

Extended Data for

Natural sensory context drives diverse brain-wide activity during *C. elegans* mating

Vladislav Susoy, Wesley Hung, Daniel Witvliet, Joshua E. Whitener, Min Wu, Core Francisco Park, Brett J. Graham, Mei Zhen, Vivek Venkatachalam, and Aravinthan D.T. Samuel

The PDF file includes:

Table E1. Functional imaging in ablated males.

Table E2. Correlations between functional and synaptic connectivity.

Figure E1. Consistency of correlations across datasets.

Figure E2. Activities of neurons during 15 randomly selected hermaphrodite contact events.

Figure E3. Activities of neurons during 15 randomly selected turning events.

Figure E4. Activities of neurons during 15 randomly selected vulva contact events.

Figure E5. Activities of neurons during nine sperm release events.

Figure E6. State-specific correlations.

Figure E7. Synaptic connectivity between correlated neurons.

Figure E8. Common synaptic input.

Figure E9. Community interaction motifs (link clustering).

Figure E10. Community interaction motifs (WSBM).

Figure E11. Position of the male rays during vulva detection events.

Figure E12. Decoding of continuous behavioral features from functional communities.

Tuning properties of individual neurons of *C. elegans* posterior brain.

Table E1. Functional imaging in ablated males. Neurons of the vulva-detecting circuit were ablated in young adult males, and the panneuronal imaging was performed on the next day. For this, the males were placed on a plate with hermaphrodites and were allowed to mate. Traces of activity were extracted for several neurons of interest. A few neurons of interest could not be seen in some males. These neurons are marked with '-'.

Ablation	Index	PCB	PCC	HOA	HOB	R2B	PVX	SPC	PCA
-HOA	102	+	+	na	+	+	+	+	+
-HOA	105	+	+	na	+	+	+	+	+
-HOA	101	+	+	na	+	+	+	+	+
-PCA/L	492	+	+	+	+	+	+	+	na
-PCA/L	501	+	+	+	+	-	+	+	na
-PCA/L	505	+	+	+	+	+	+	+	na
-HOA -PCB/L	450	na	+	na	+	+	+	+	+
-HOA -PCB/L	453	na	+	na	-	+	+	+	-
-HOA -PCB/L	1023	na	+	na	+	-	+	+	-
-HOA -PCC/L	568	+	na	na	+	+	+	+	+
-HOA -PCC/L	1025	+	na	na	+	+	+	+	+
-HOA -PCC/L	1032	+	na	na	+	+	+	+	+
-HOA -HOB	560	+	-	na	na	-	+	+	+
-HOA -HOB	561	+	-	na	na	-	+	+	+
-HOA -HOB	562	+	+	na	na	+	+	+	+
-HOA -HOB	1022	+	+	na	na	+	+	+	+

Table E2. Correlations between functional correlations and synaptic connectivity. We calculated Pearson and partial correlation coefficients on 8 variants of synaptic connectivity matrices. The different variants of the connectivity matrices were generated using (i) symmetrized or original connectivity, (ii) validated or original gap junctions, and (iii) synapse count or synaptic size as a measure of connectivity.

Symmetrized connectivity	Validated gap junctions	Connectivity measure	Chemical		Electrical	
			Pearson correlation	Partial correlation	Pearson correlation	Partial correlation
1	1	count	r=0.18 p=0.0014	r=0.13 p=0.014	r=0.34 p=0.0011	r=0.33 p=7e-04
			r=0.12 p=0.012	r=0.08 p=0.062	r=0.29 p=0.0029	r=0.28 p=0.0012
1	0	count	r=0.18 p=0.0015	r=0.14 p=0.0061	r=0.33 p=1e-04	r=0.33 p<0.0001
			r=0.12 p=0.0092	r=0.08 p=0.073	r=0.37 p<0.0001	r=0.37 p<0.0001
0	1	count	r=0.14 p=0.0087	r=0.1 p=0.063	r=0.36 p=1e-04	r=0.36 p=1e-04
			r=0.11 p=0.028	r=0.08 p=0.089	r=0.29 p=0.0033	r=0.29 p=0.001
0	0	count	r=0.14 p=0.0081	r=0.12 p=0.029	r=0.35 p<0.0001	r=0.35 p<0.0001
			r=0.11 p=0.025	r=0.08 p=0.096	r=0.37 p<0.0001	r=0.37 p<0.0001

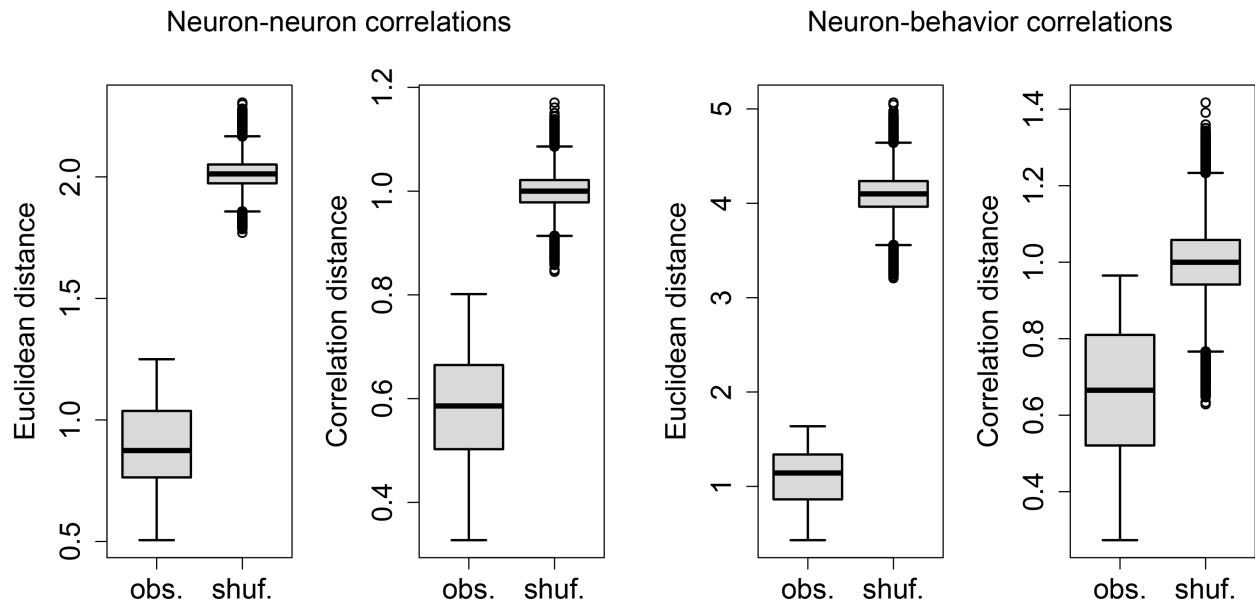


Figure E1. Consistency of correlations across datasets. Pairwise Euclidean and correlation distances between neuron-neuron and neuron-behavior correlation matrices compared to distances between 10,000 matrices with shuffled neuronal ids. Neuron-neuron correlations: $t(35) = -35.92, p < 0.0001$, $t(35) = -21.79, p < 0.0001$ for Euclidean and correlation distances respectively; neuron-behavior correlations $t(27) = -47.26, p < 0.0001$, $t(27) = -9.66, p < 0.0001$.

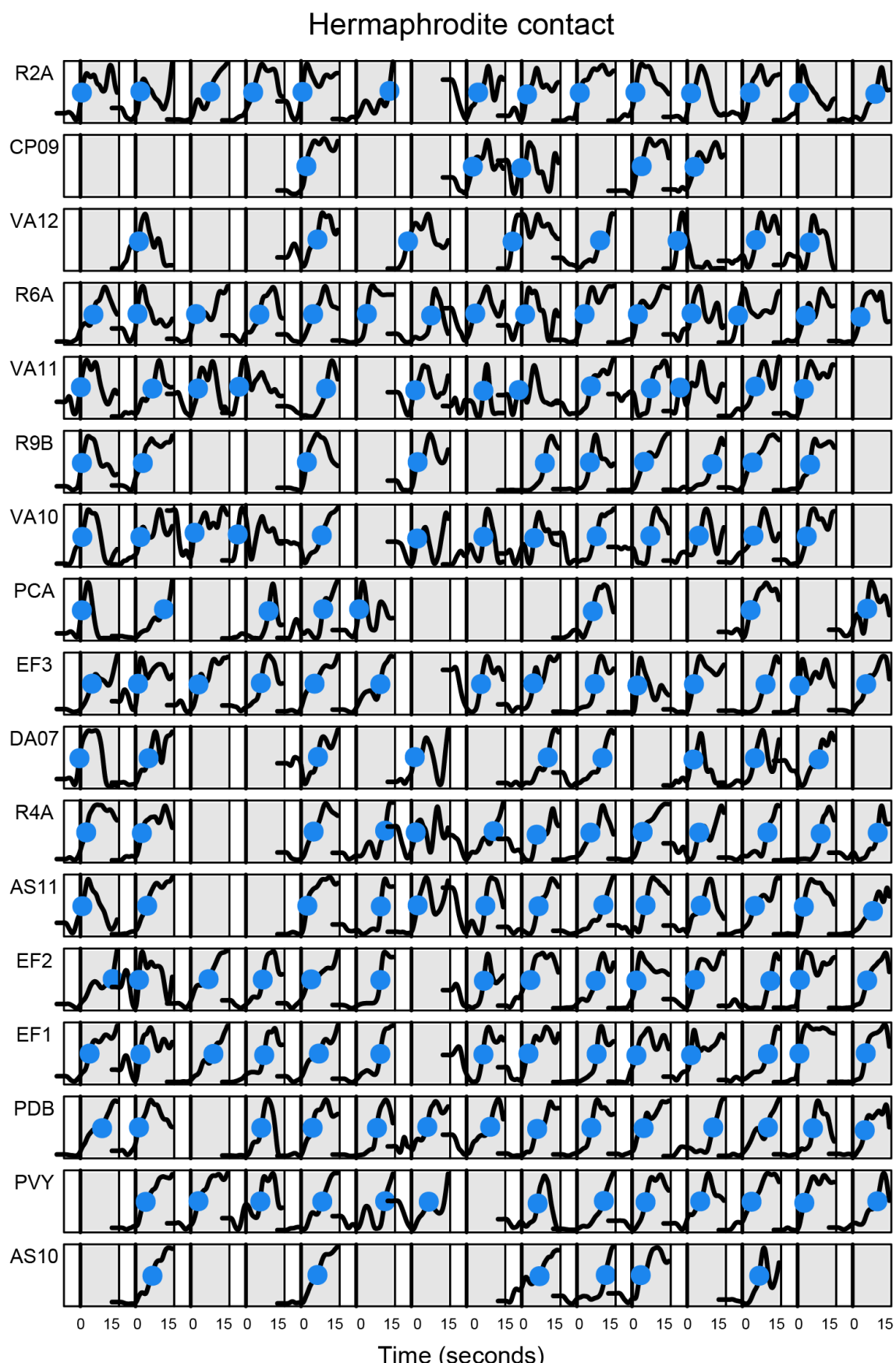


Figure E2. Activities of neurons during 15 randomly selected hermaphrodite contact events. Activity traces of neurons associated with hermaphrodite contact plotted for 15 instances of the contact events. Blue dots indicate half-peak response times.

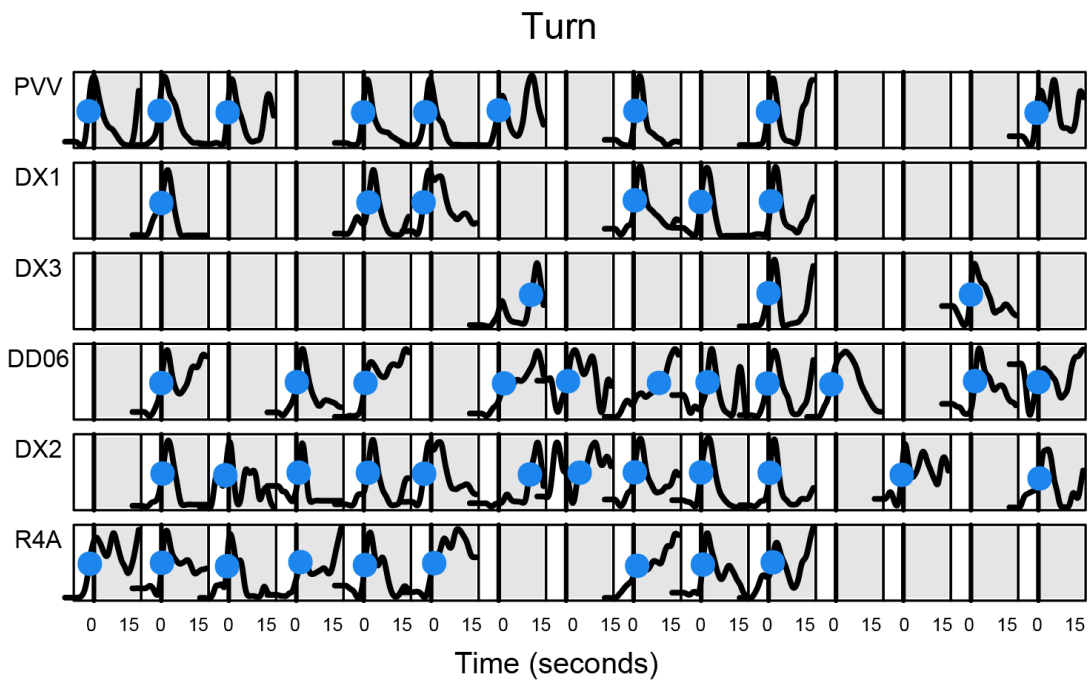


Figure E3. Activities of neurons during 15 randomly selected turning events. Activity traces of neurons associated with turning plotted for 15 instances of turning events. Blue dots indicate half-peak response times.

Vulva contact

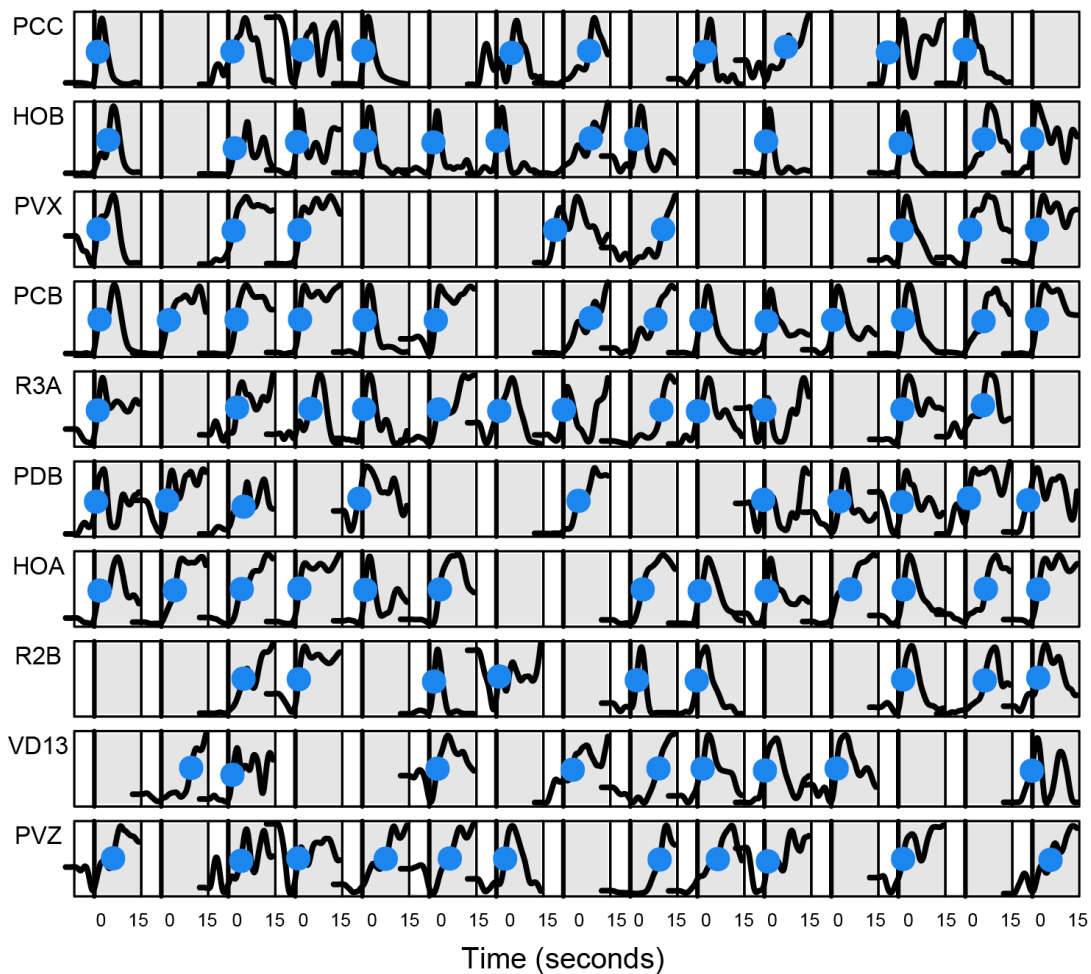


Figure E4. Activities of neurons during 15 randomly selected vulva contact events. Activity traces of neurons associated with vulva location plotted for 15 instances of the vulva contact events. Blue dots indicate half-peak response times.

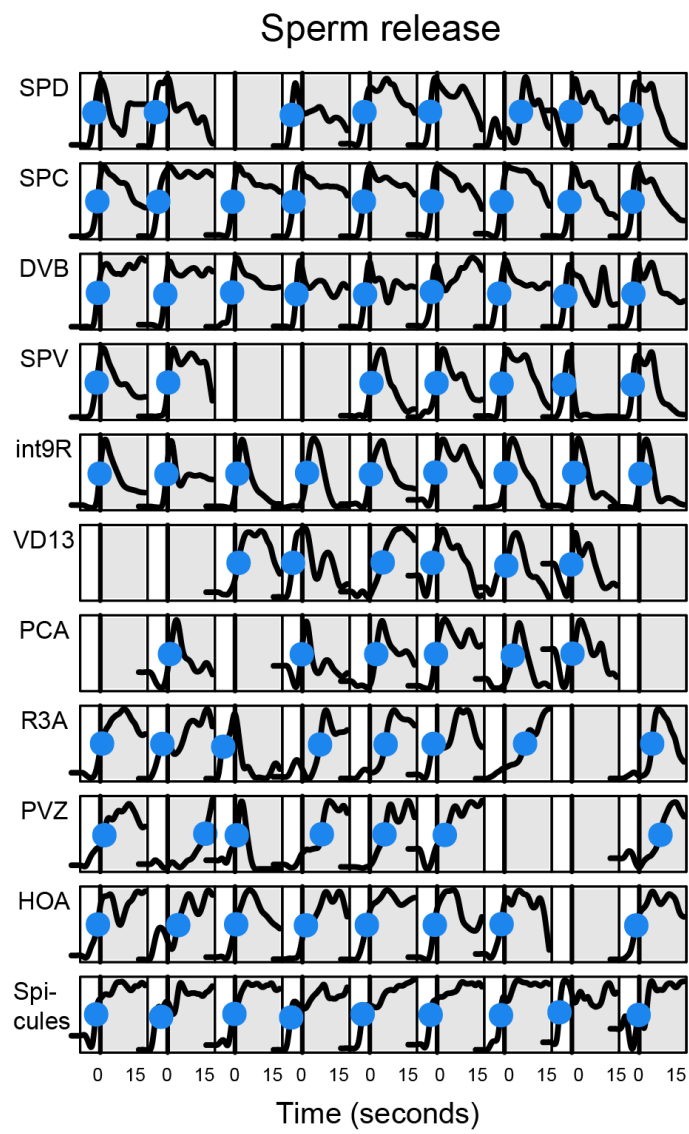


Figure E5. Activities of neurons during nine sperm release events. Activity traces of neurons associated with copulation plotted for 9 instances of the sperm release events. Blue dots indicate half-peak response times. The change in the spicule position is plotted alongside neuron activities.

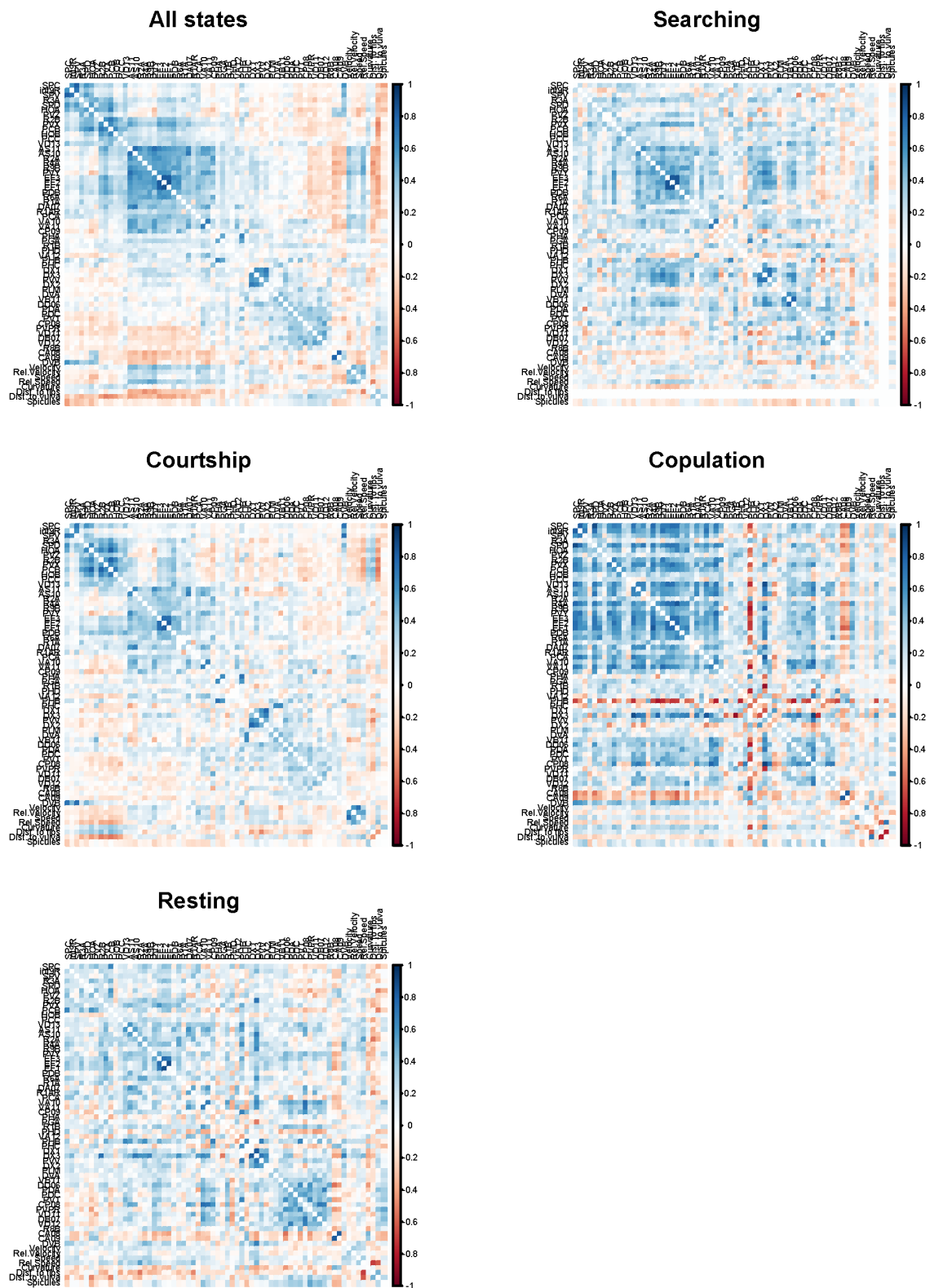


Figure E6. State-specific correlations. Consensus cross-correlation matrices for four major behavioral states: searching, courtship, copulation, and resting.

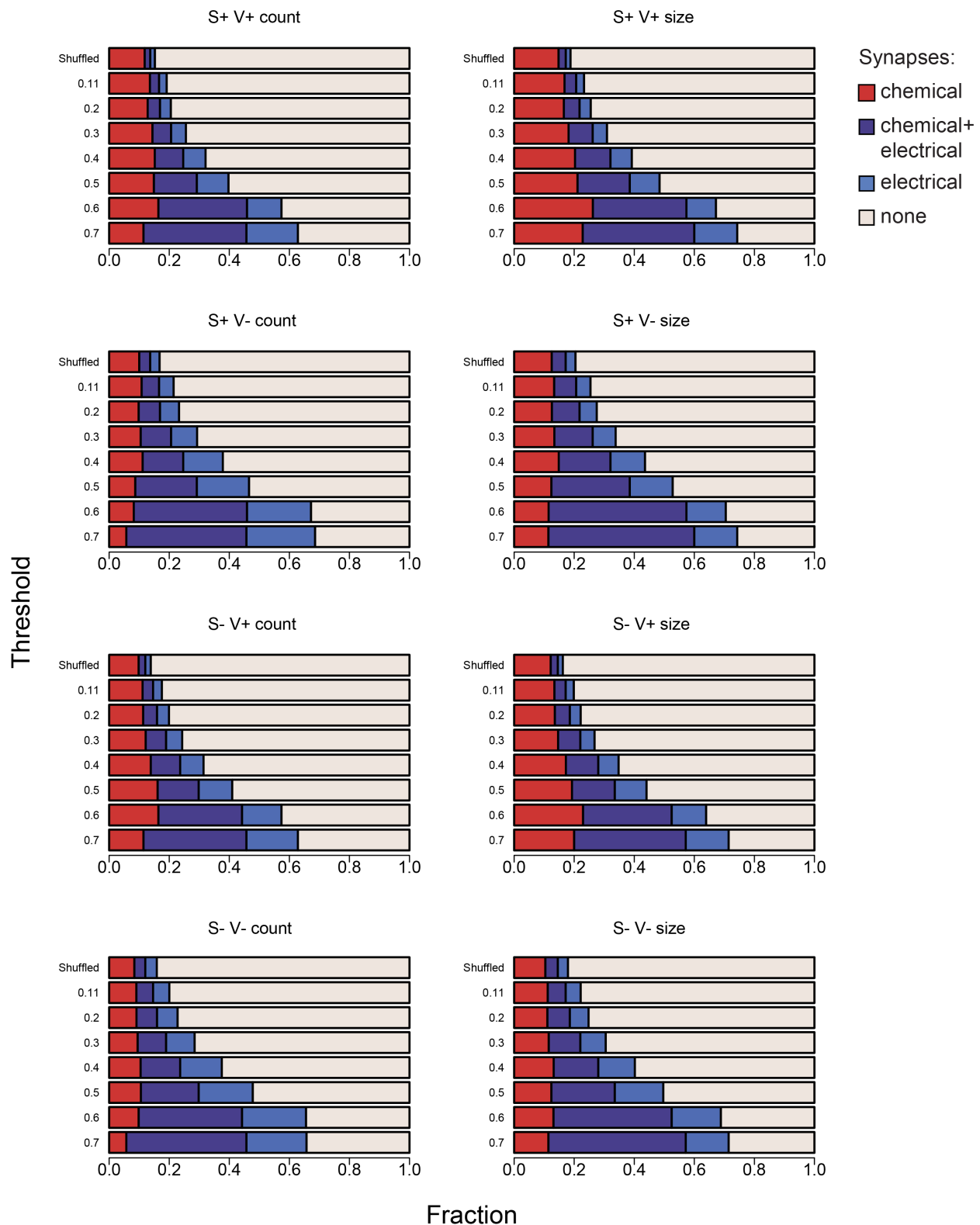


Figure E7. Synaptic connectivity between correlated neurons. Fraction of neurons with positive functional correlations above the threshold that are connected by chemical and electrical synapses. Analysis was performed on eight different variants of the synaptic connectivity matrix (see methods): "S+" – symmetrized, "S-" – not symmetrized, "V+" validated synapses, "V-" original synapses, "count" – synapse count, "size" – synaptic connectivity size.

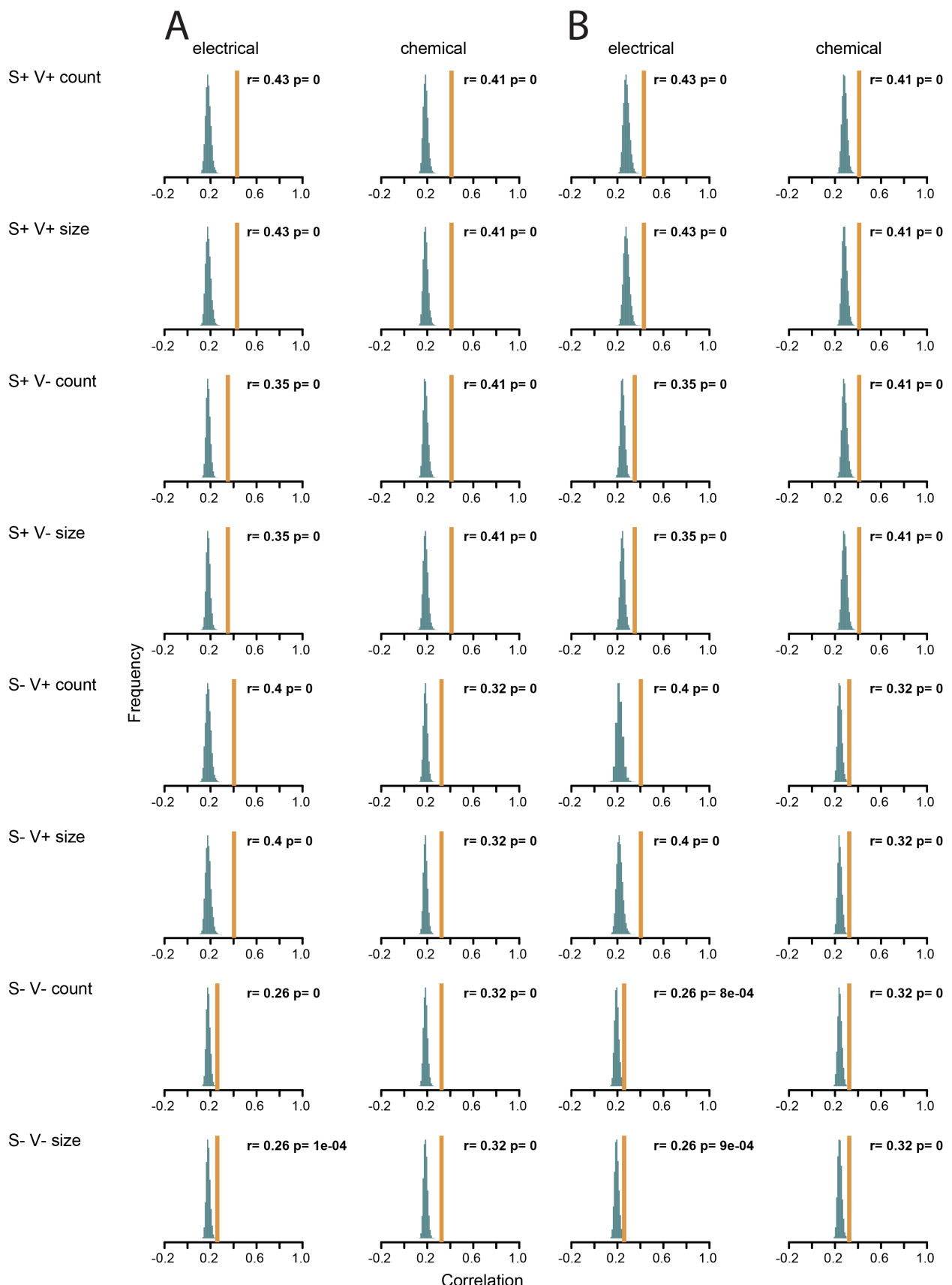


Figure E8. Common synaptic input. (A) Mean correlation between neurons that have common synaptic input (orange line) compared to correlations obtained when ids of the consensus correlation matrix were shuffled (histogram). Shuffling procedure was performed 10,000 times. (B) Same as in (A), except shuffling procedure was performed in a way that preserved left-right functional symmetries. These analysis was performed on eight different variants of the synaptic connectivity matrix (see methods): "S+" – symmetrized, "S-" – not symmetrized, "V+" – validated synapses, "V-" original synapses, "count" – synapse count, "size" – synaptic connectivity size.

Community interaction motifs (link clustering)

assortative □ core-periphery □ disassortative

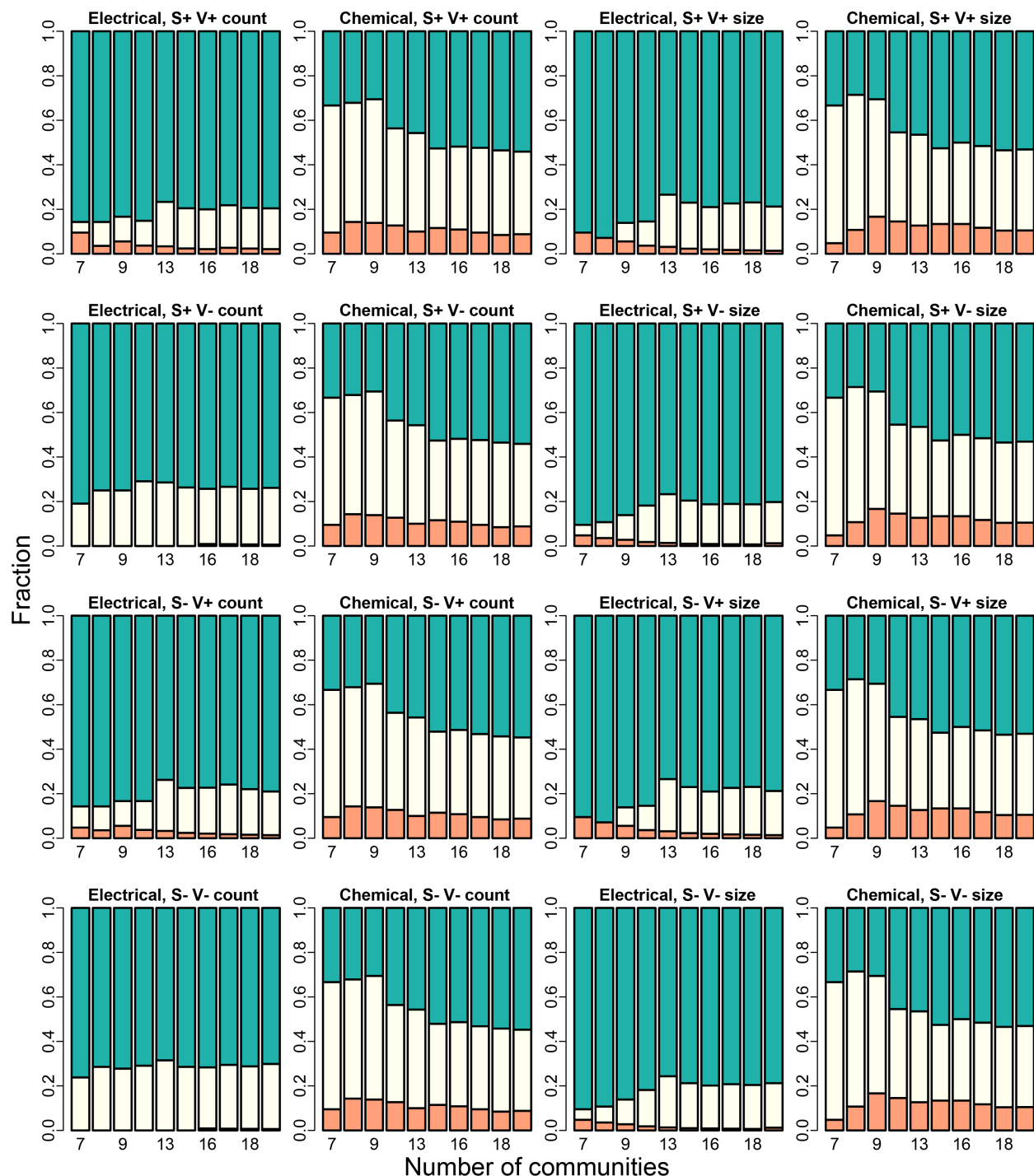


Figure E9. Community interaction motifs (link clustering). Analysis was performed on eight different variants of the synaptic connectivity matrix (see methods): "S+" – symmetrized, "S-" – not symmetrized, "V+" validated synapses, "V-" original synapses, "count" – synapse count, "size" – synaptic connectivity size.

Community interaction motifs (WSBM)

█ assortative █ core-periphery █ disassortative

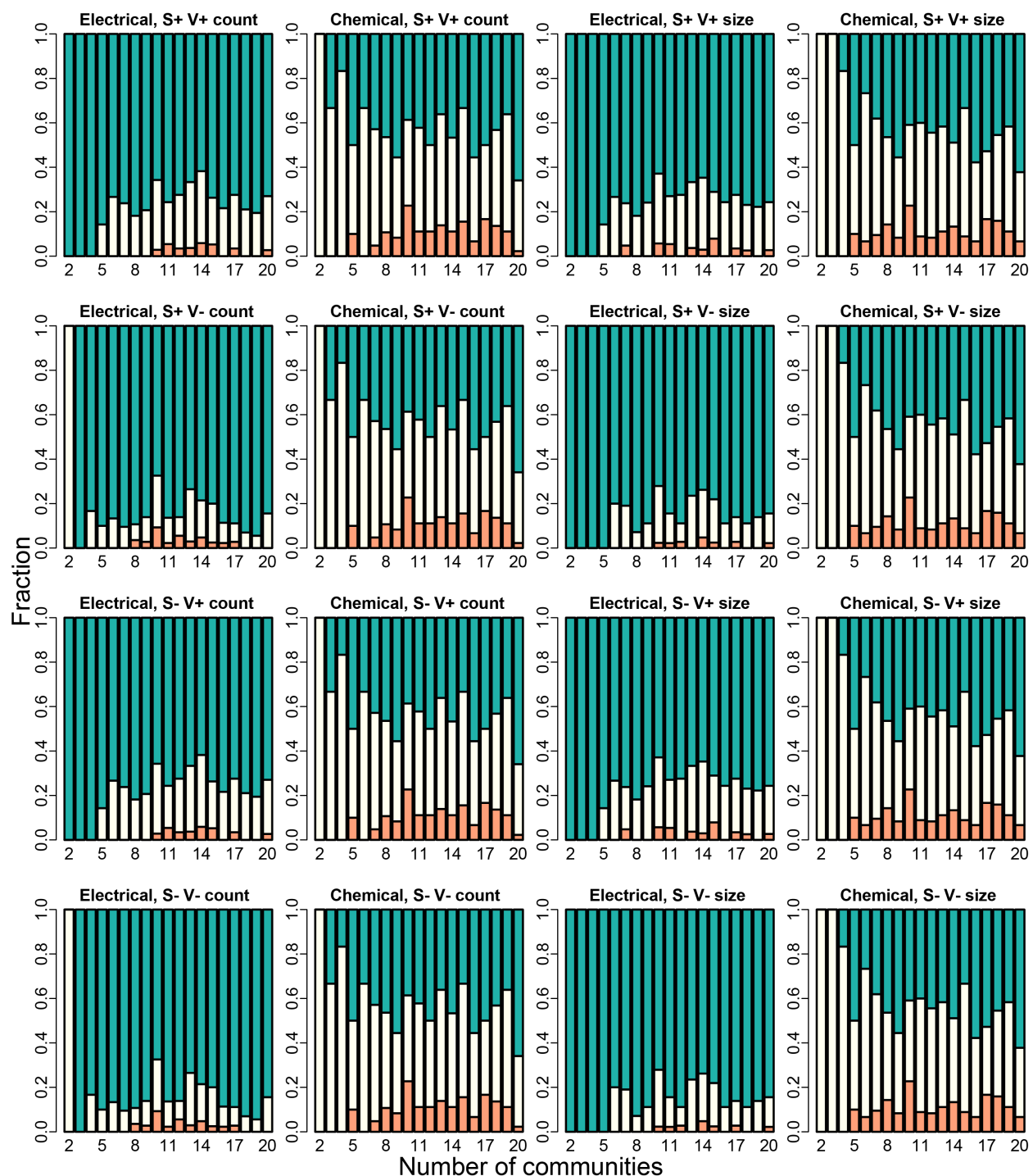


Figure E10. Community interaction motifs (WSBM). Analysis was performed on eight different variants of the synaptic connectivity matrix (see methods): "S+" – symmetrized, "S-" – not symmetrized, "V+" – validated synapses, "V-" – original synapses, "count" – synapse count, "size" – synaptic connectivity size.

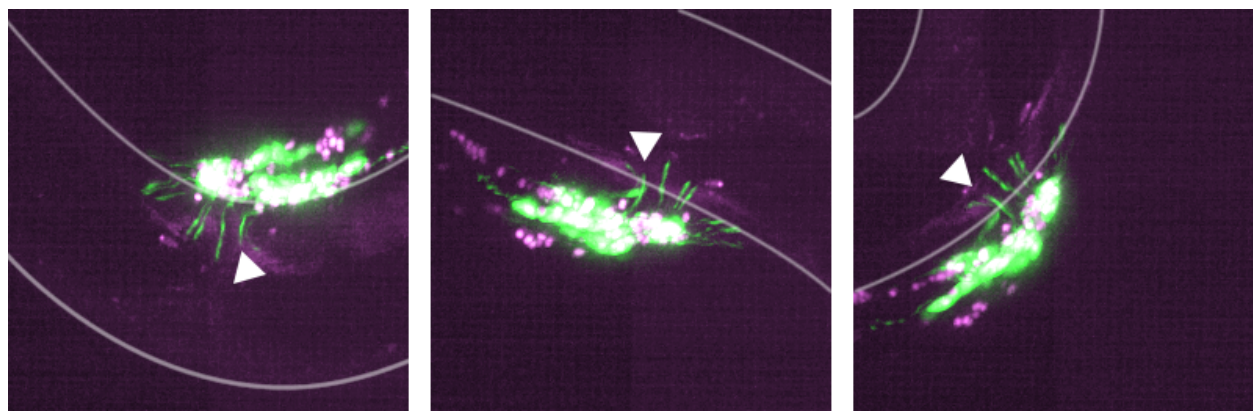


Figure E11. Position of the male rays during vulva detection events. When the male stops at the vulva, some of its rays are positioned opposite of the opening of the vulva. B-type ray neurons expressing pPkd-2::GFP are shown in green. Arrows point at the second ray. Hermaphrodite's vulva can be seen in magenta. Right lateral aspect. Maximum intensity projections are shown.

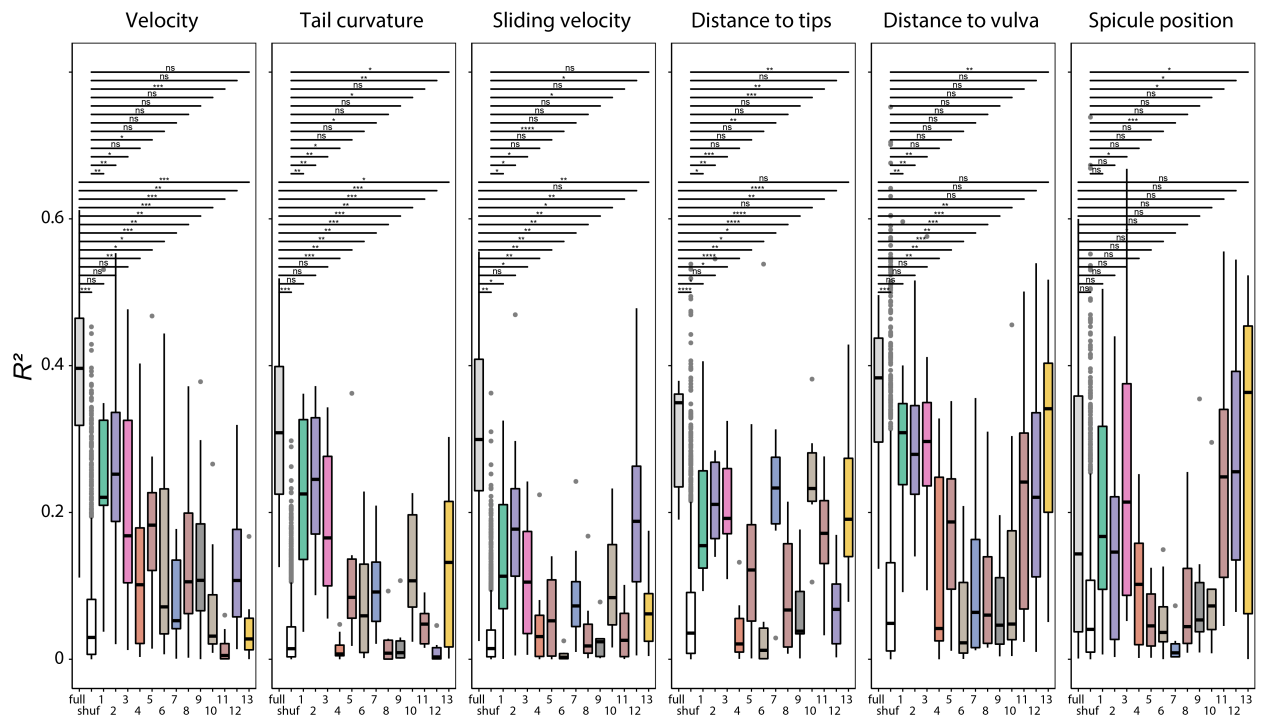
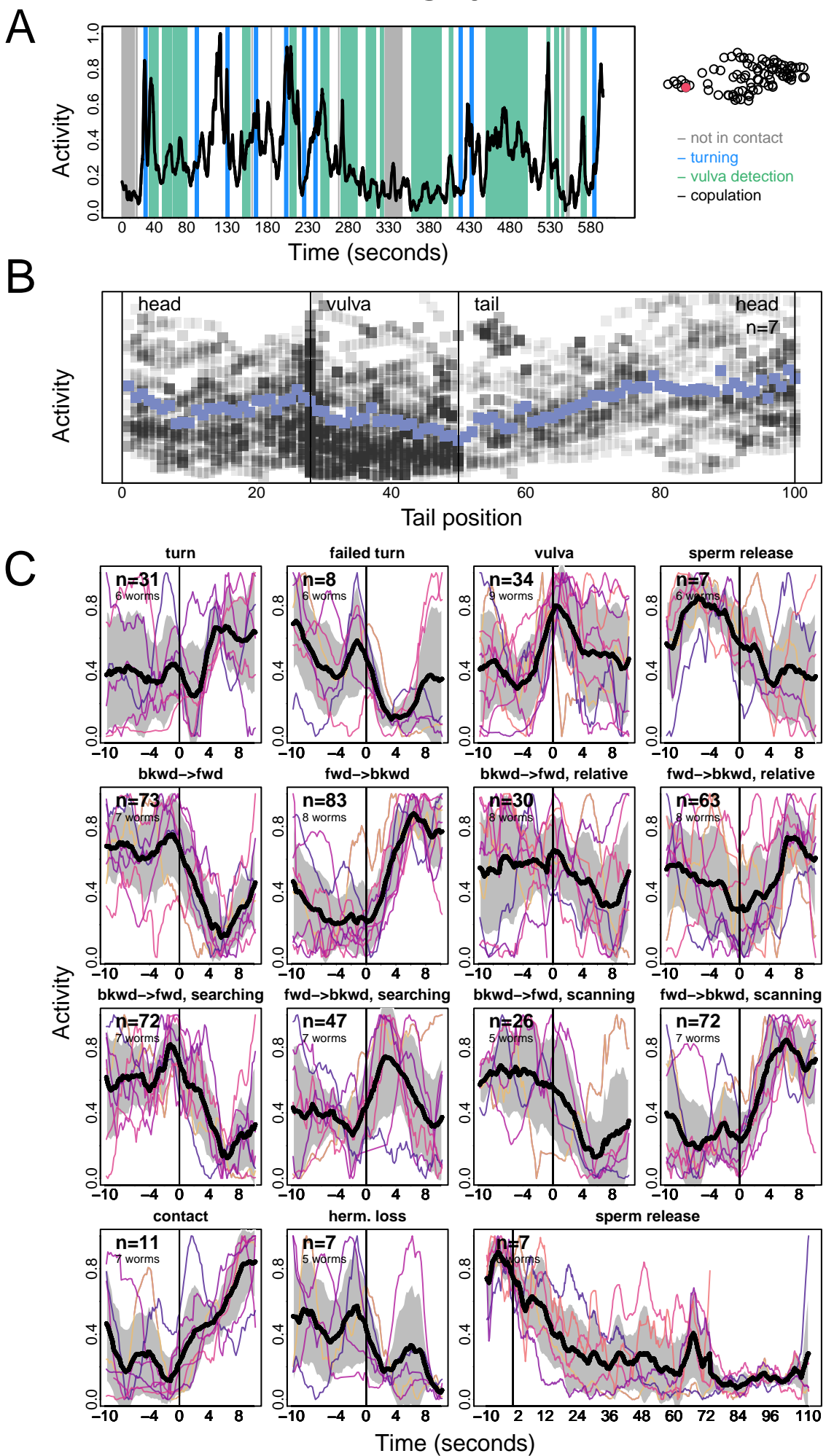


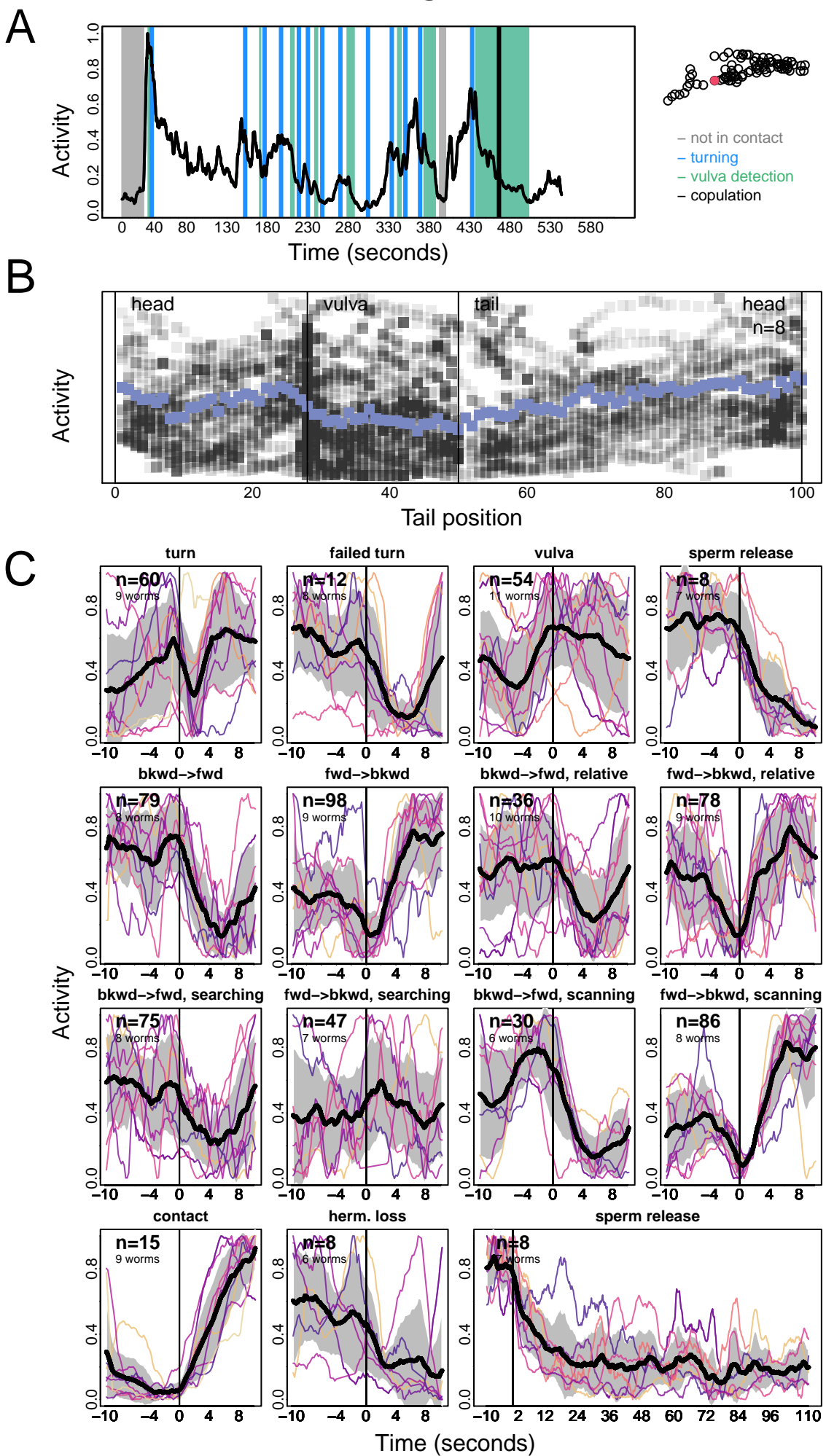
Figure E12. Decoding of continuous behavioral features from functional communities. Prediction accuracy for models built and tested using neurons that belong to different functional communities identified with link clustering. 'full' – models built using all neurons; 'shuf' – models built using all neurons and tested using shuffled ids in the testing set; 1-13 and models built and tested using activities of neurons that belong to different communities as in Figure 3C and Figure S2B. The color code is the same as in Figure 3C and Figure S2B. * $p<0.05$, ** $p<0.01$, *** $p<0.001$, ns – not significant.

Tuning properties of individual neurons of *C. elegans* posterior brain. For each recorded neuron in the male tail, its activity patterns are shown. **(A)** Neuron activity plotted for an entire mating behavior for a representative dataset. The neuron's location in the posterior brain is shown in red. **(B)** Neuron activities from up to seven males as a function of the tail position on the hermaphrodite (as in **Figure 5**). Mean activity for all males is shown in blue. **(C)** Neuron activities from all males aligned to the onset of discrete behavioral events. The discrete events include (in the order of appearance) turning, failed turning, vulva contact, sperm release, switching from backward to forward movement (tabulated for the entire behavior), switching from forward to backward movement (tabulated for the entire behavior), switching from backward to forward sliding (relative to the hermaphrodite), switching from forward to backward sliding (relative to the hermaphrodite), switching from backward to forward movement (during searching), switching from forward to backward movement (during searching), switching from backward to forward movement (during scanning), switching from forward to backward movement (during scanning), hermaphrodite contact, hermaphrodite loss, and sperm release (an extended time window is shown). 'n' is number of times that each neuron was recorded during the onset of specific motifs. Colored lines show normalized mean activities for individual males. The mean activity for all males is in black and standard deviation is indicated in gray.

AS10

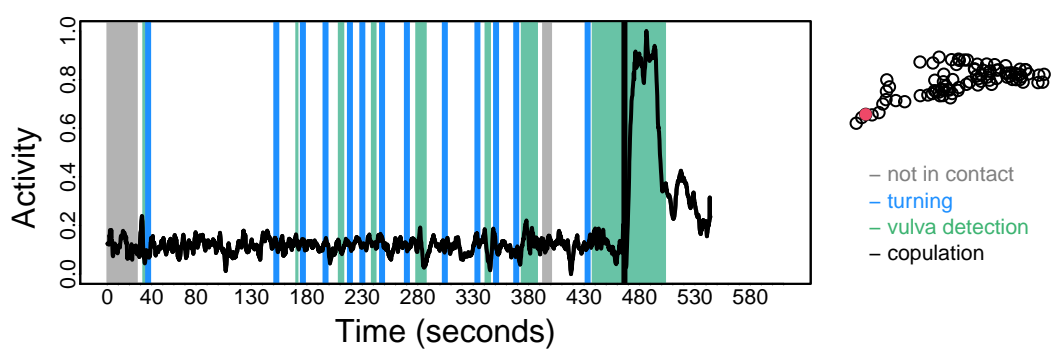


AS11

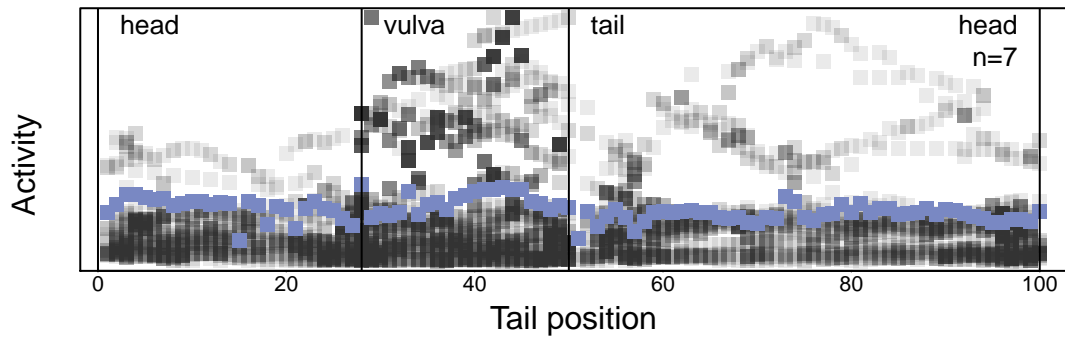


CA08

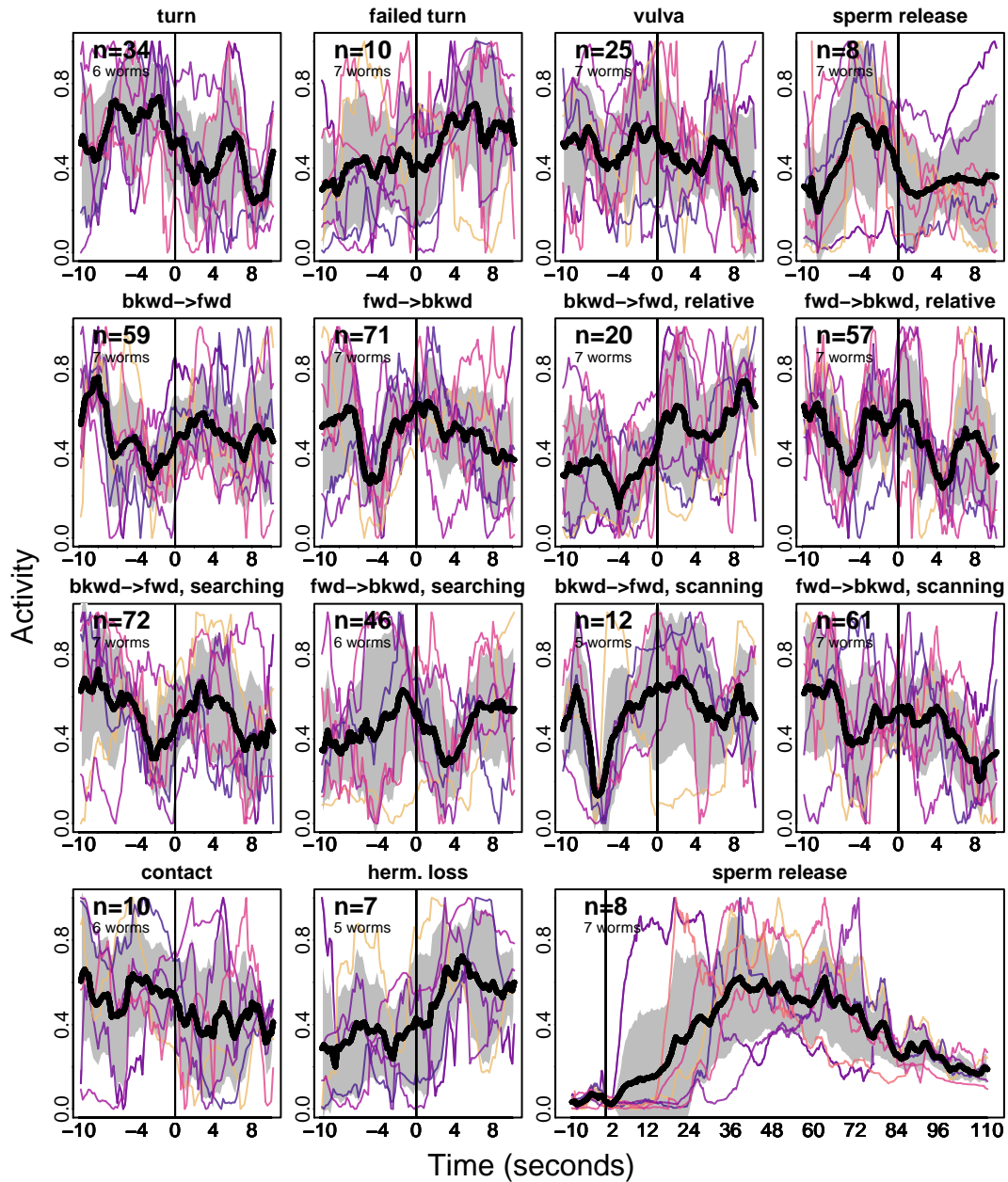
A



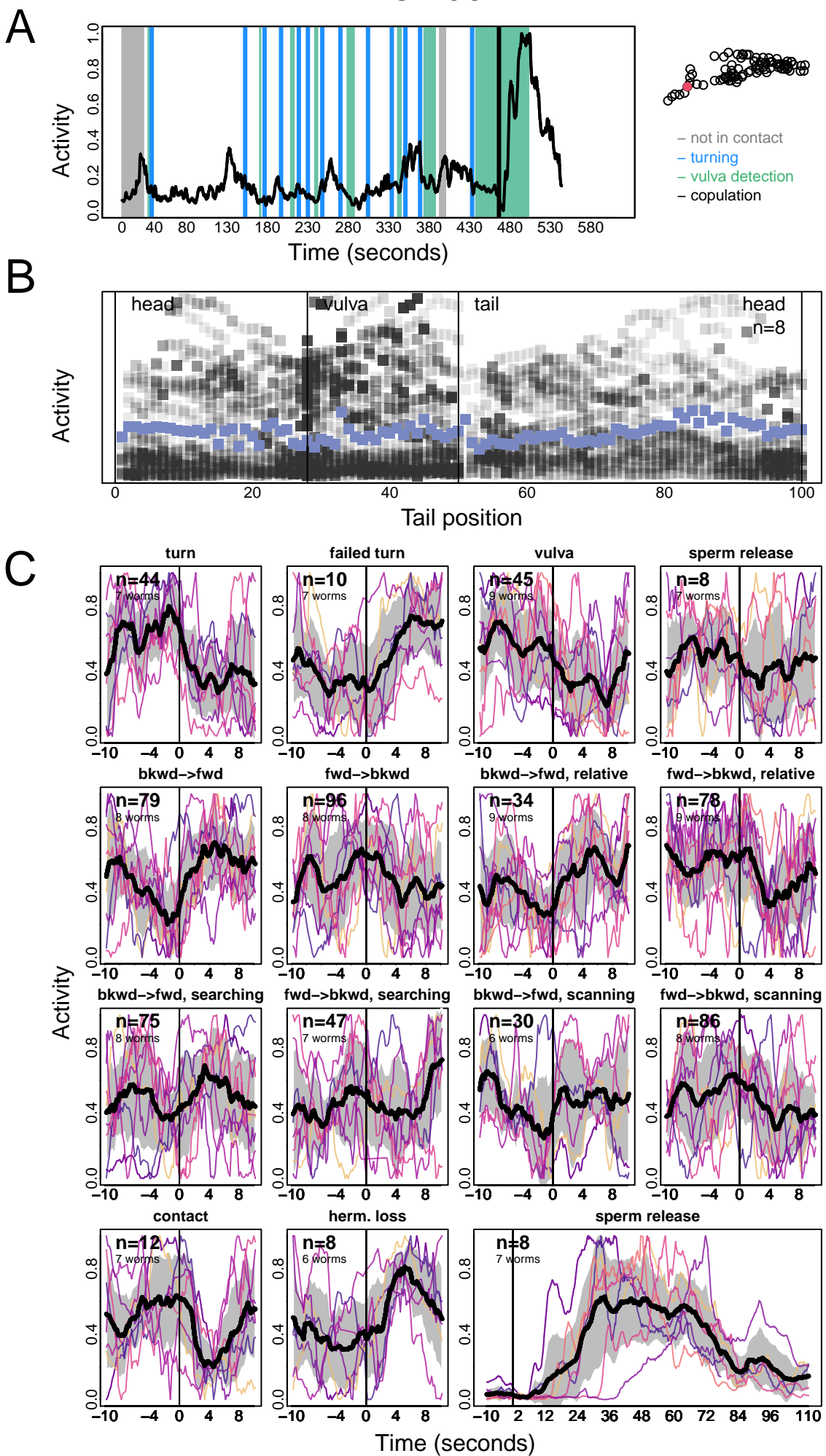
B



C

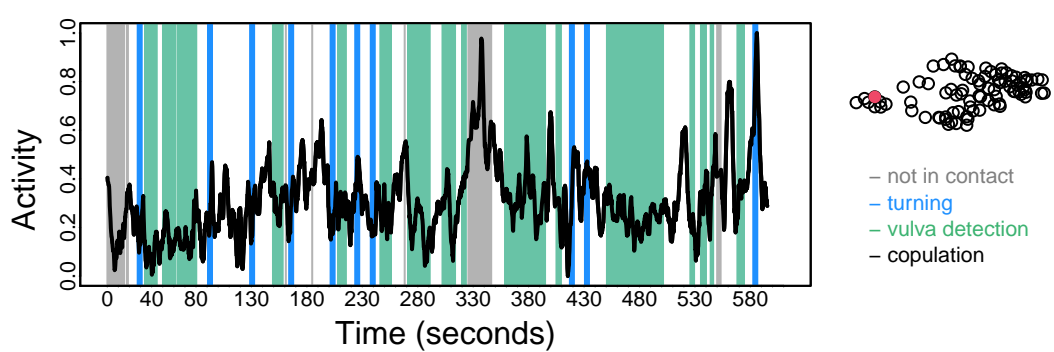


CA09

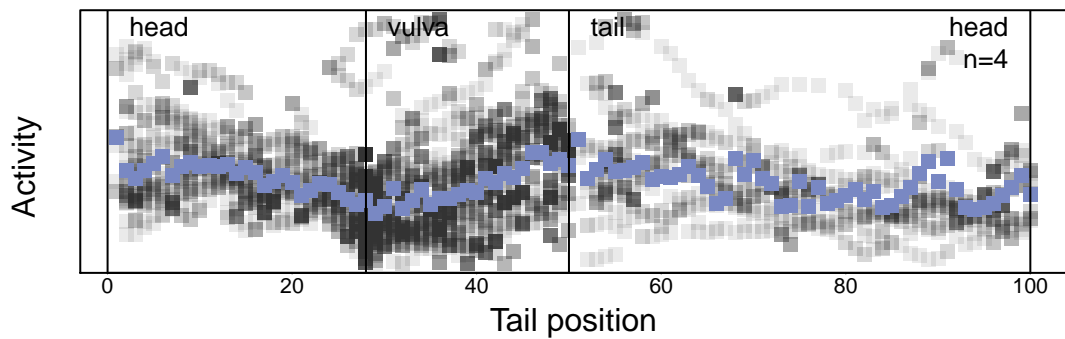


CP08

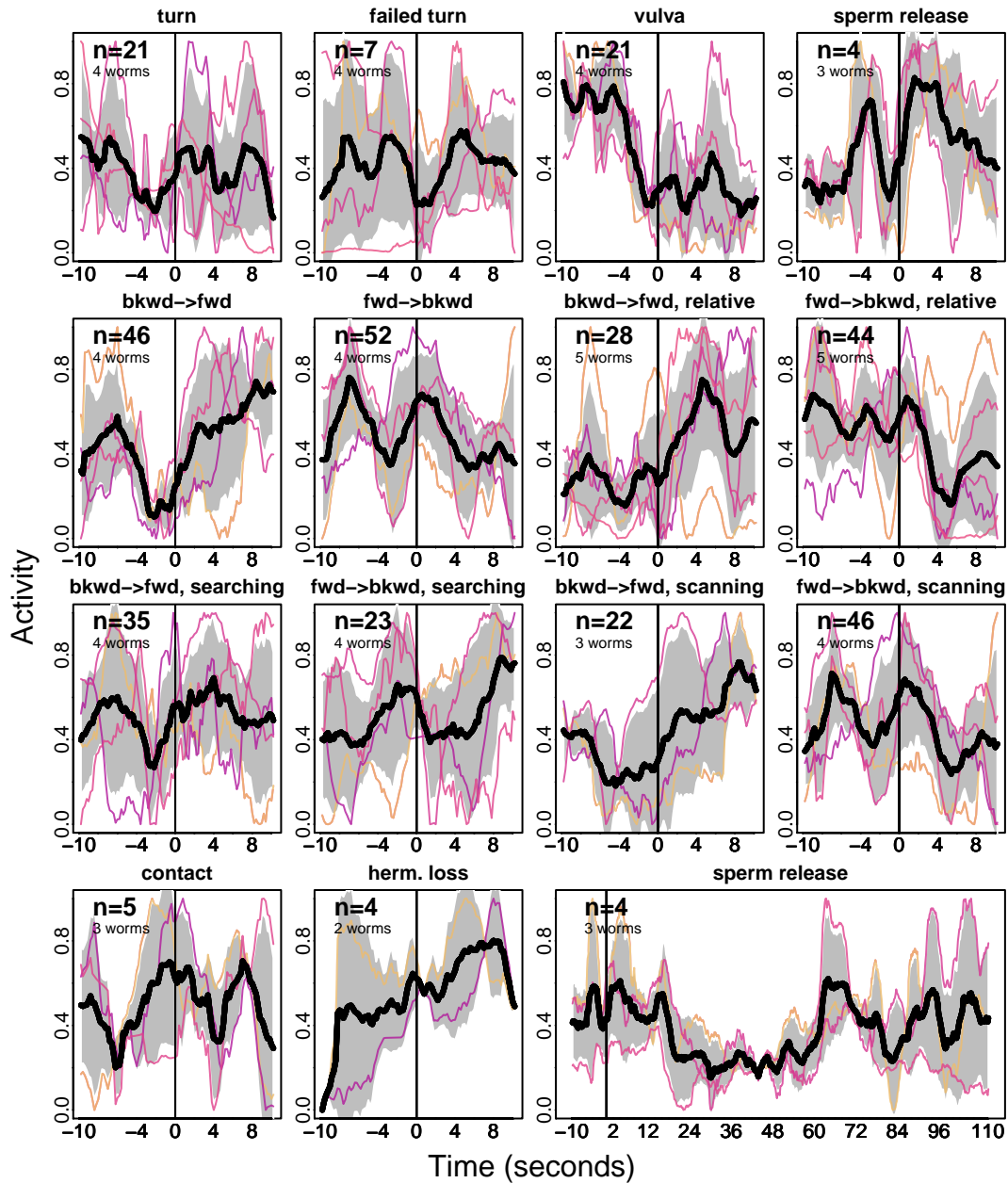
A



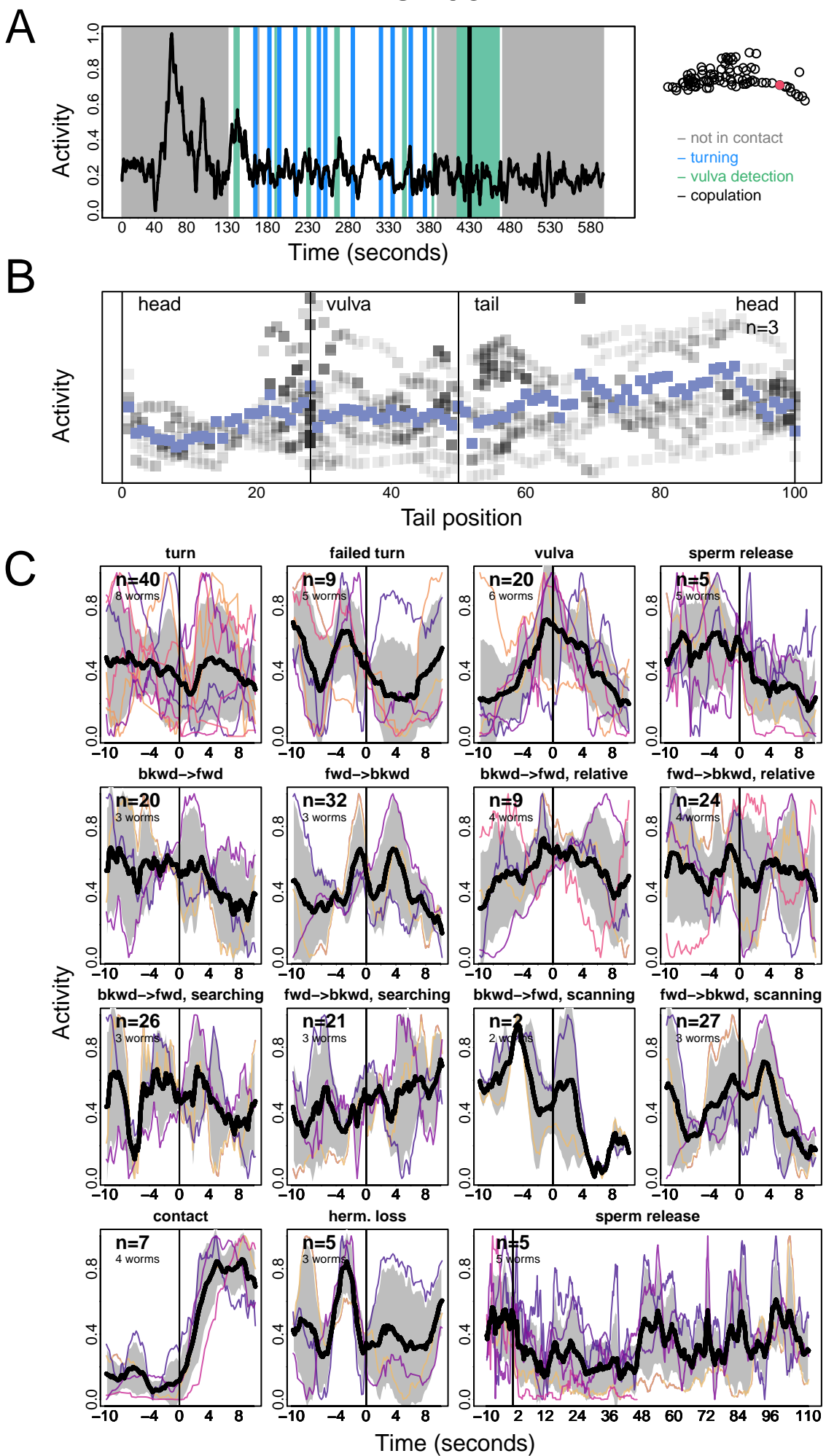
B



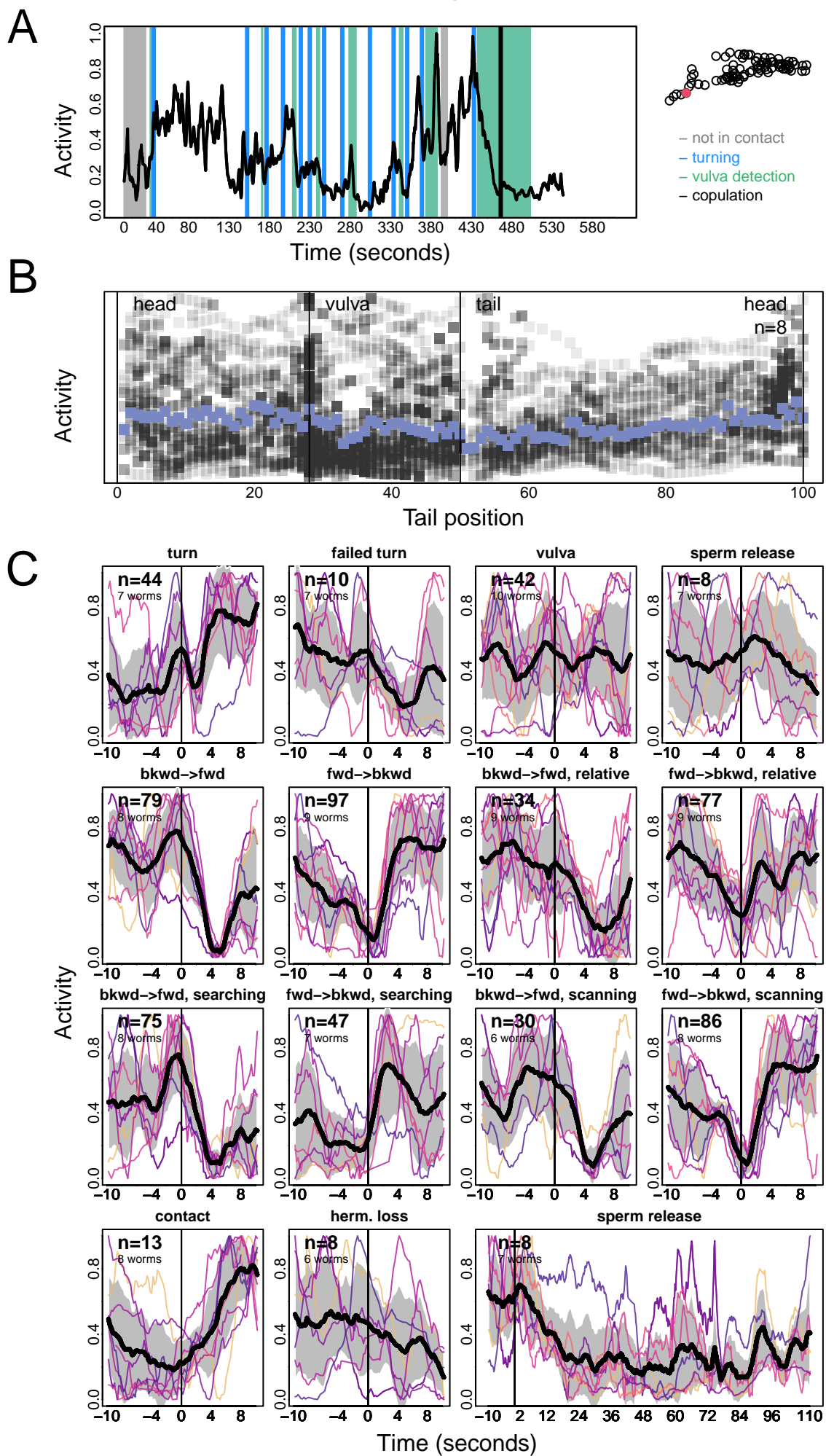
C



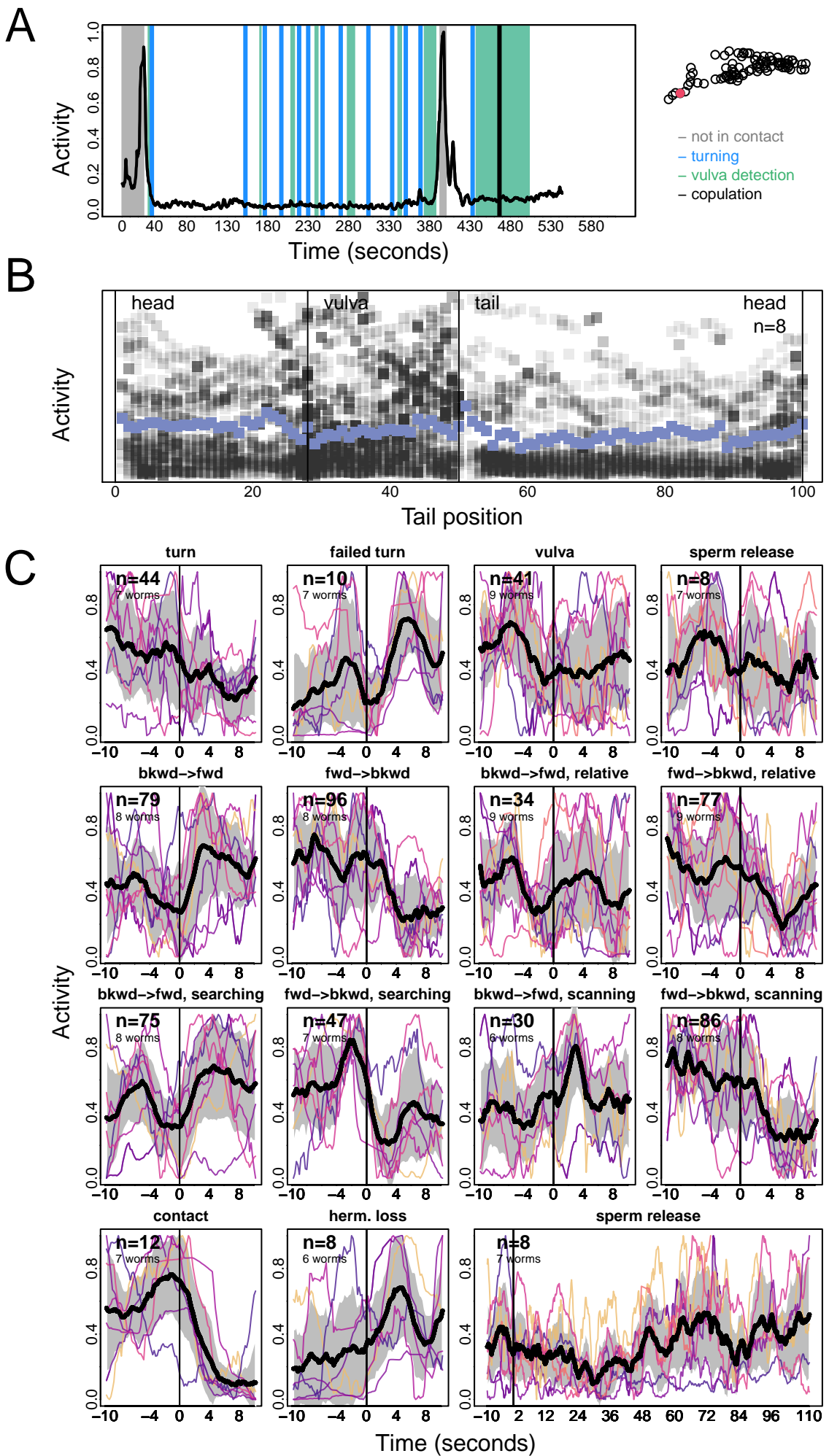
CP09



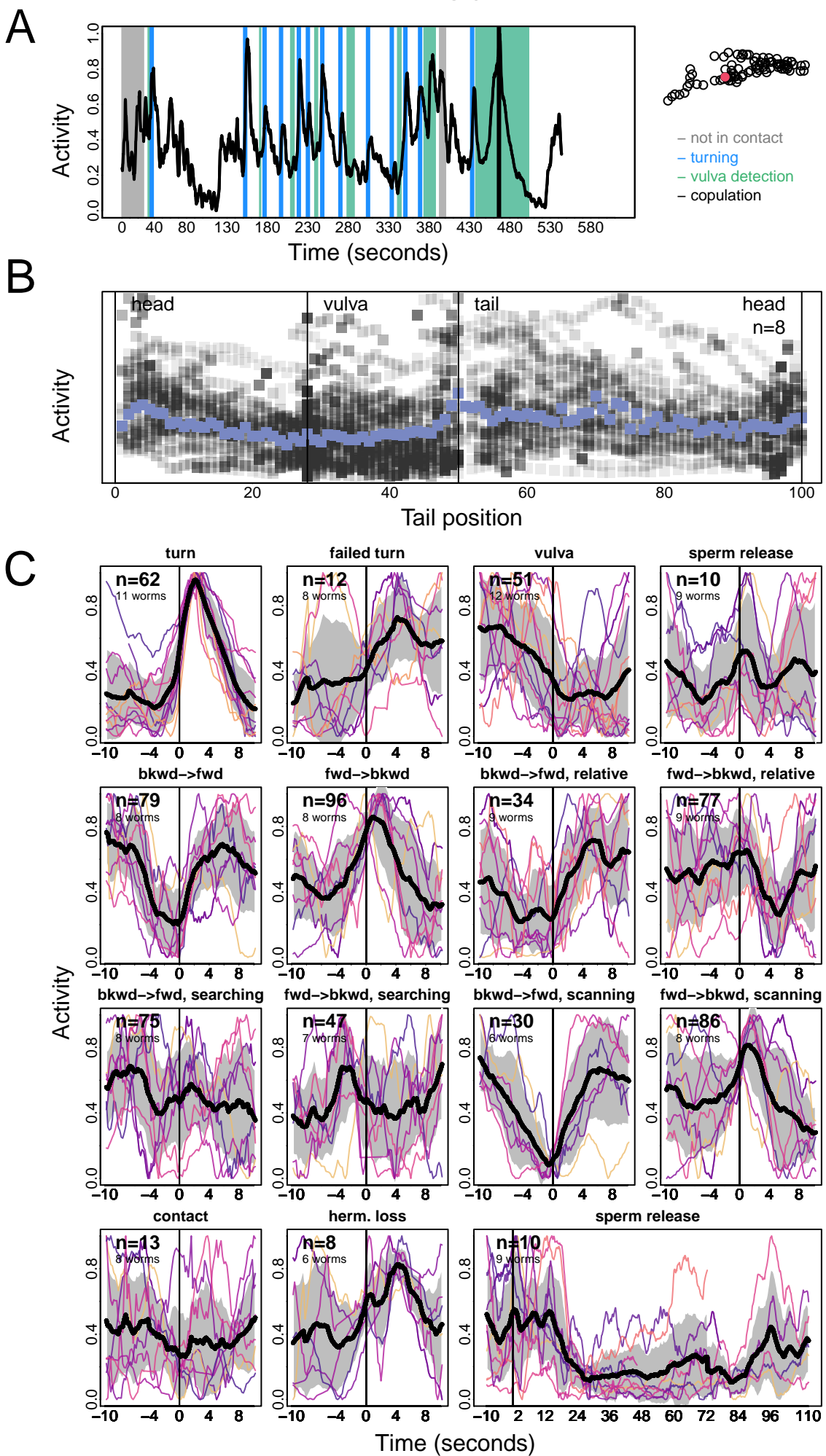
DA07



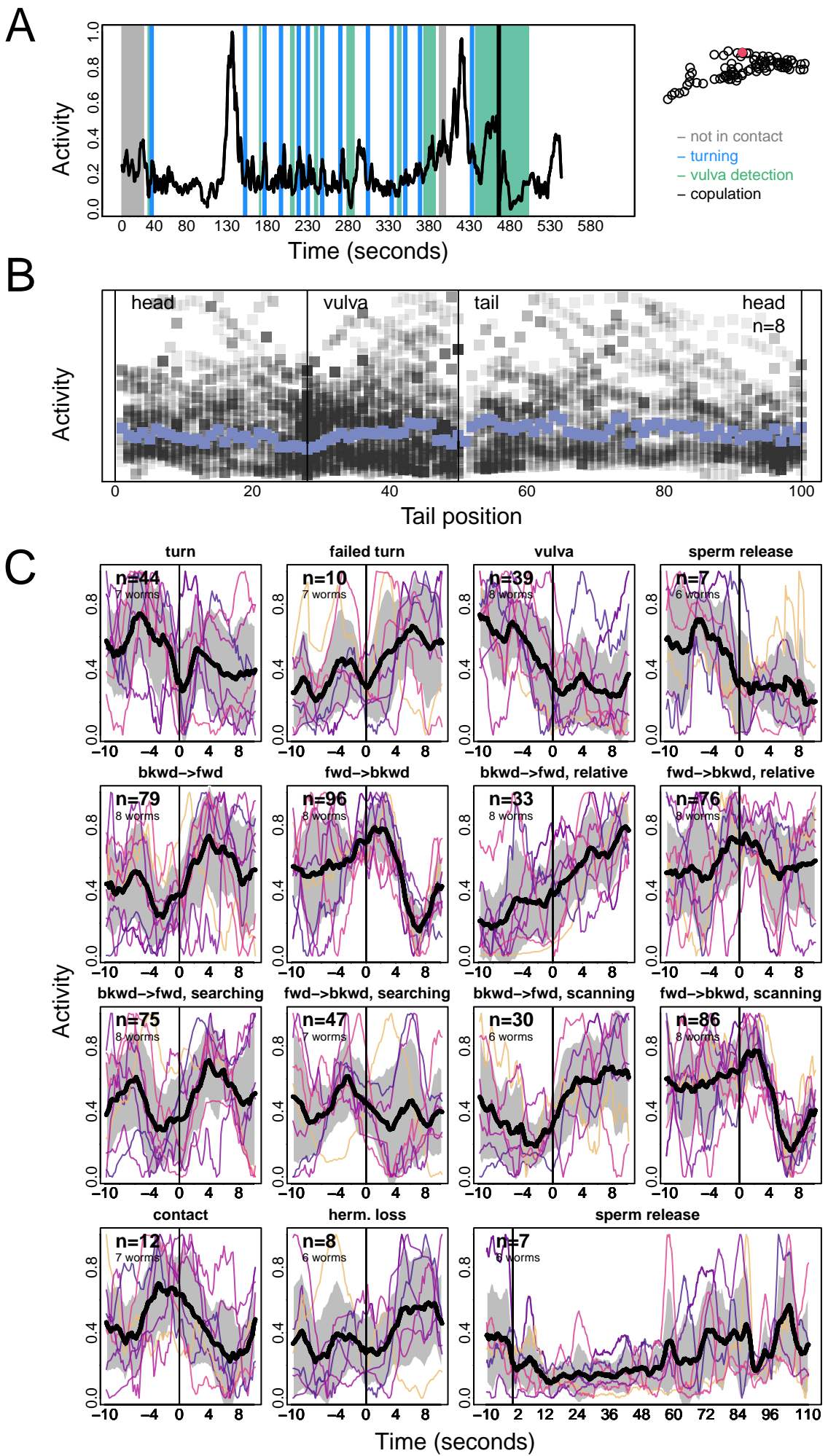
DB07



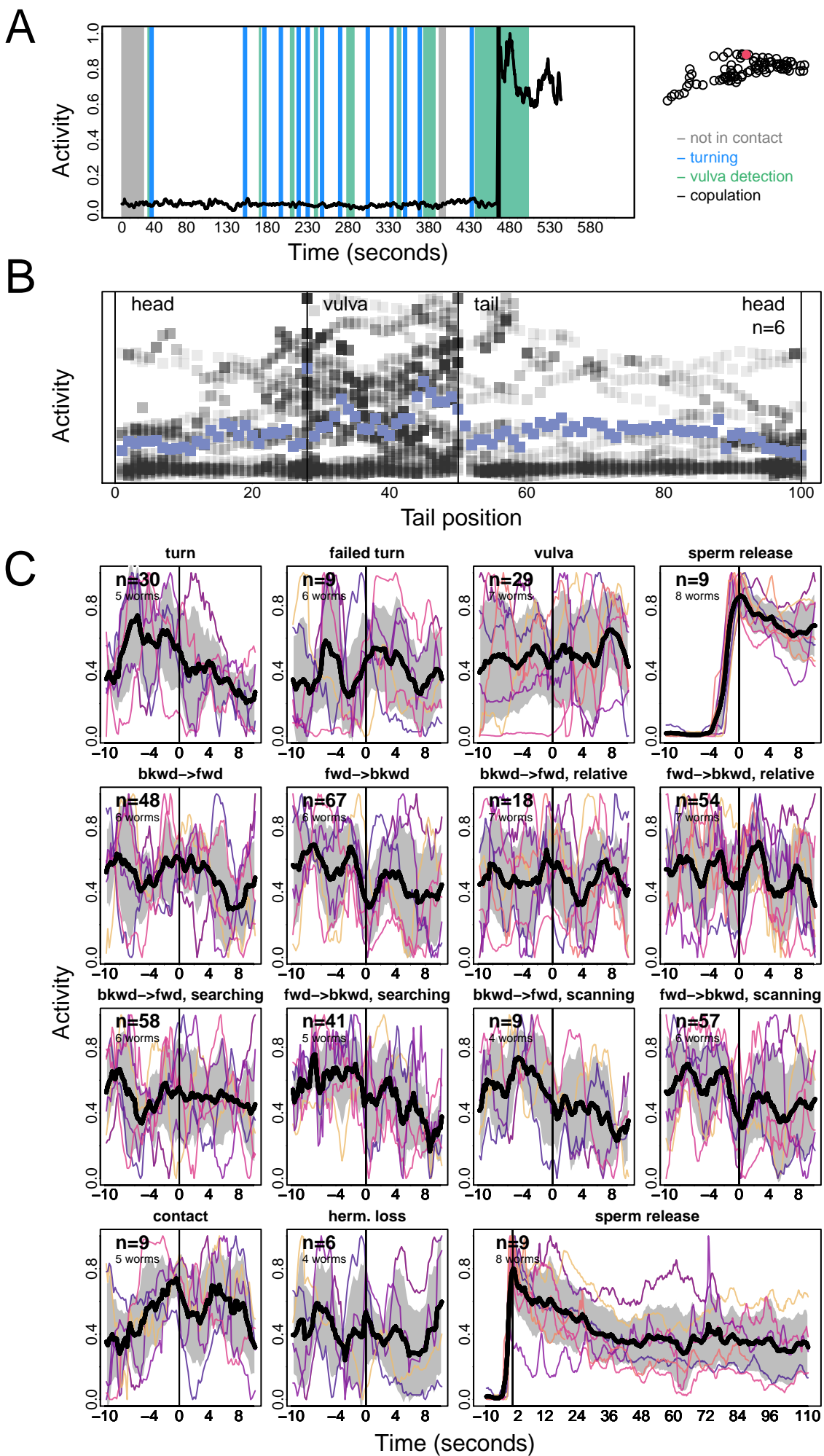
DD06



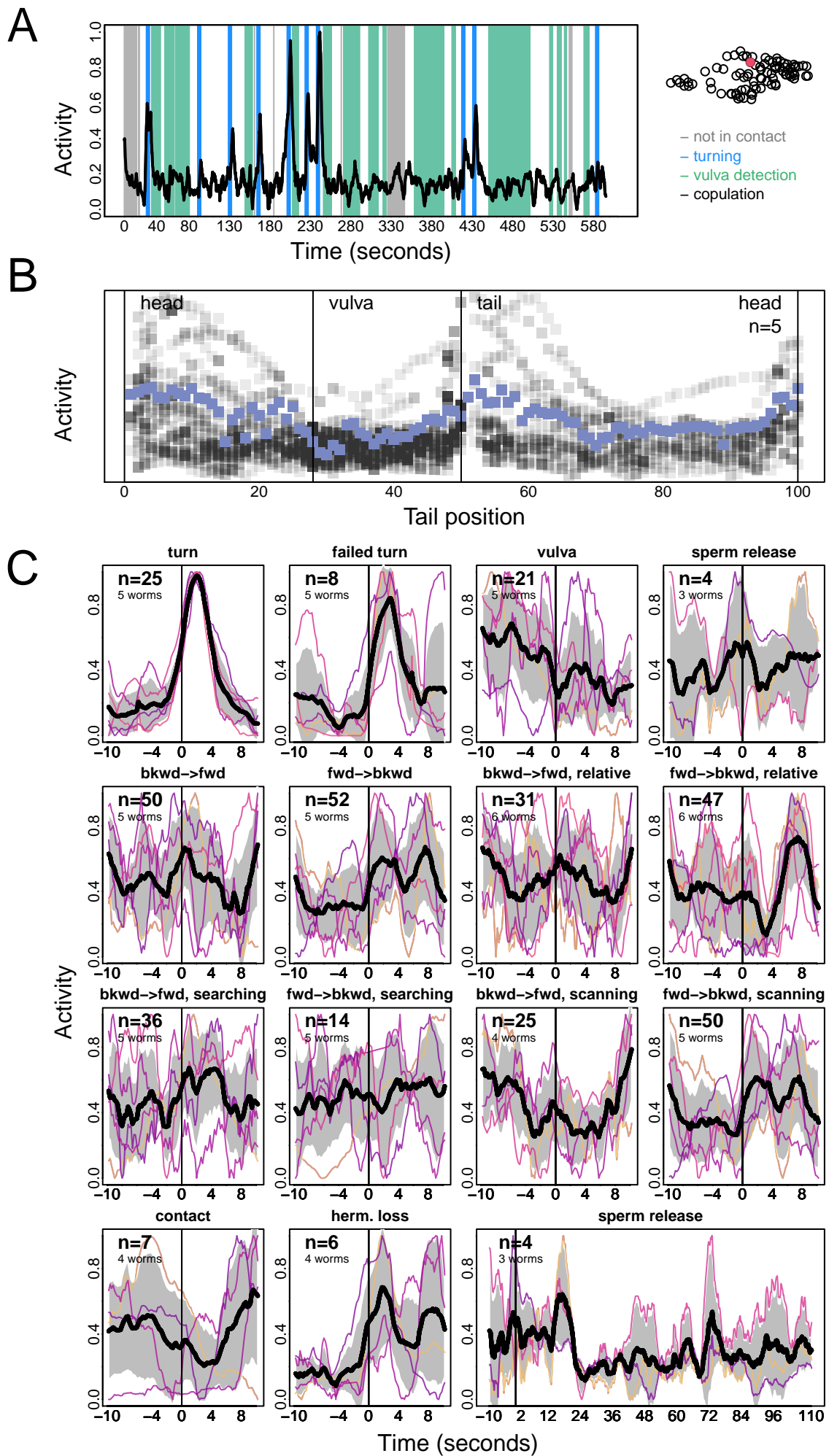
DVA



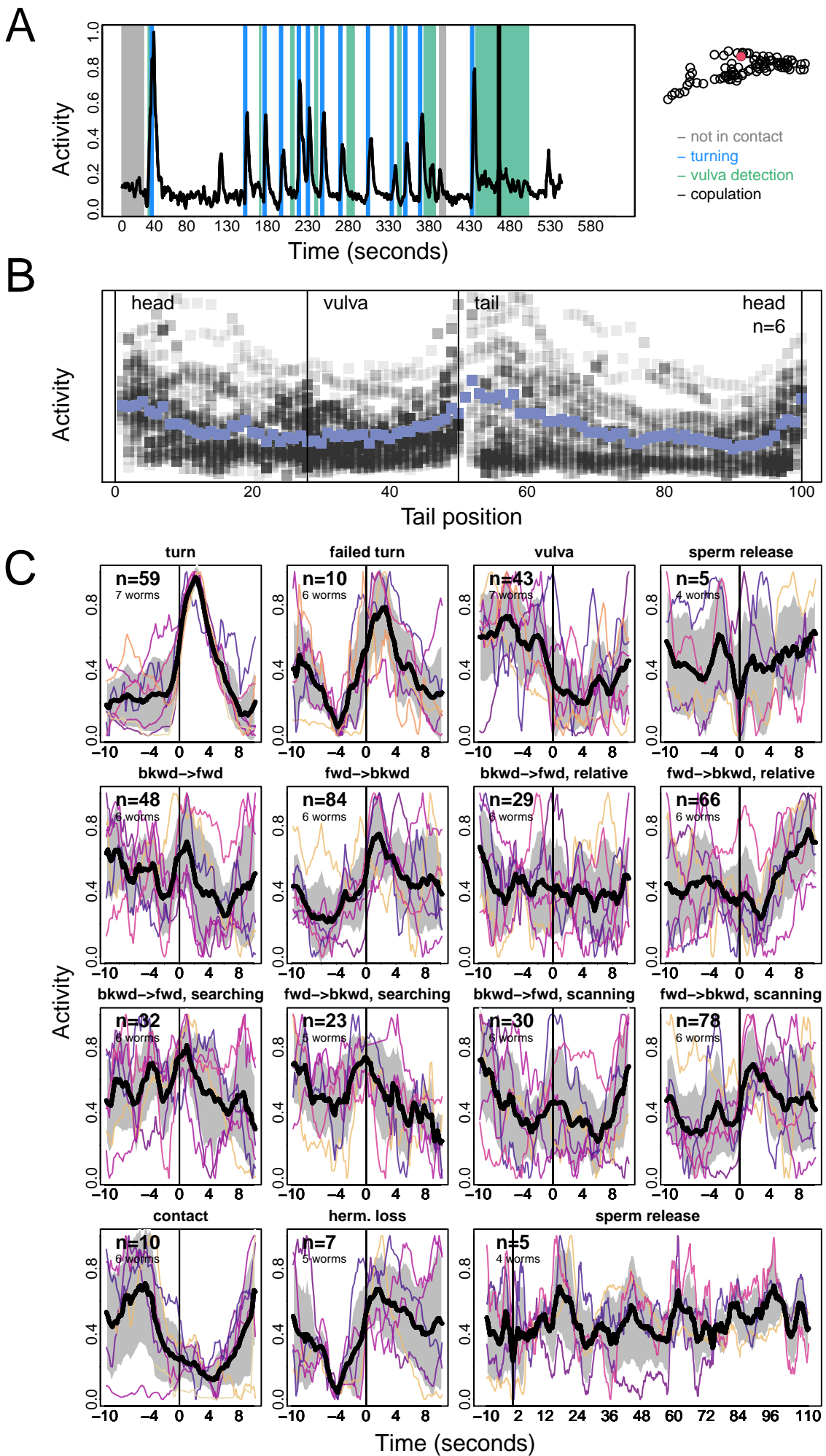
DVB



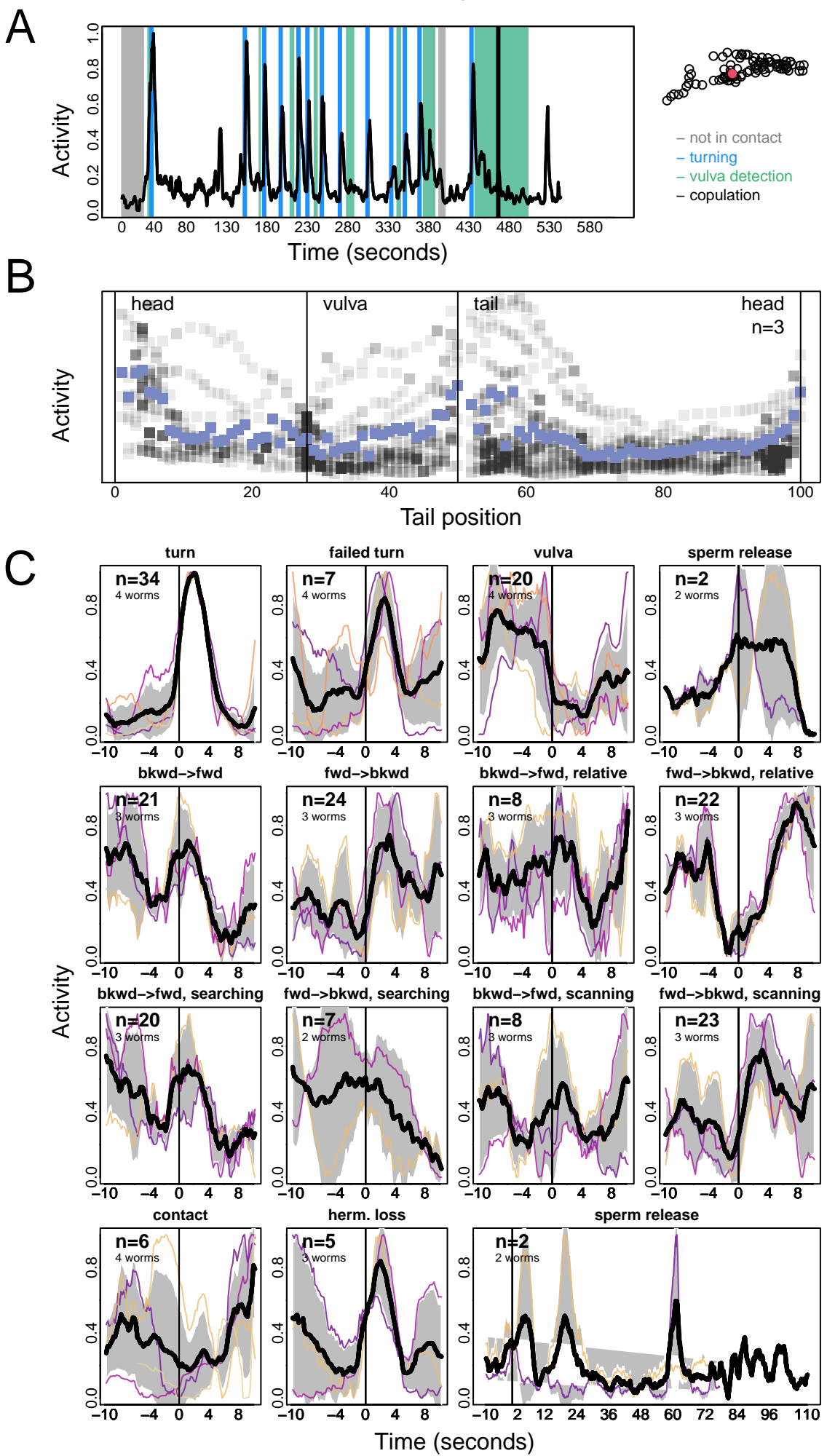
DX1



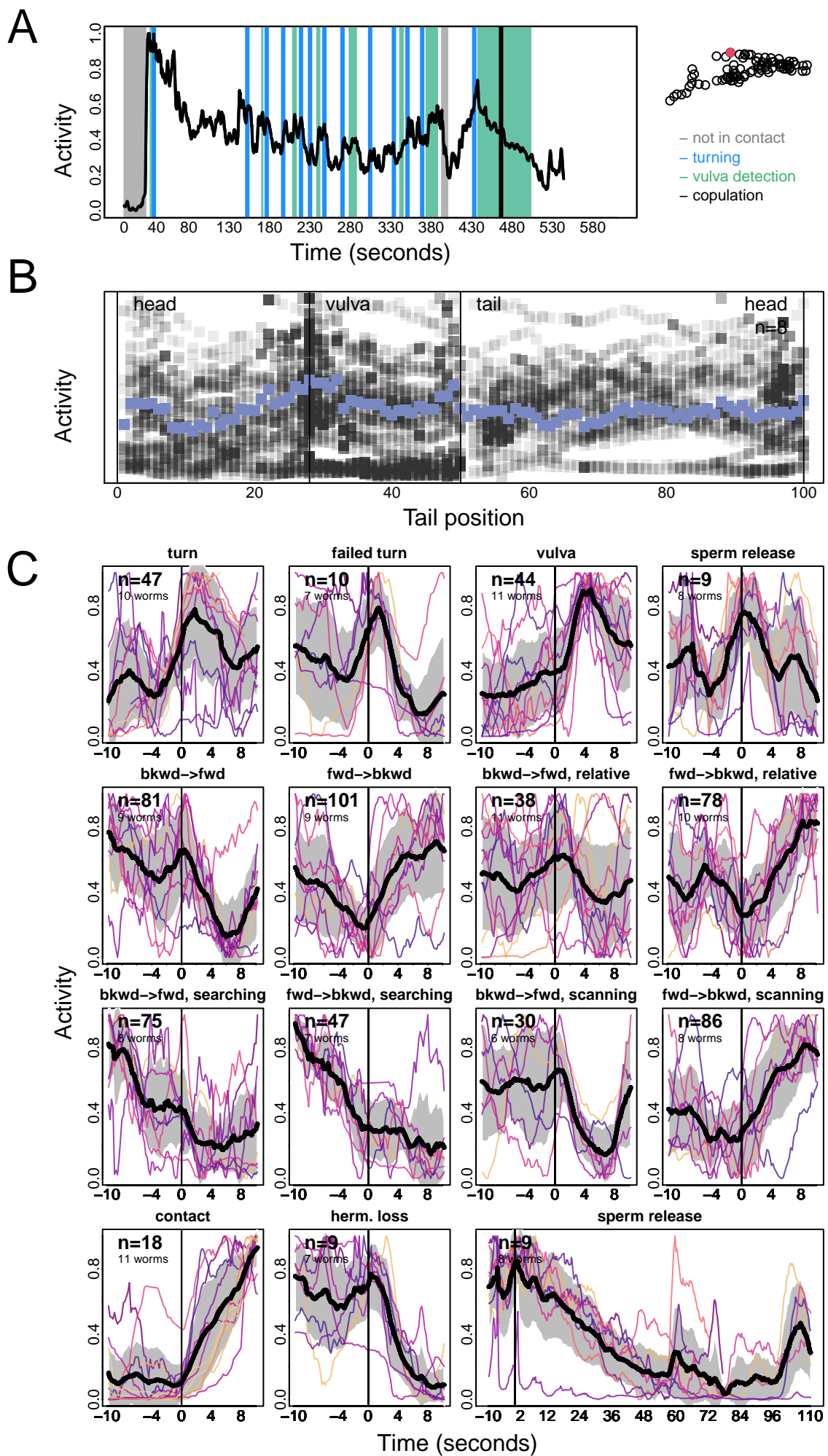
DX2



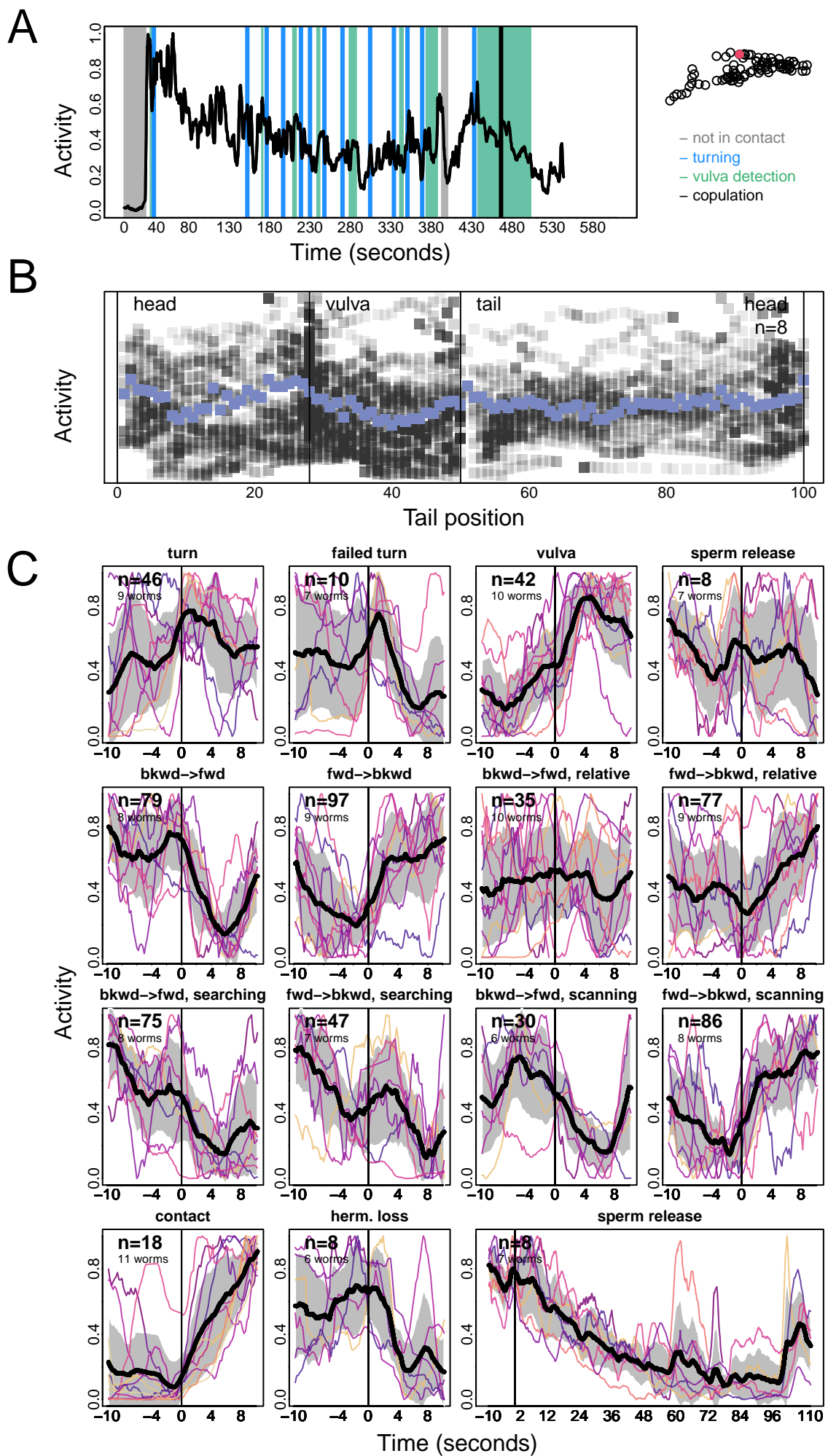
DX3



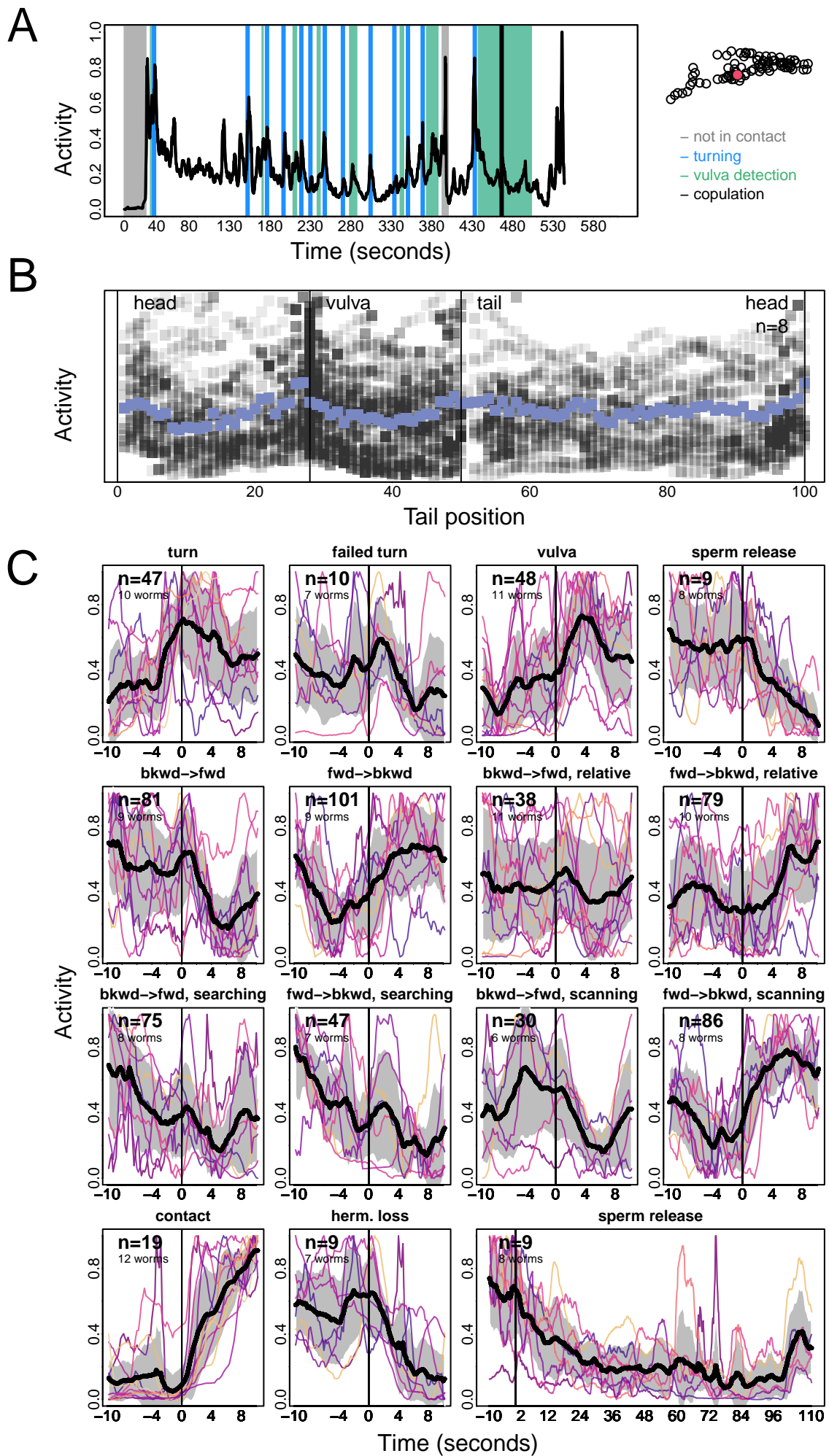
EF1



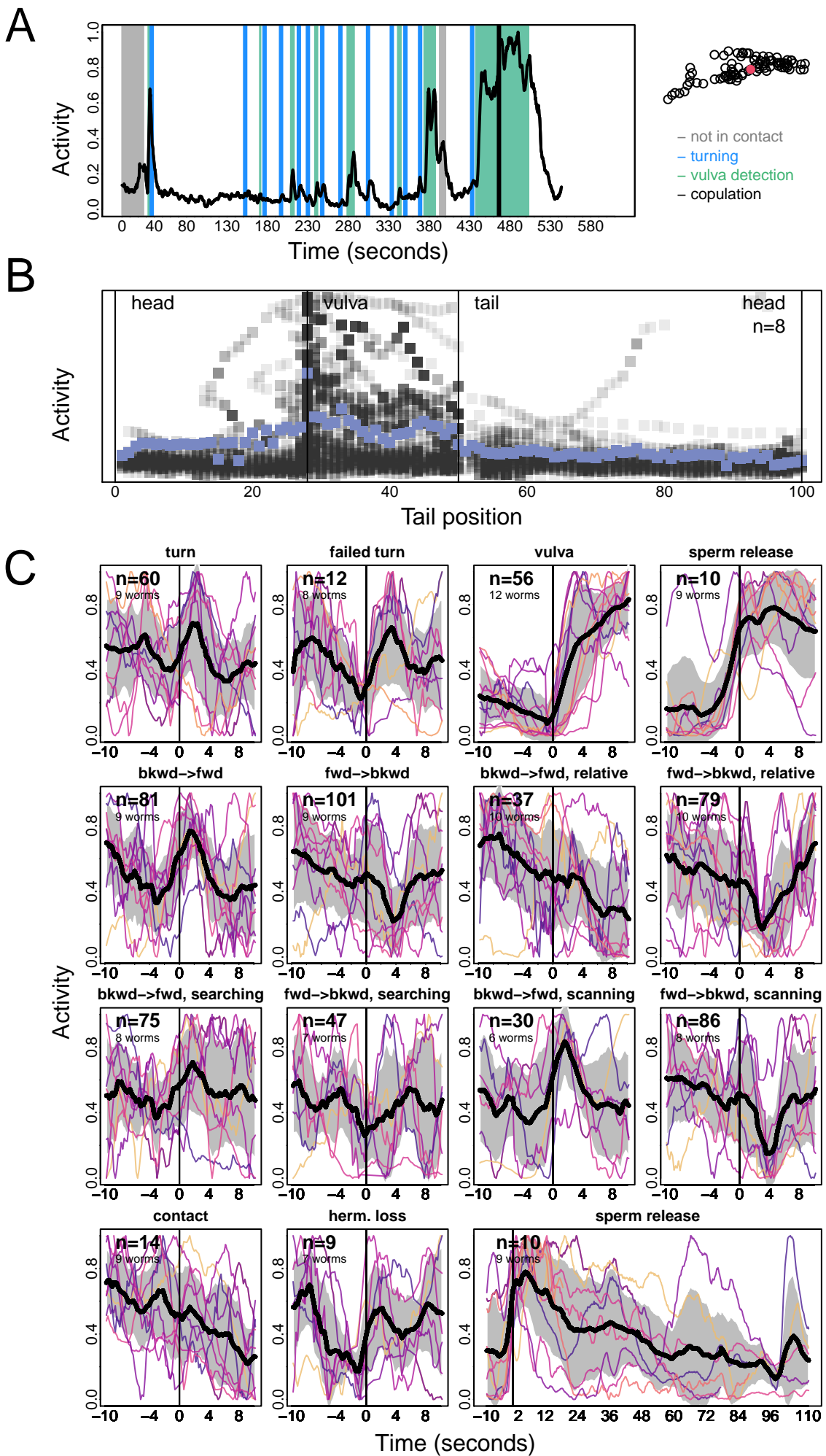
EF2



EF3

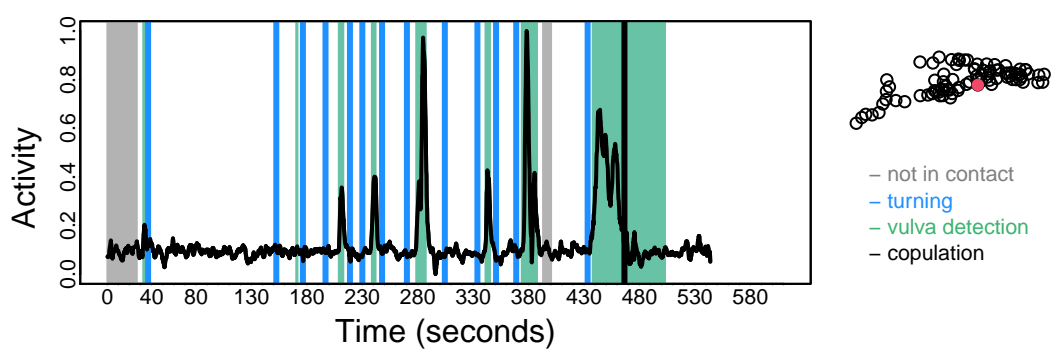


HOA

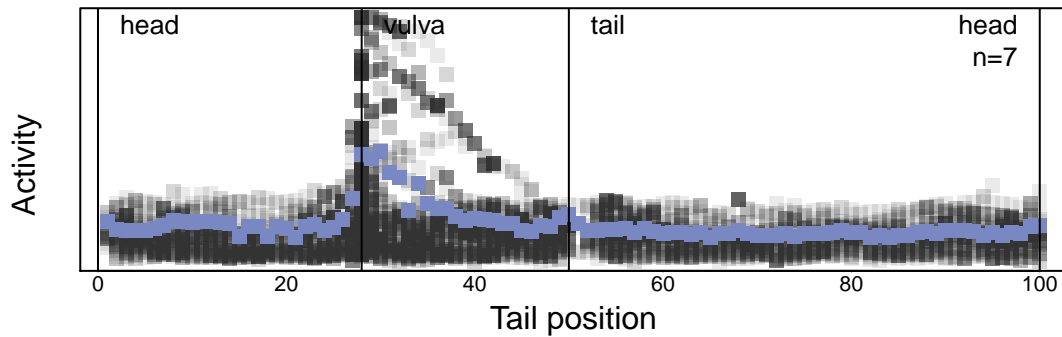


HOB

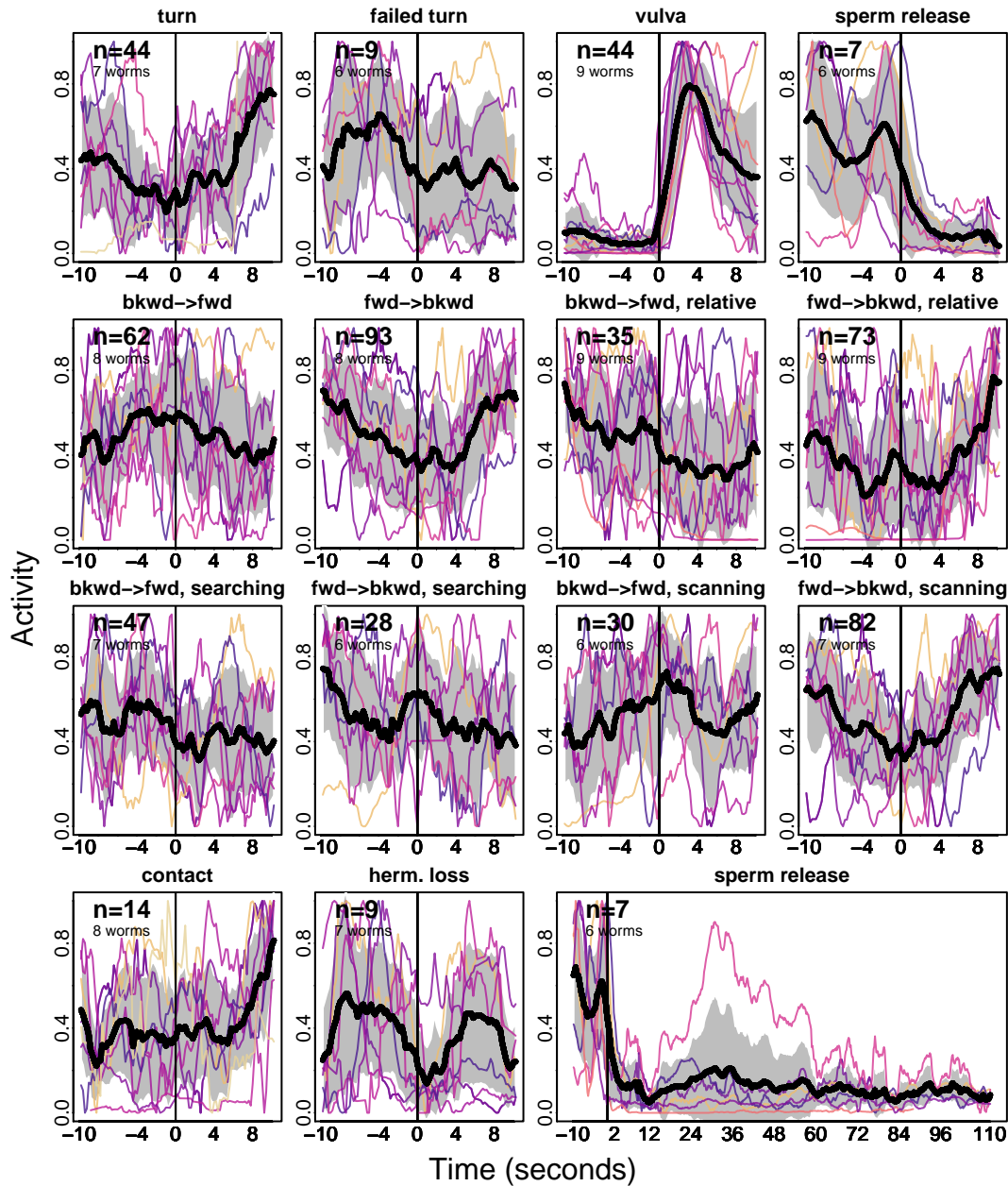
A



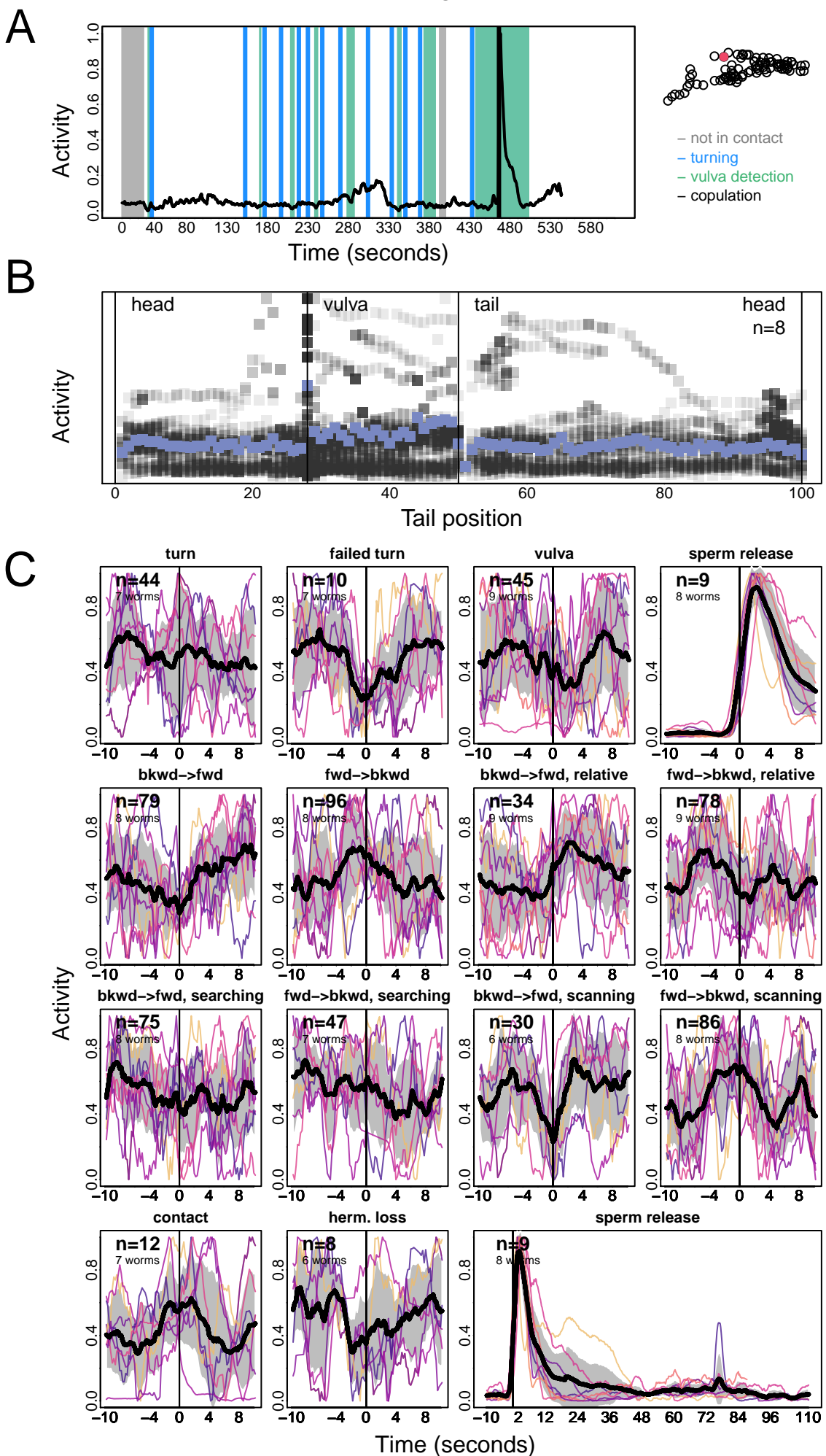
B



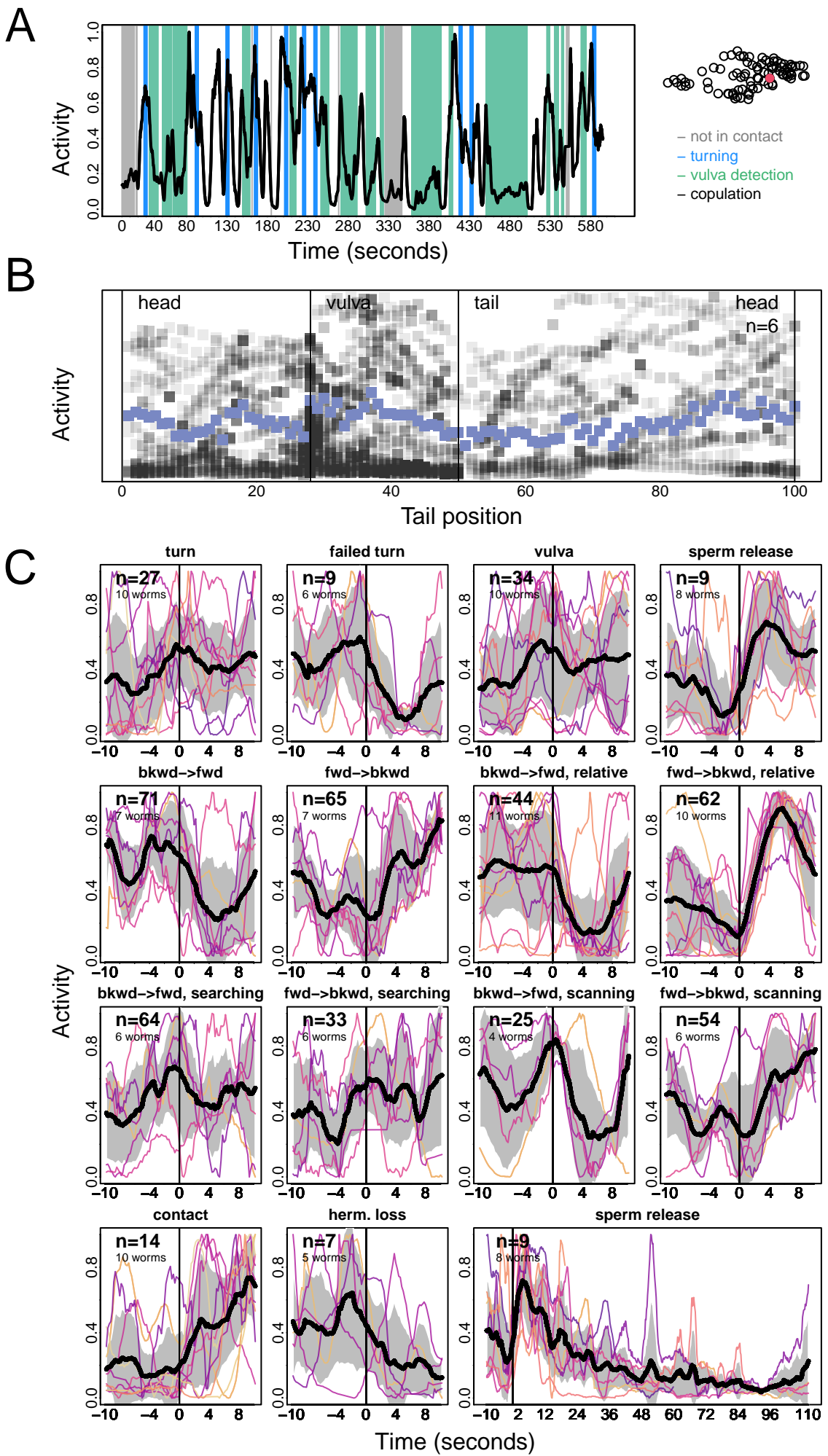
C



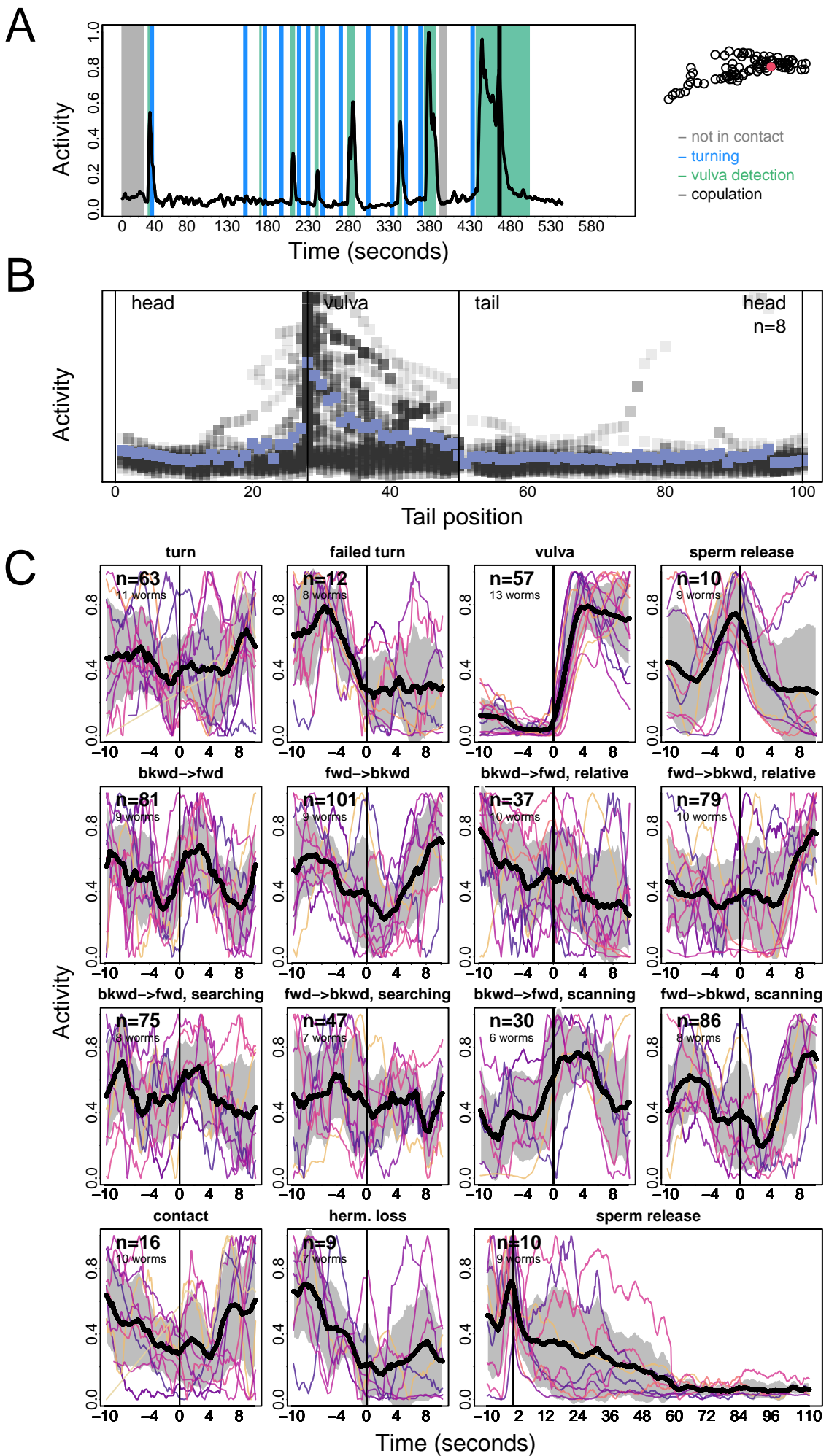
int9R



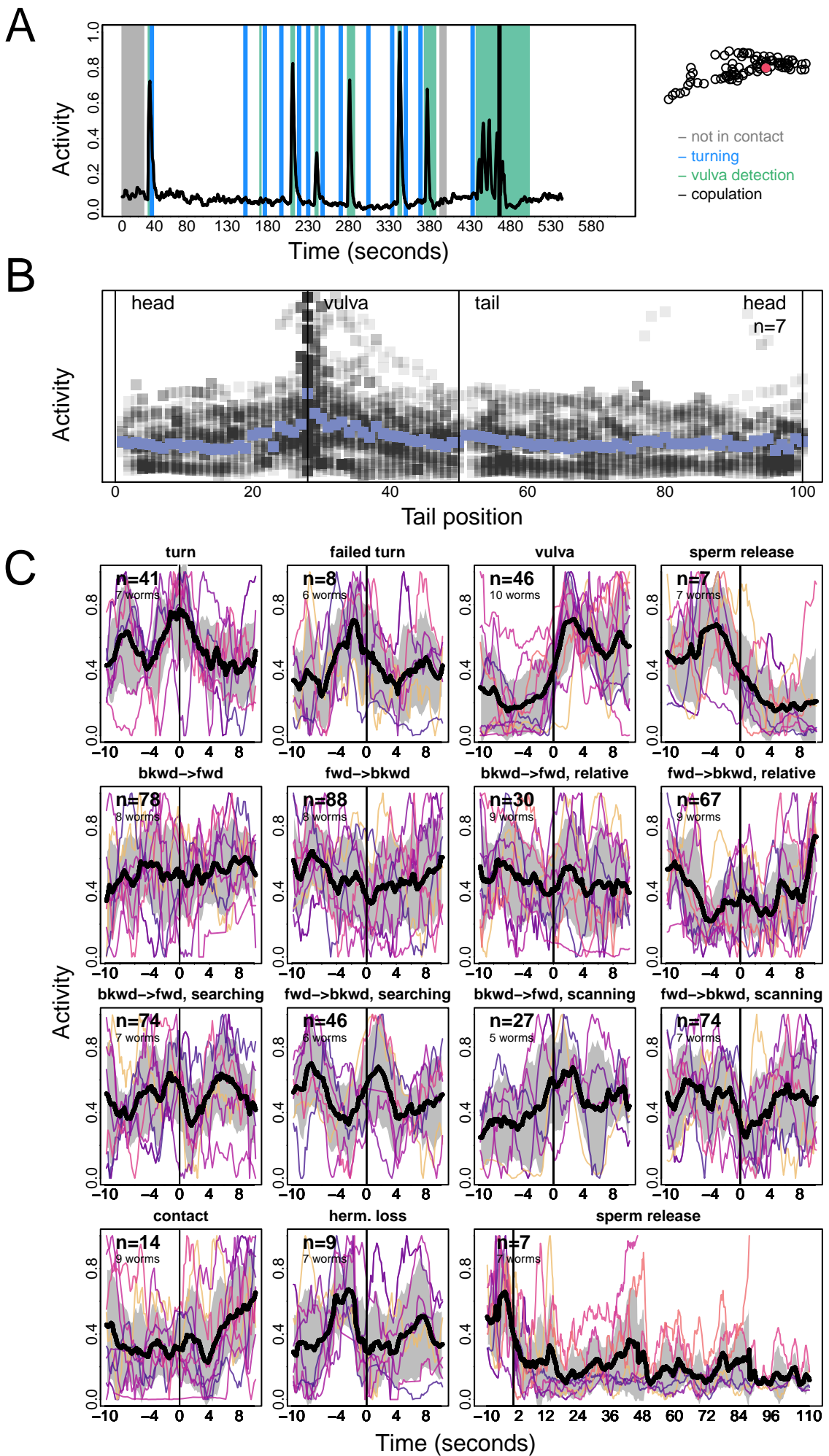
PCA



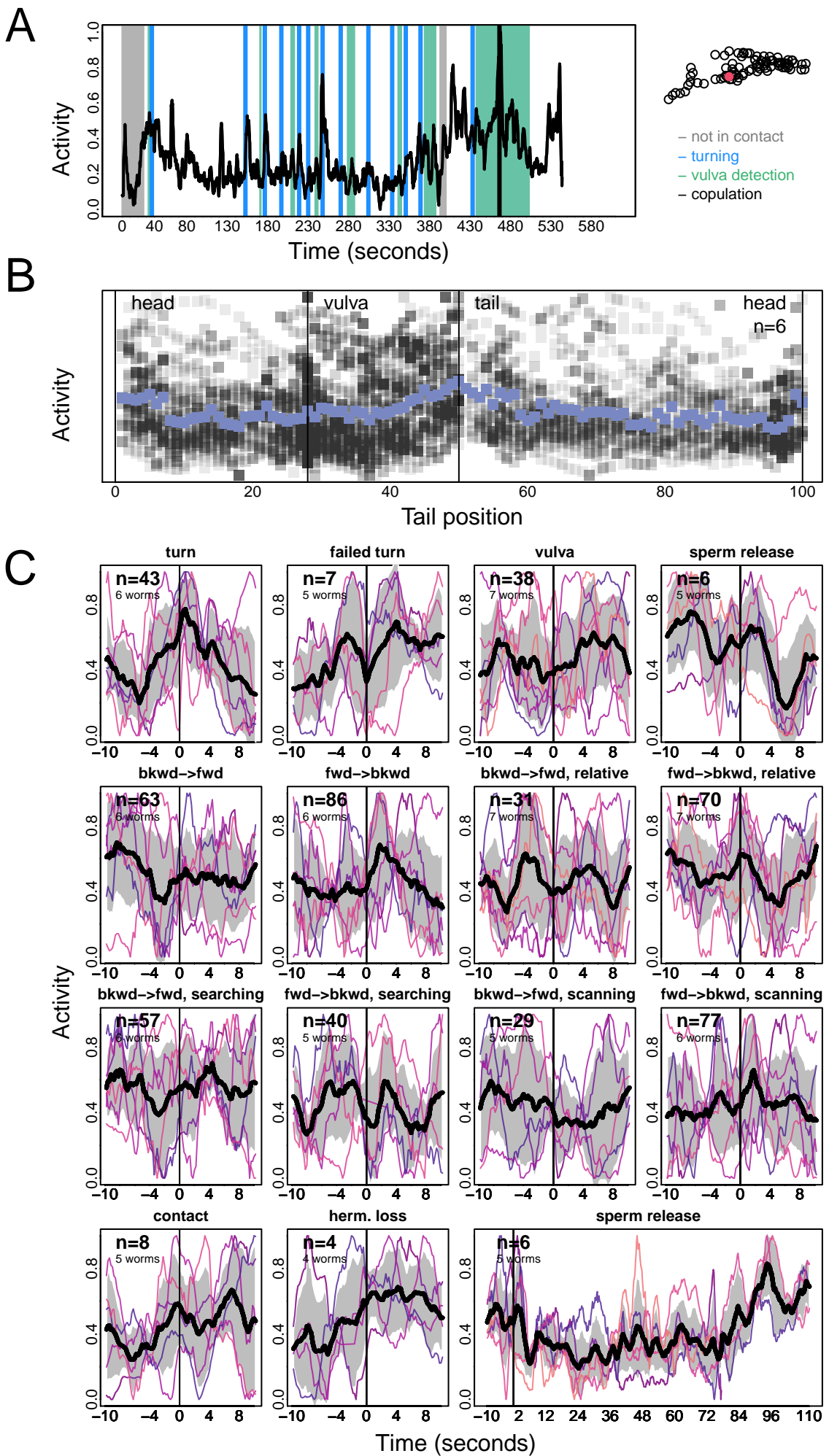
PCB



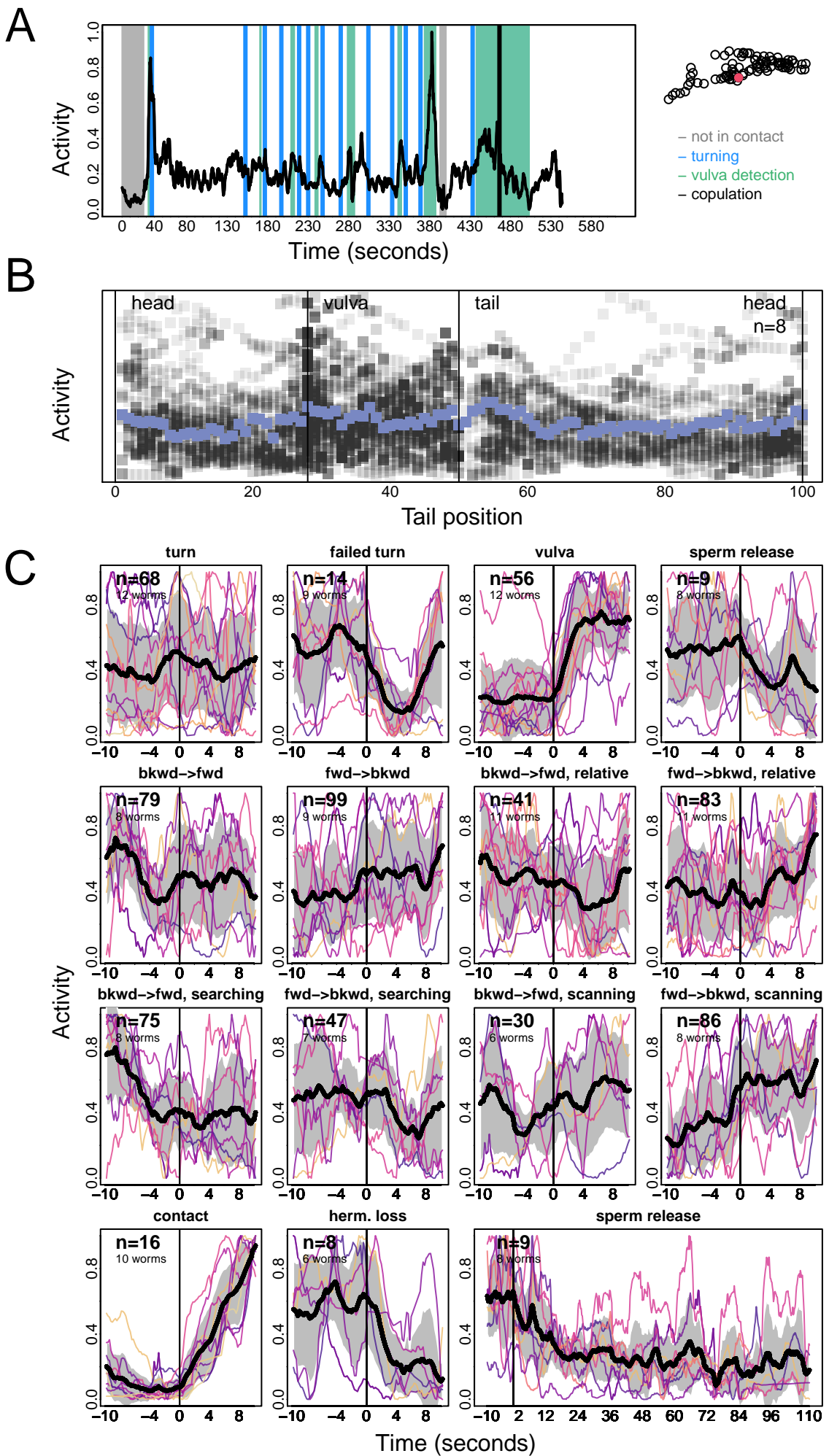
PCC



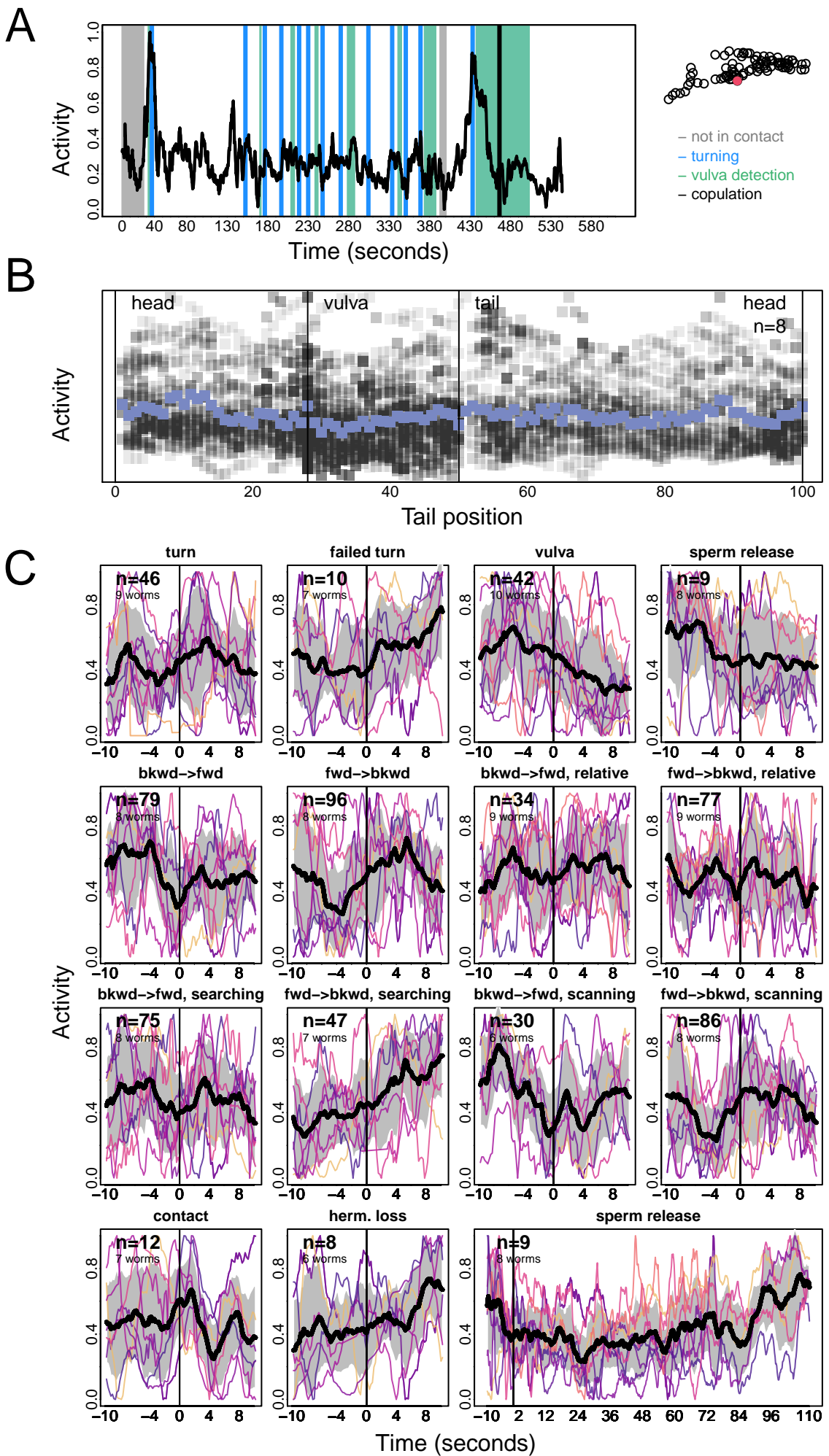
PDA



PDB

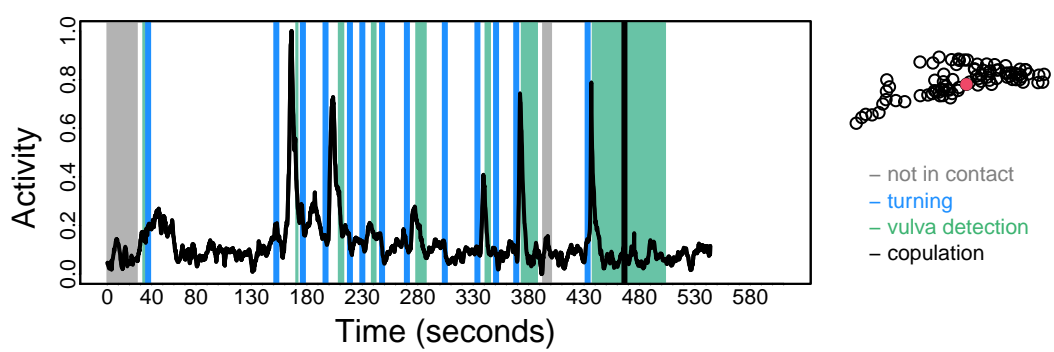


PDC

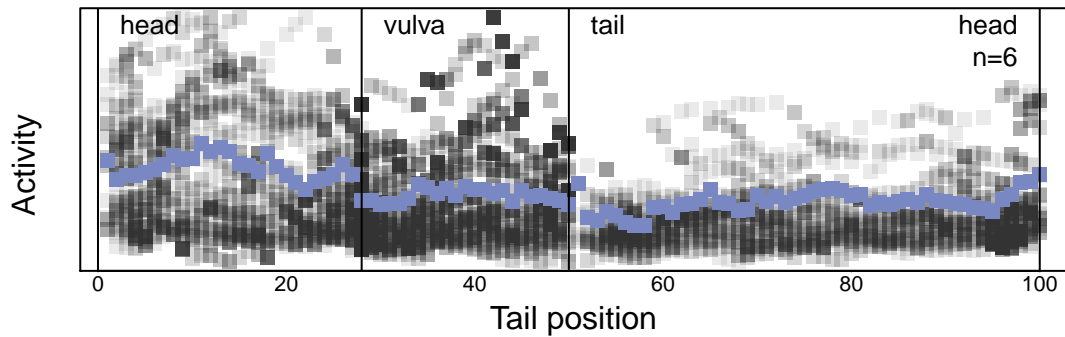


PGA

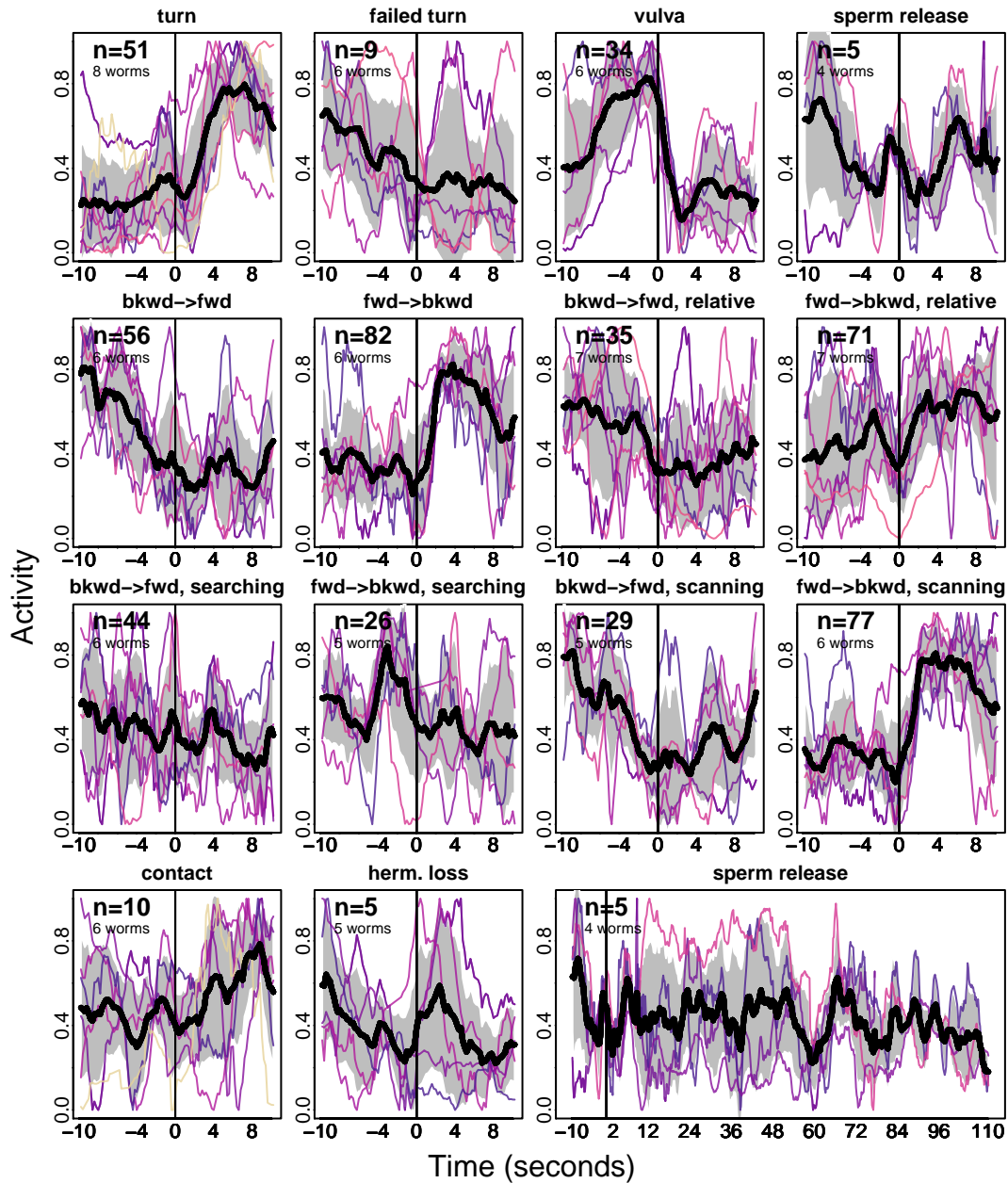
A



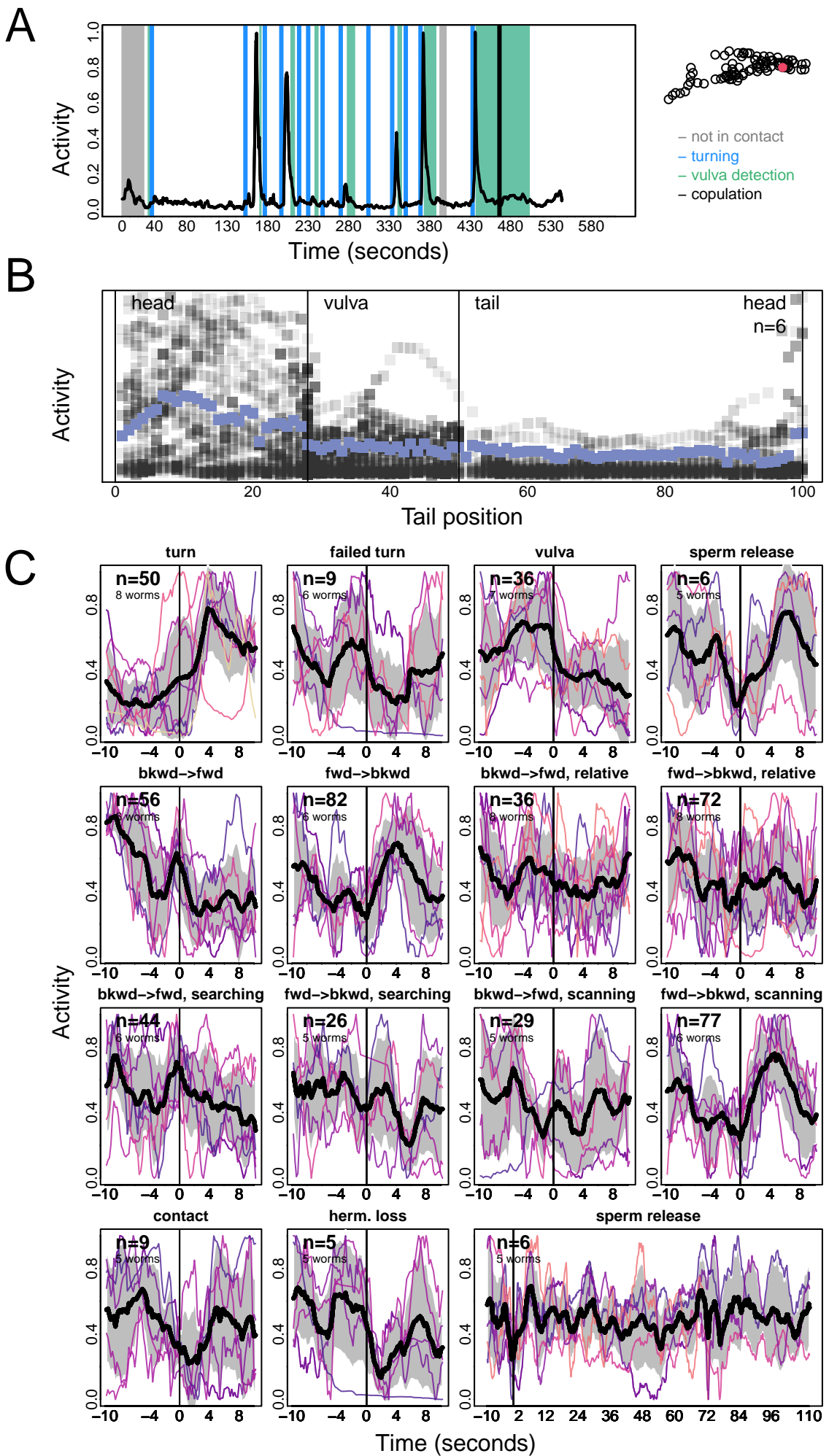
B



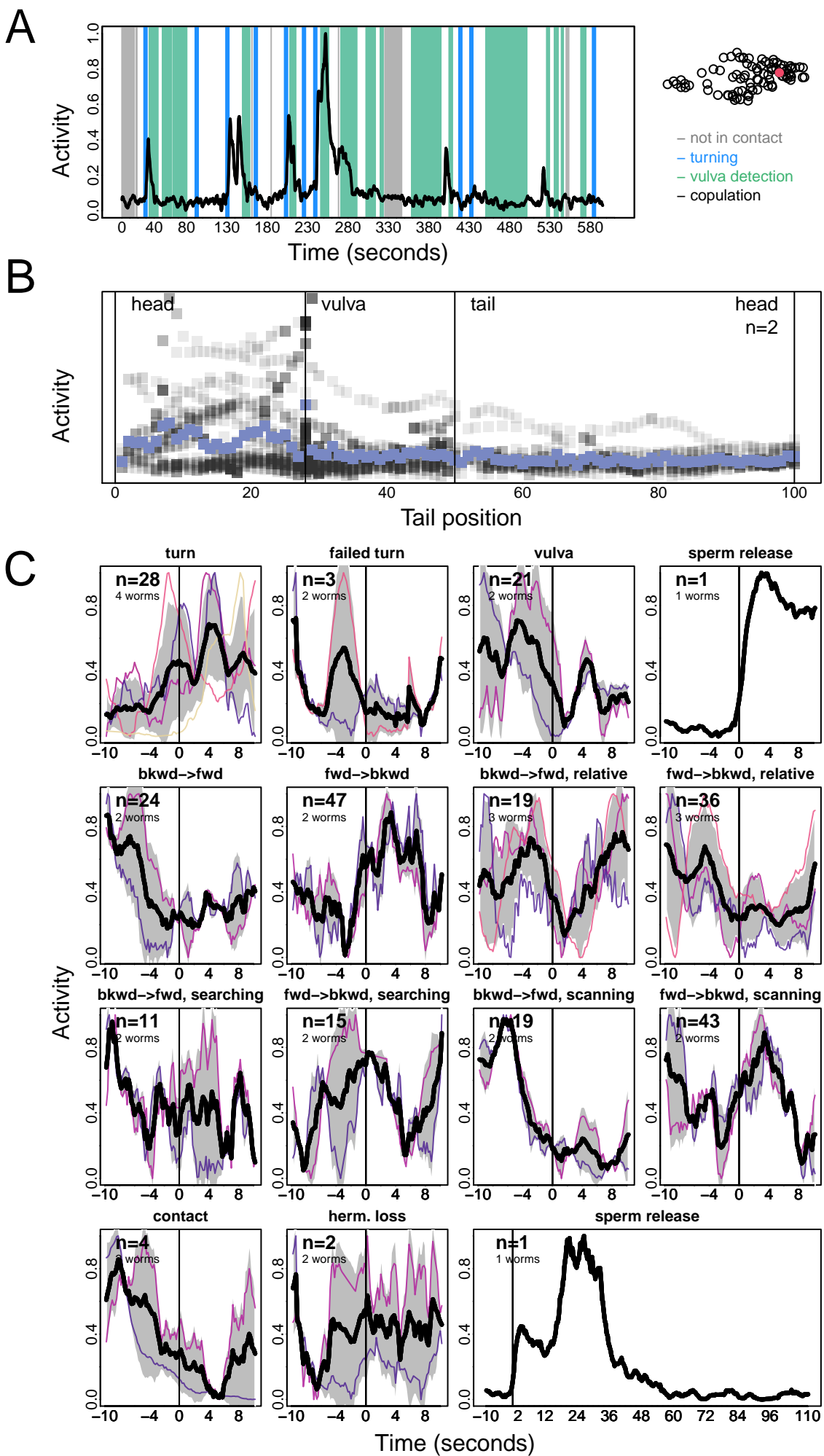
C



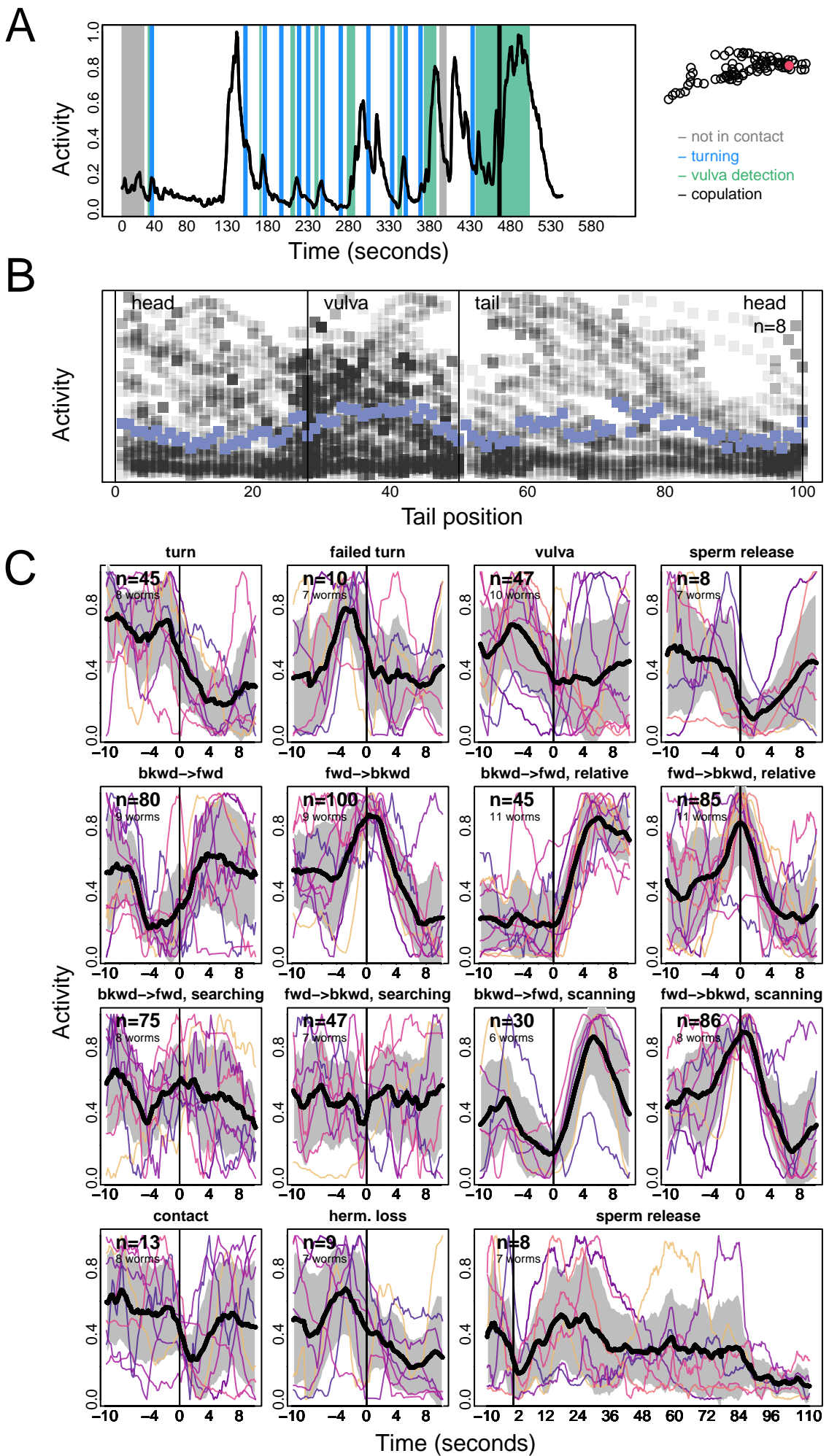
PHA



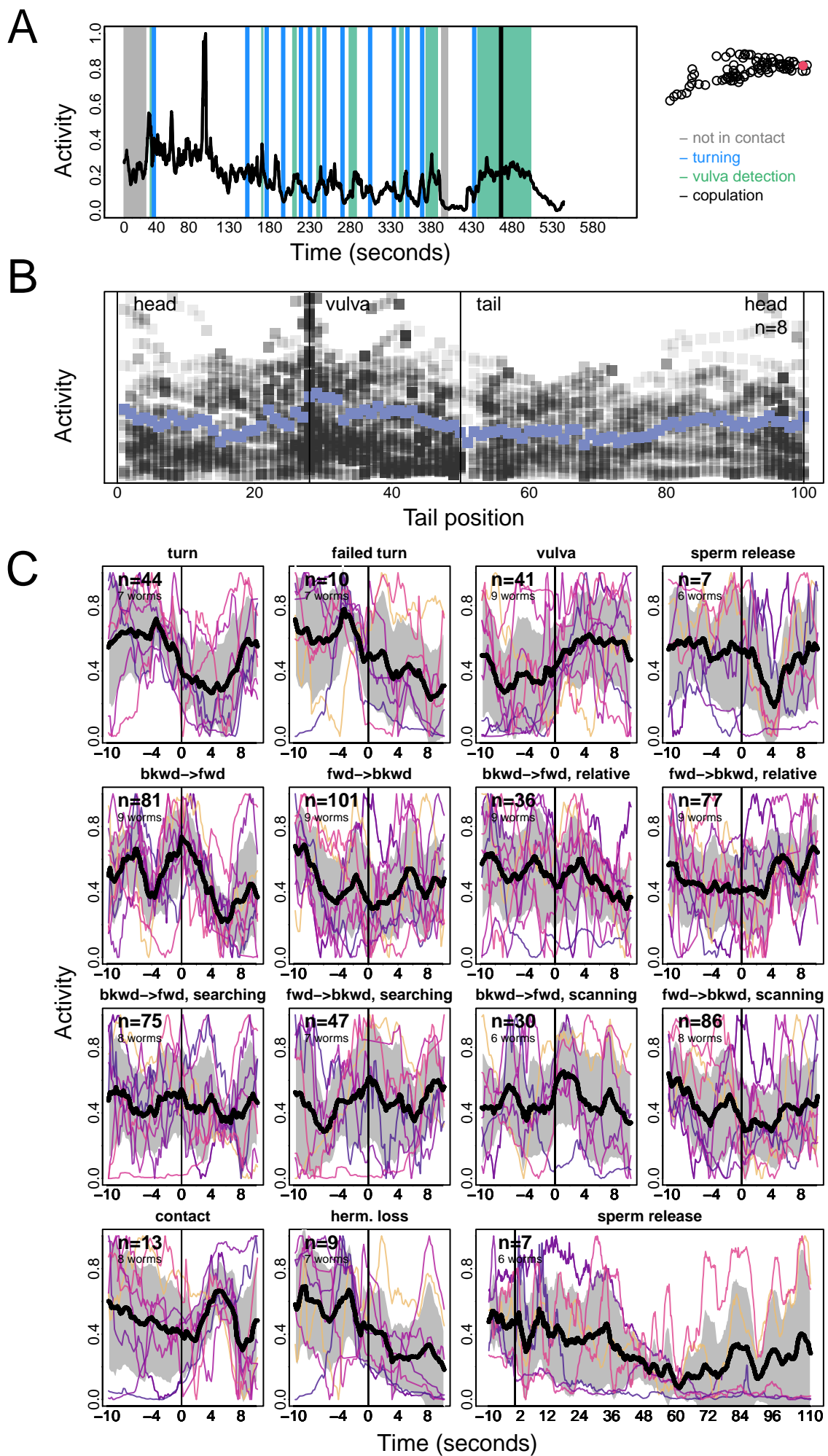
PHB



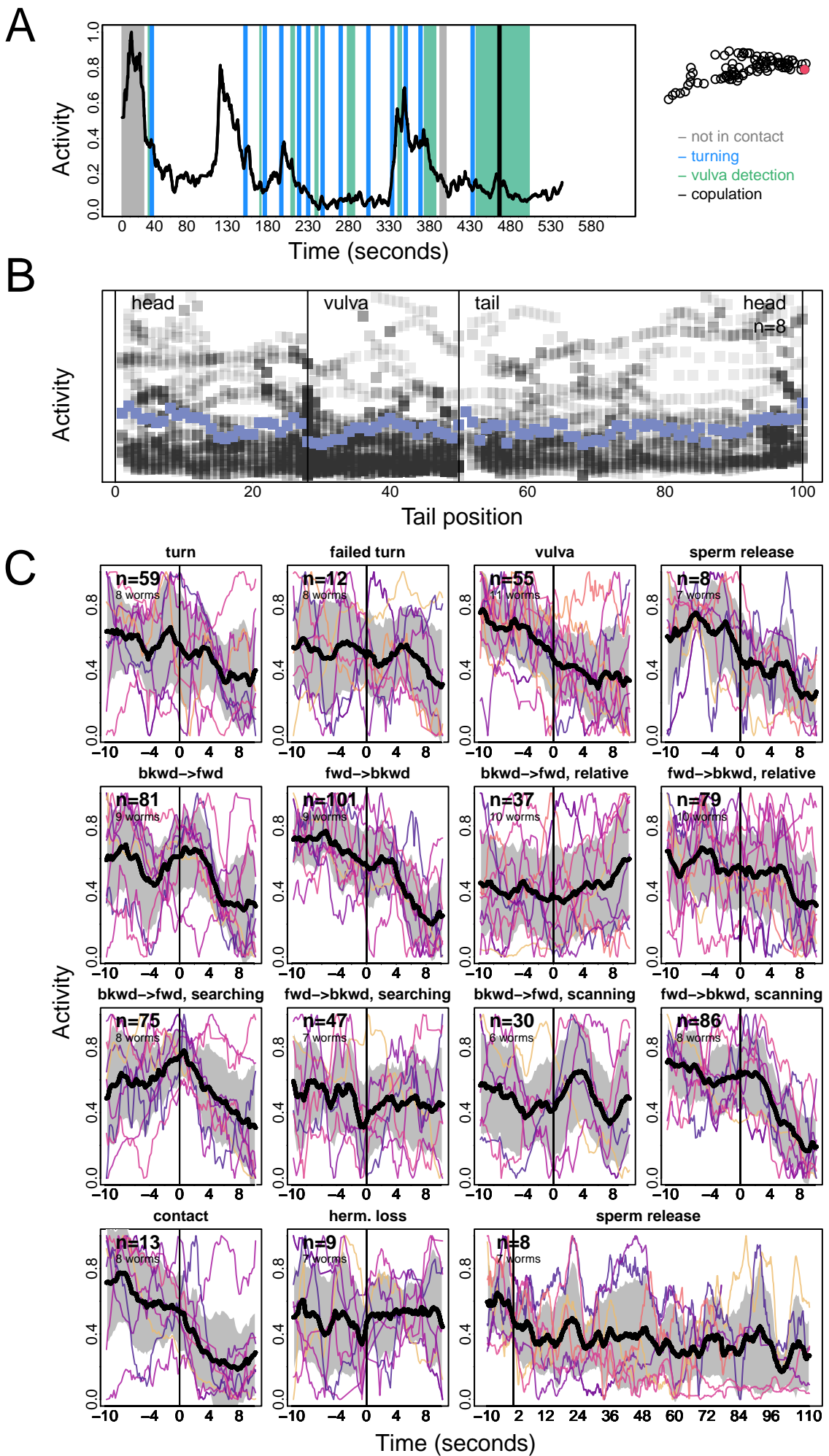
PHC



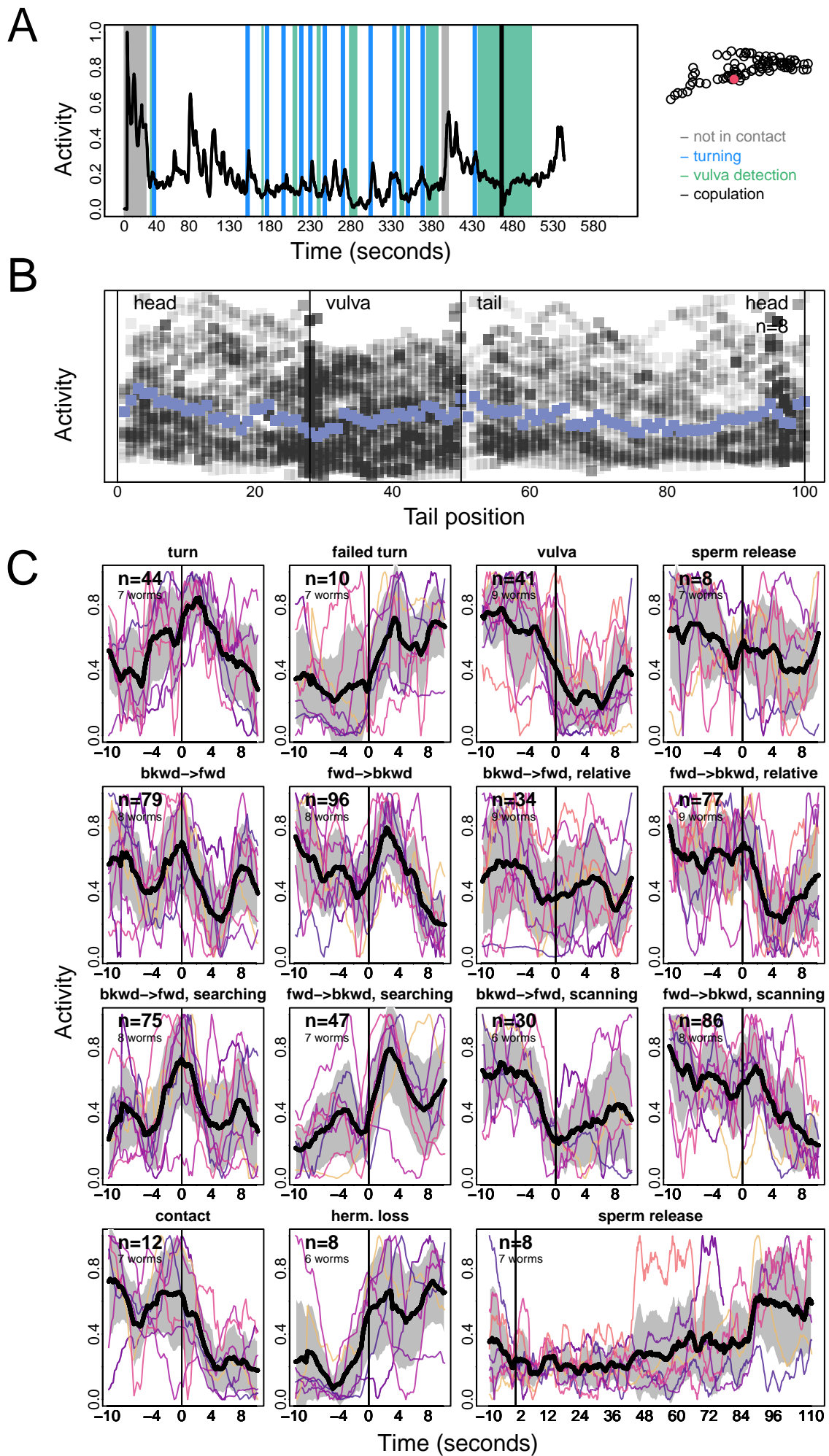
PHD



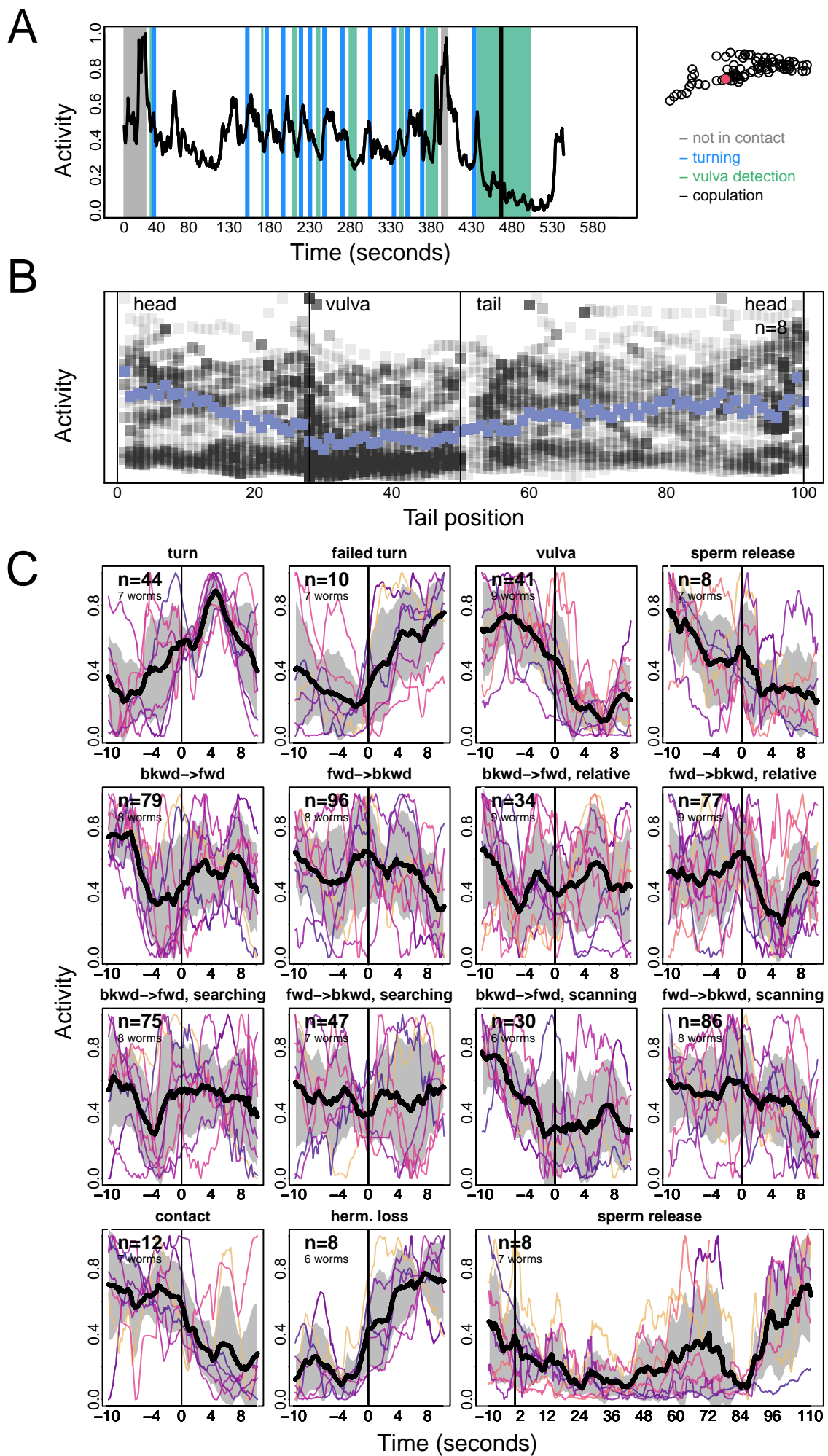
PLM



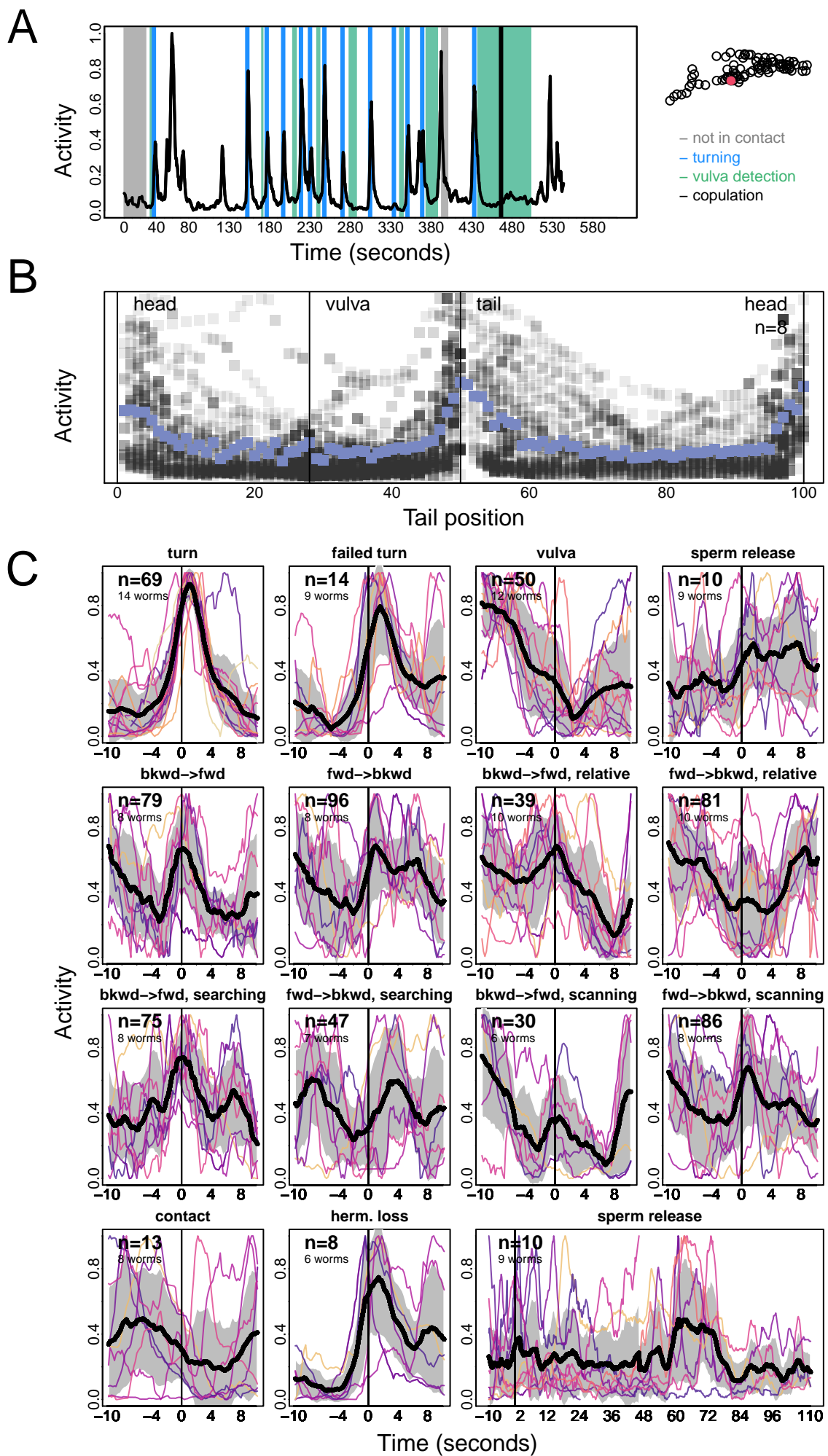
PVPR



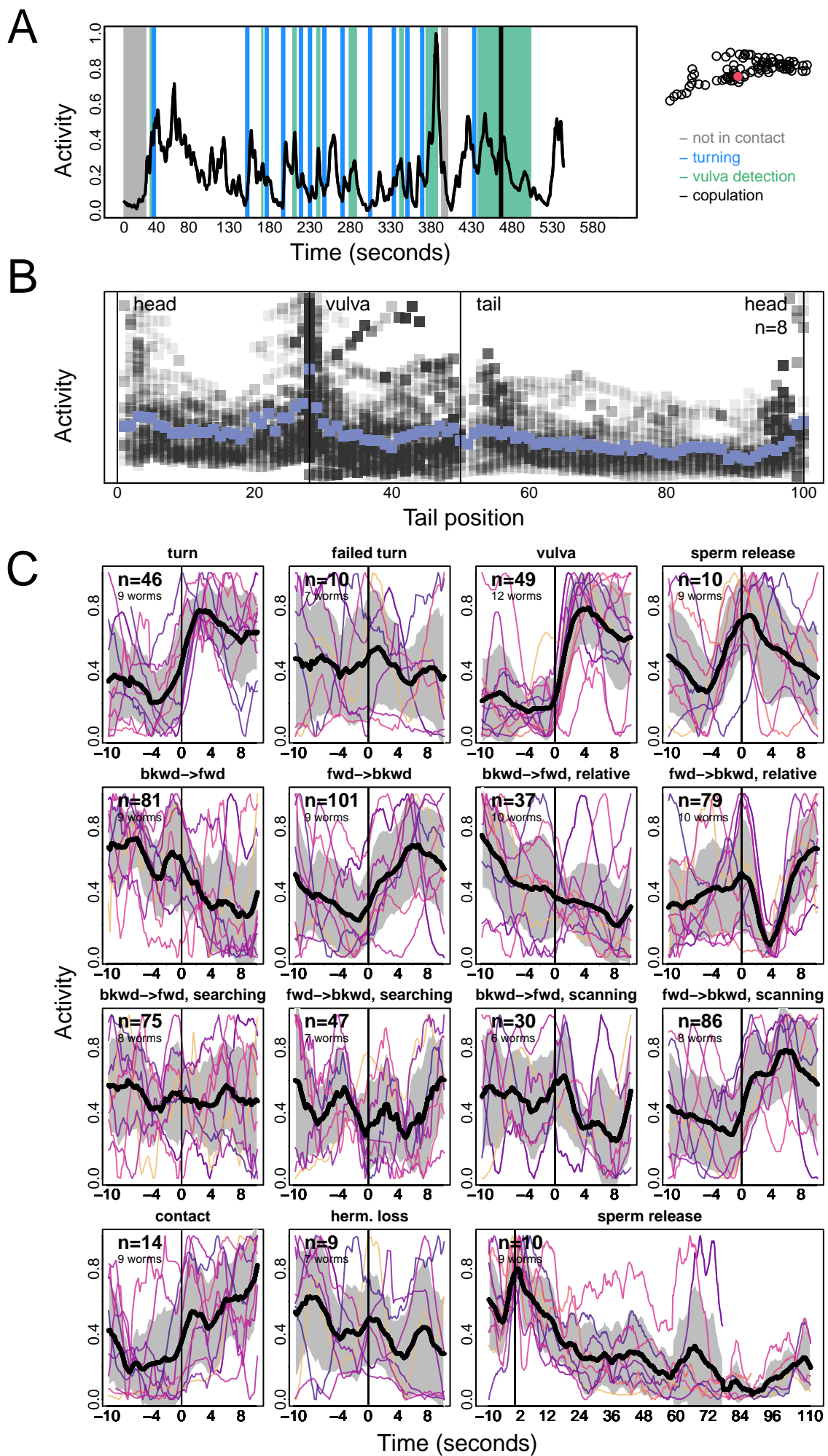
PVT



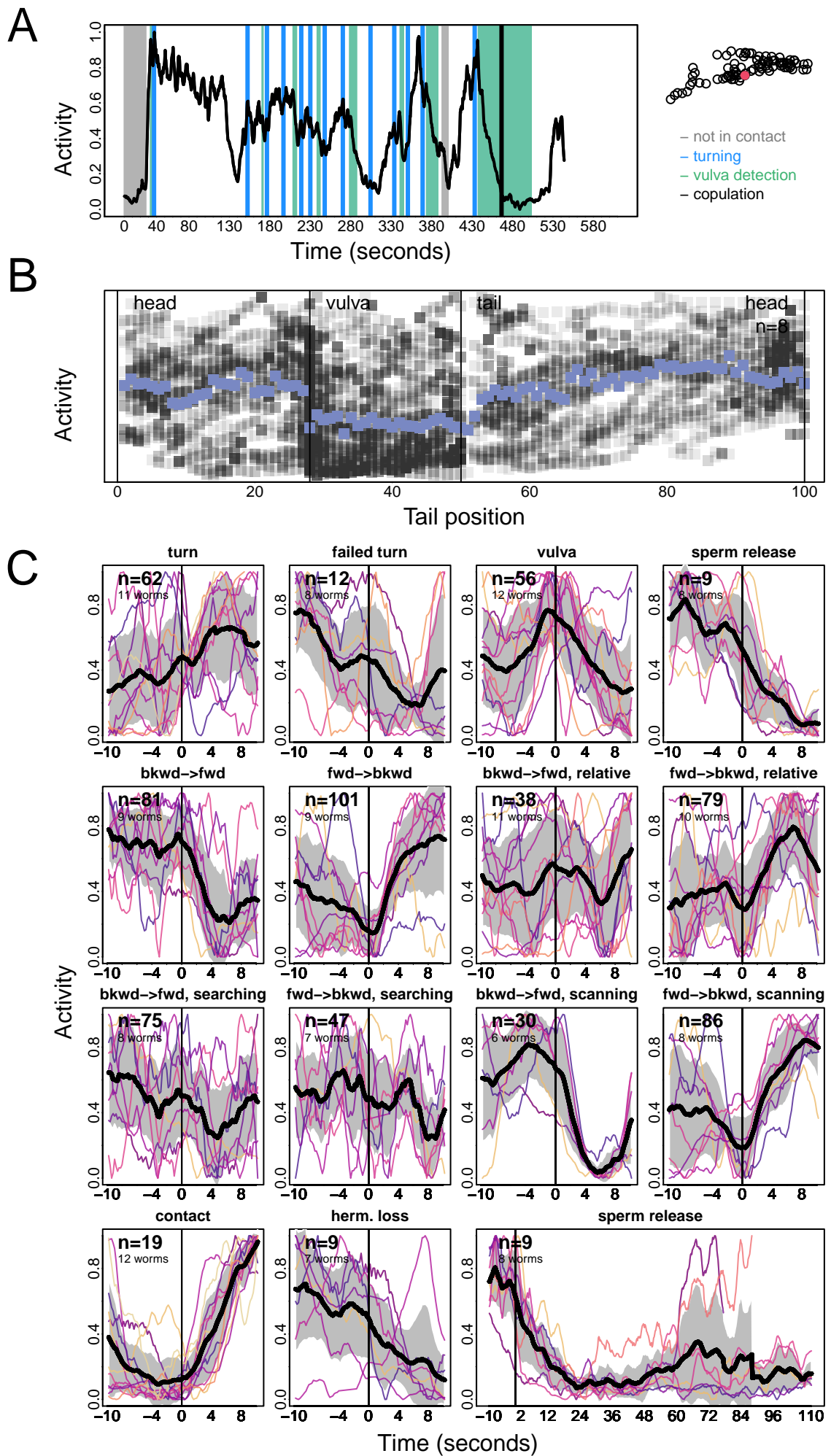
PVV



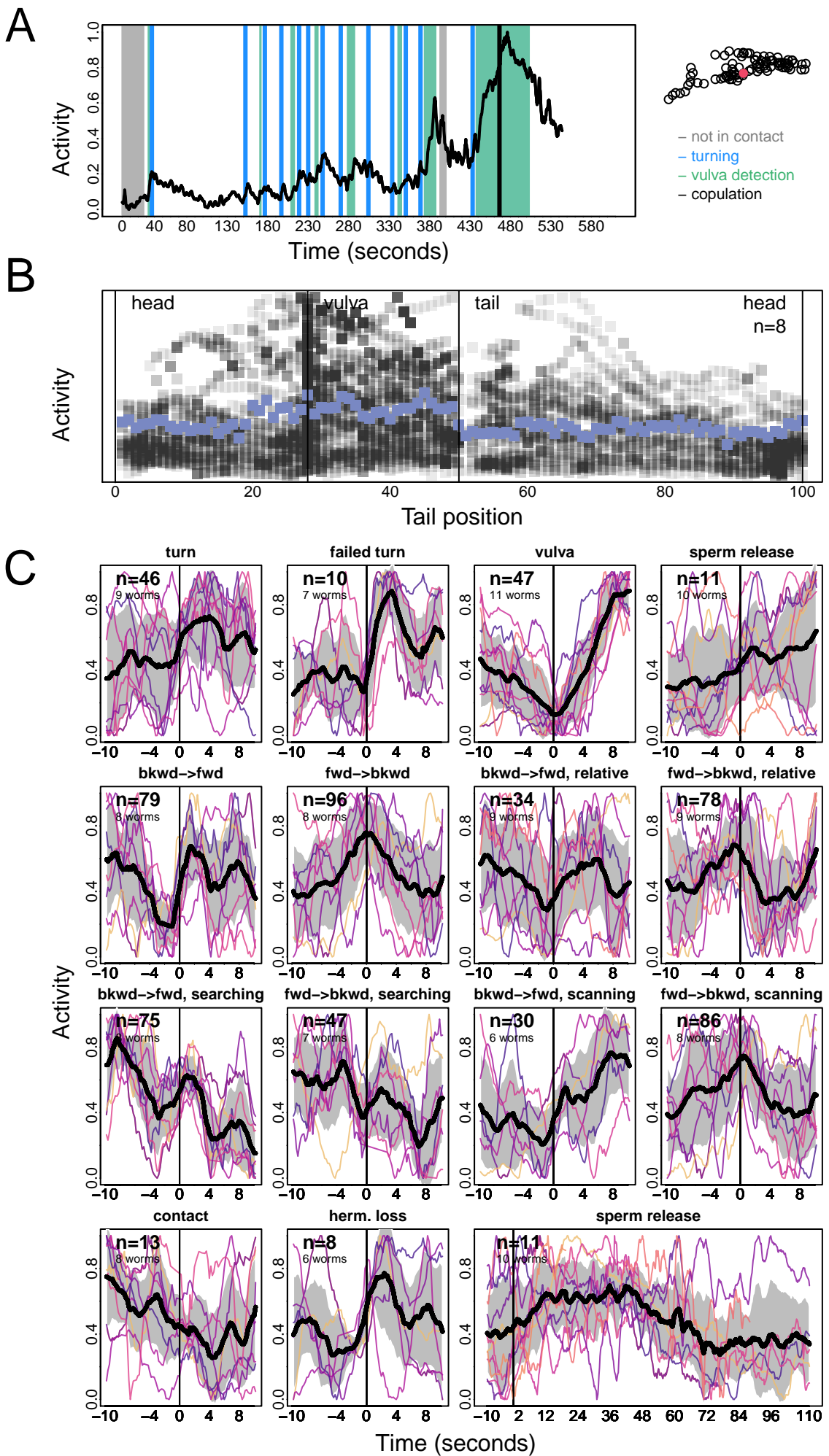
PVX



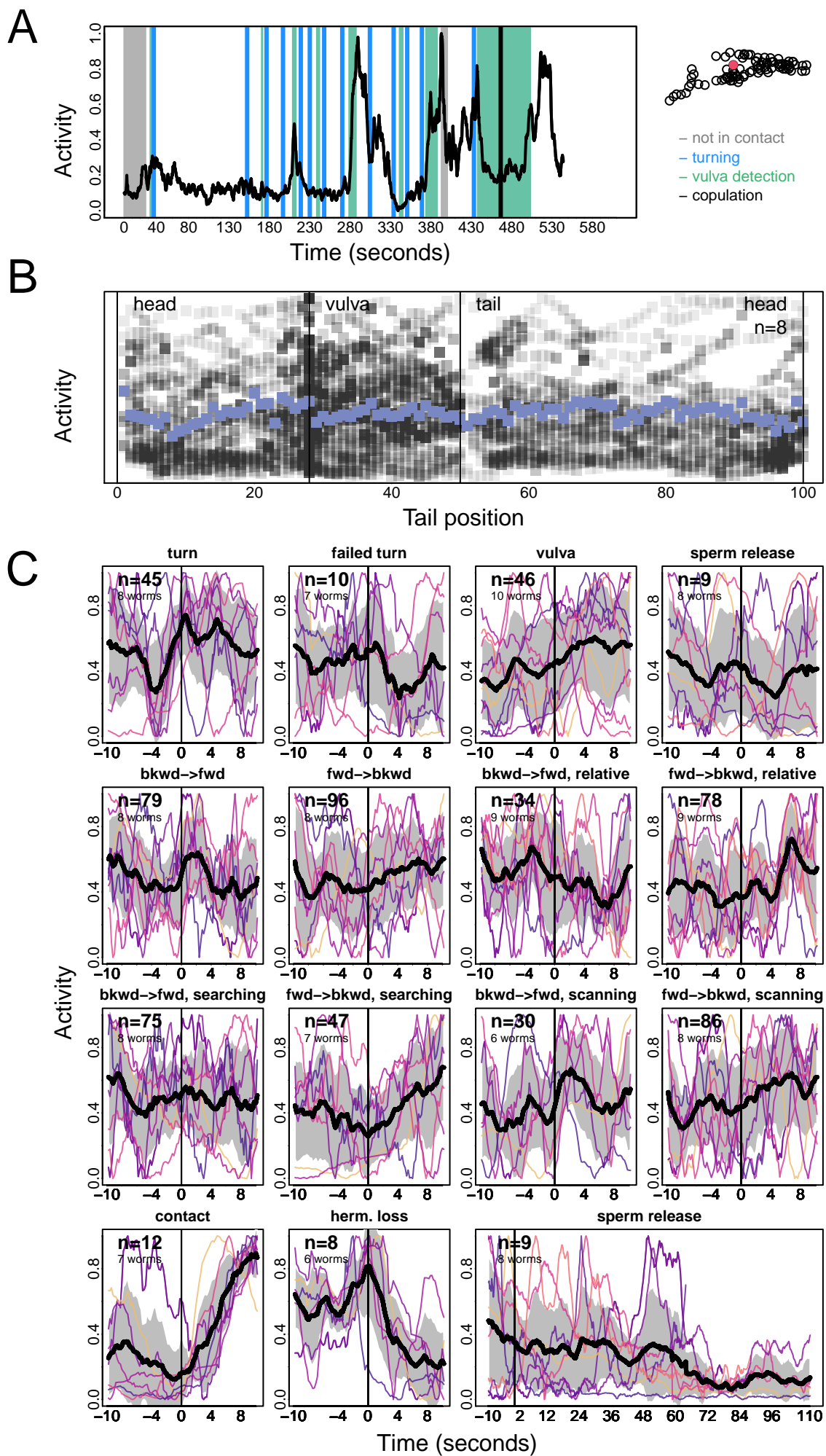
PVY



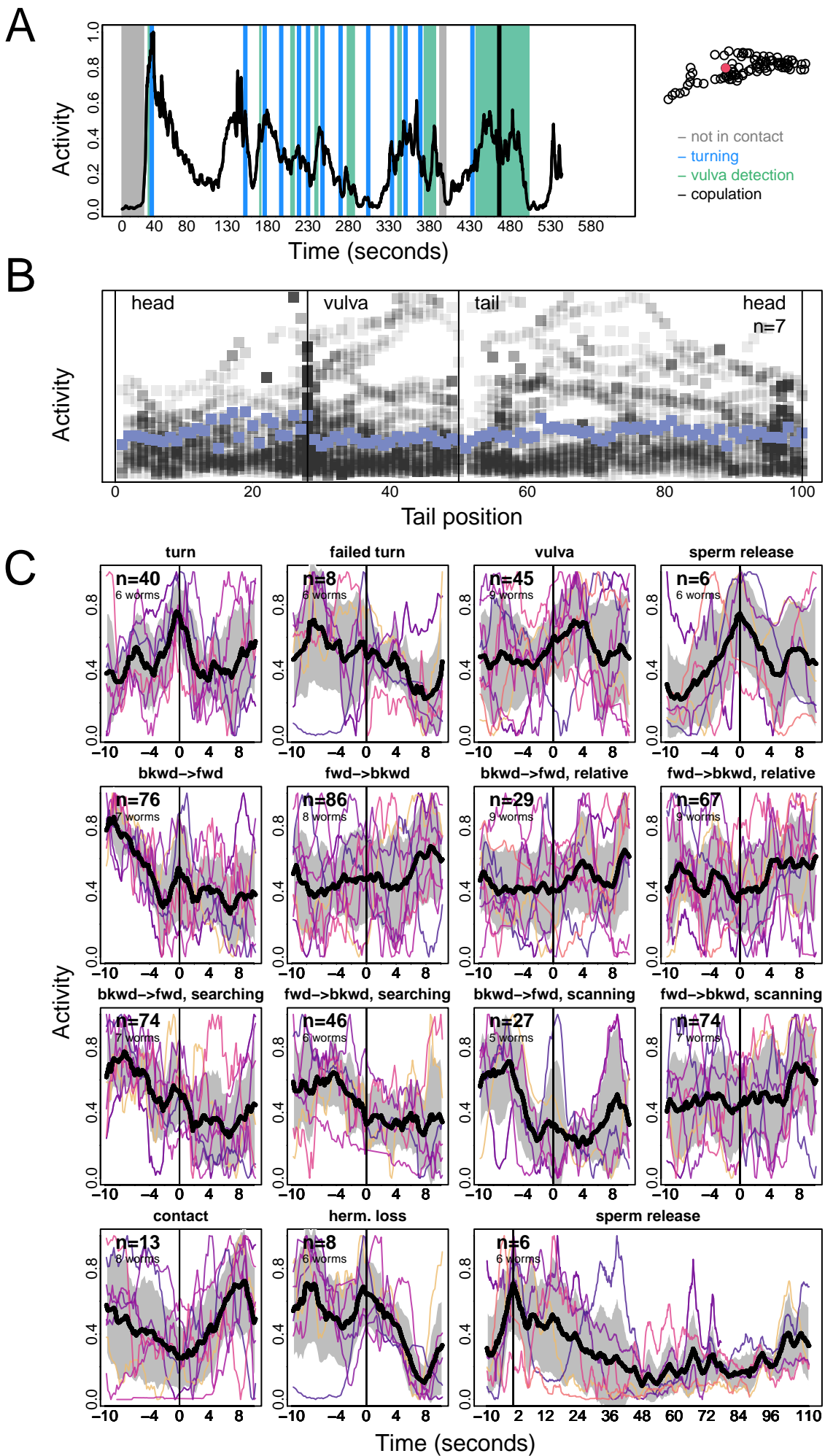
PVZ



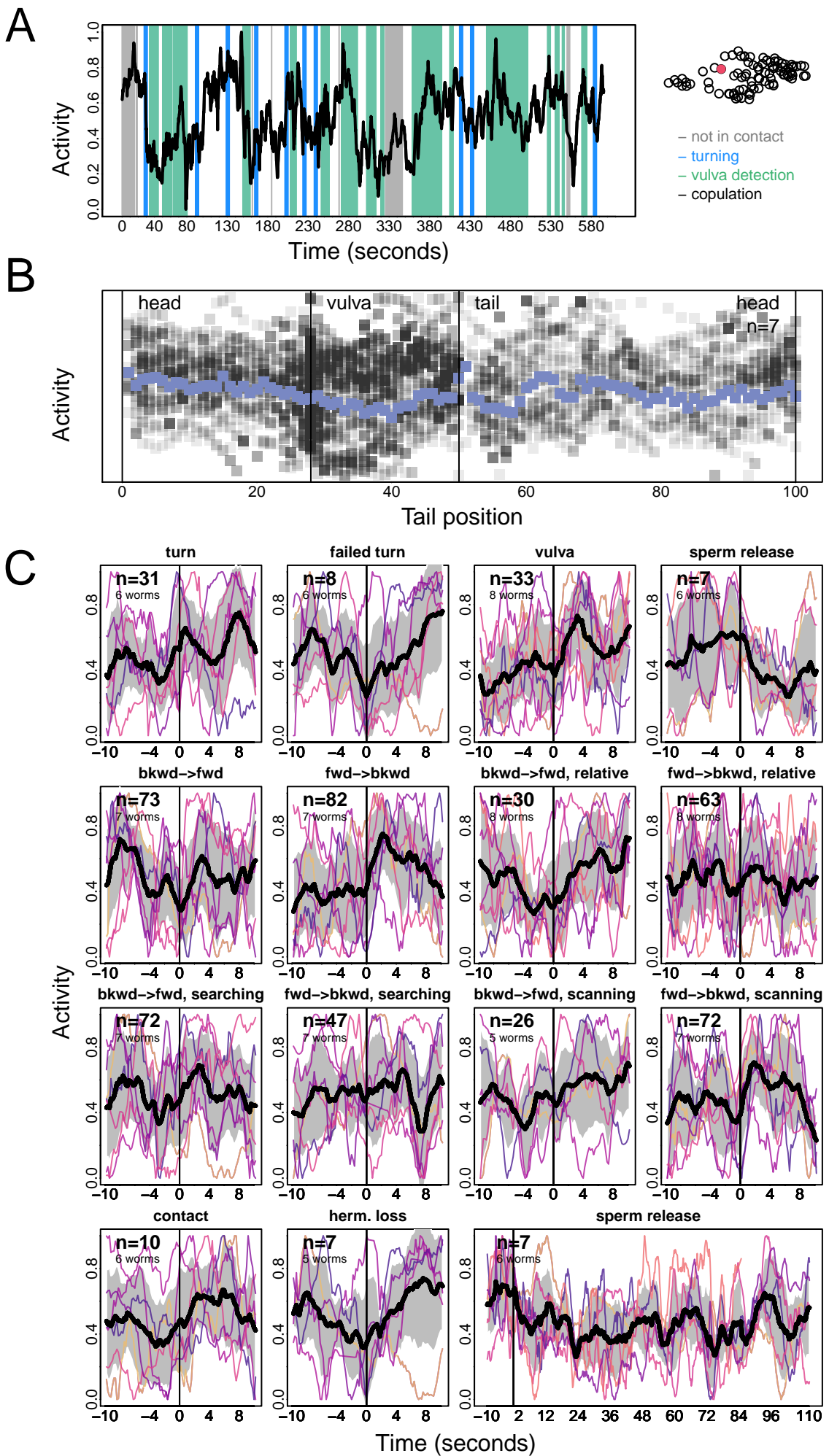
R1A



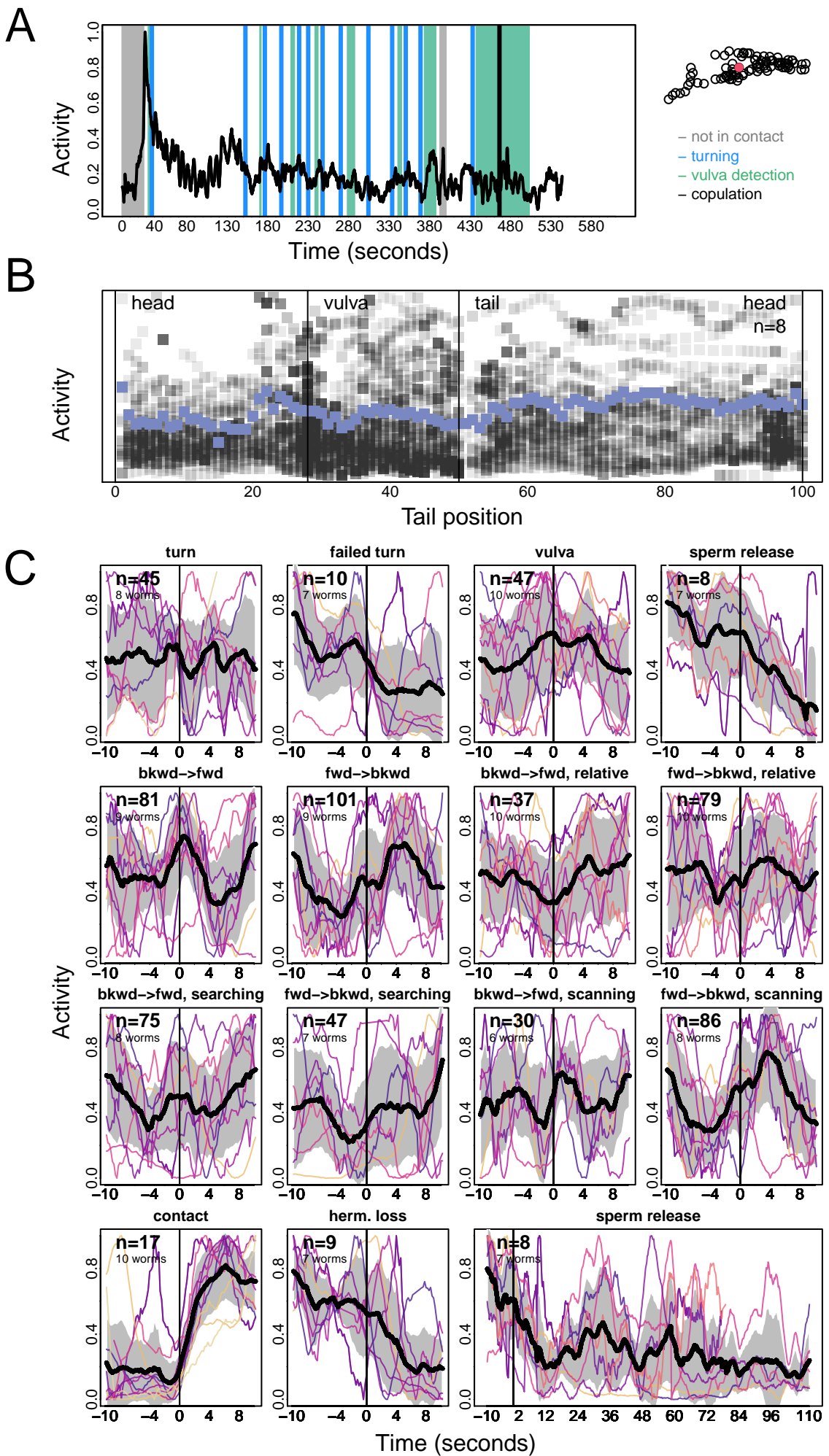
R1AR



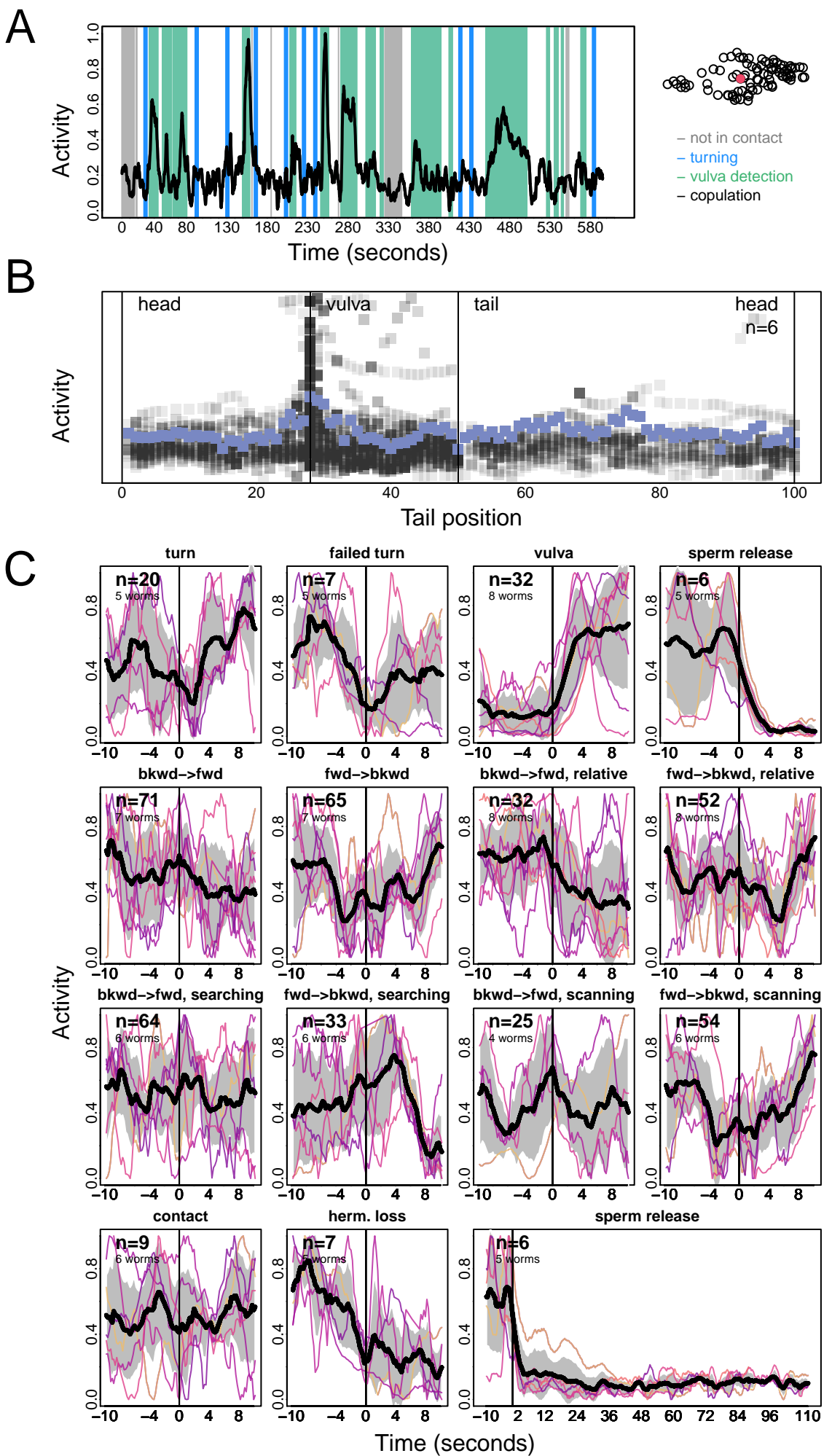
R1B



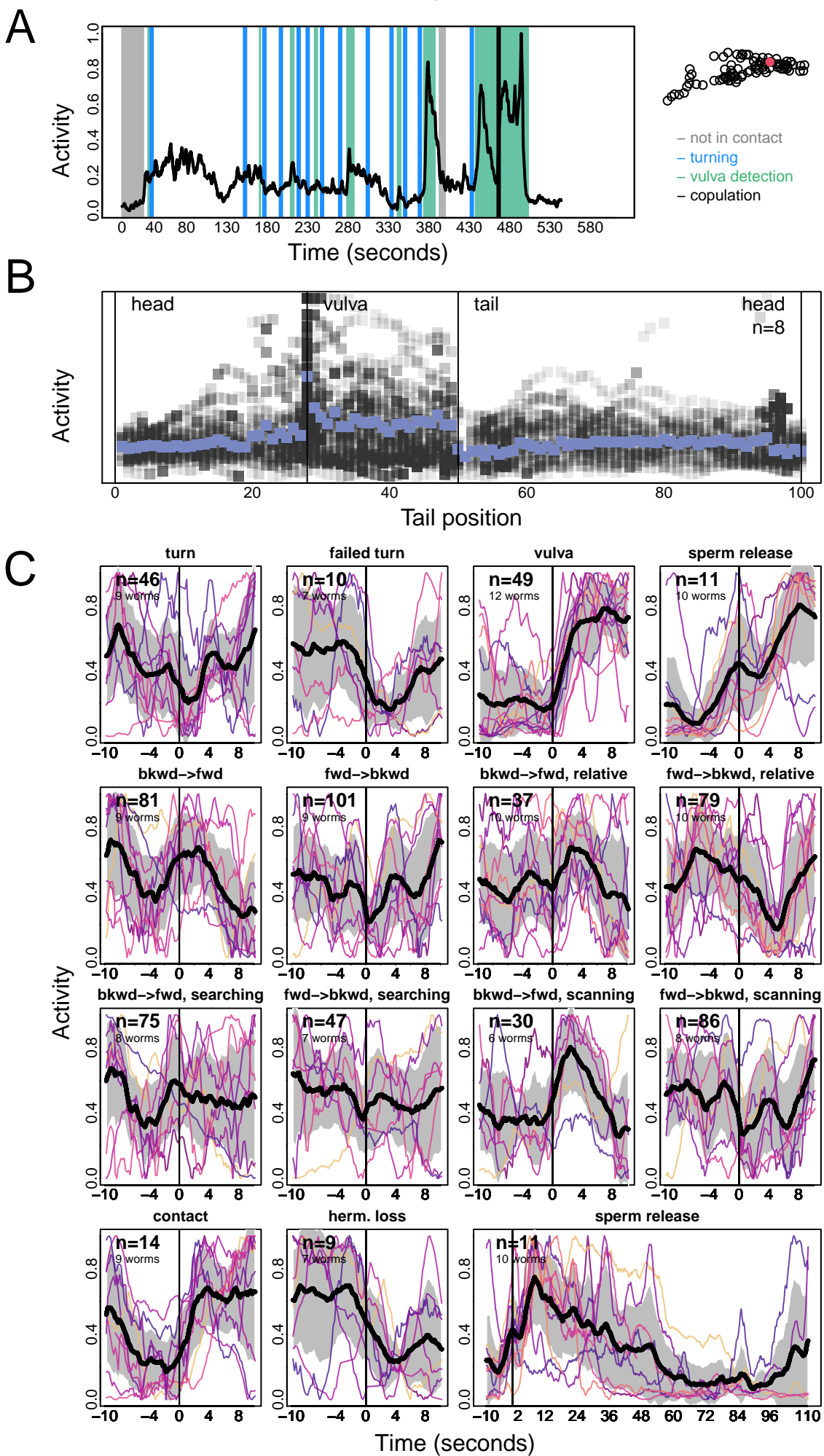
R2A



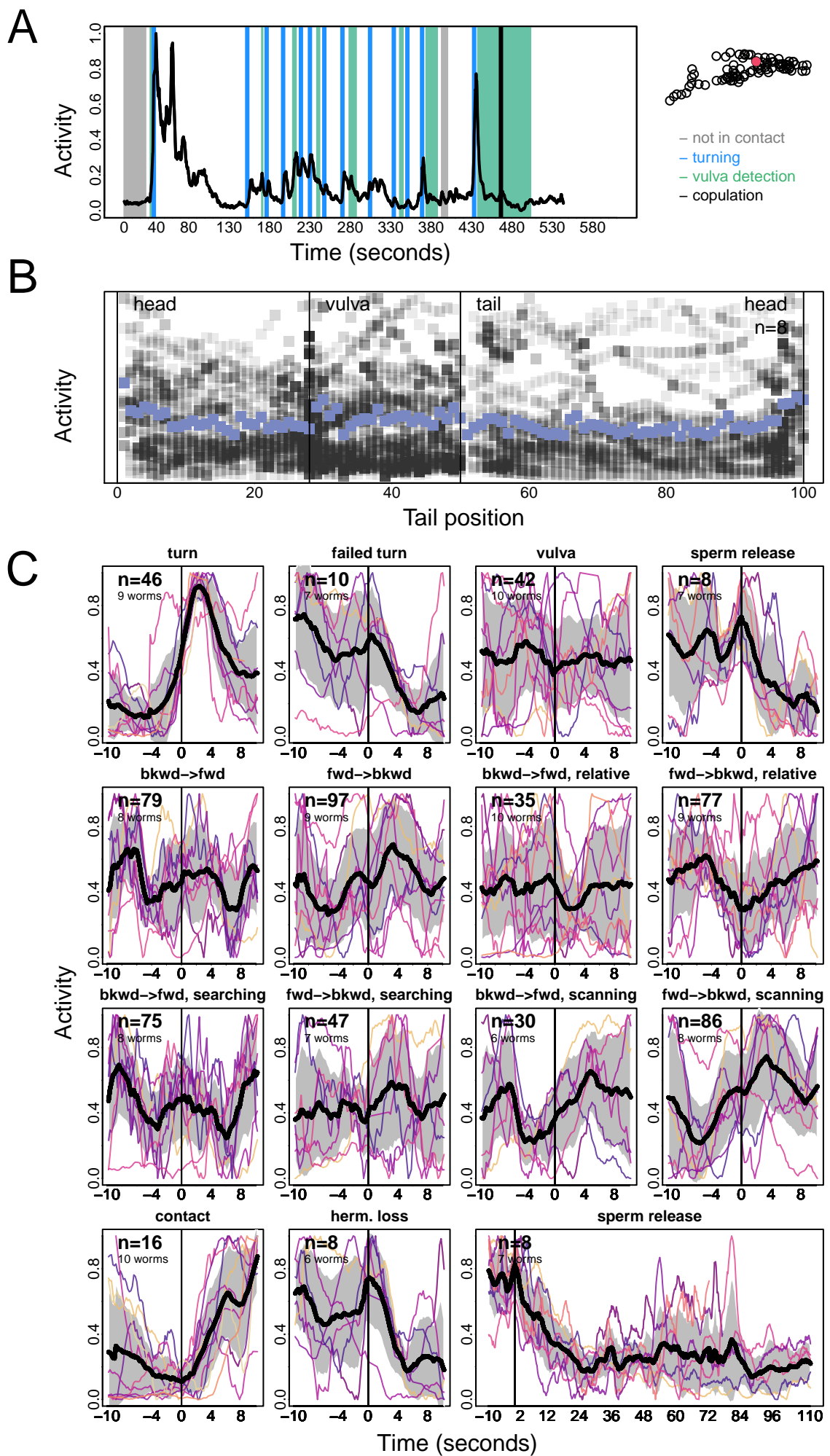
R2B



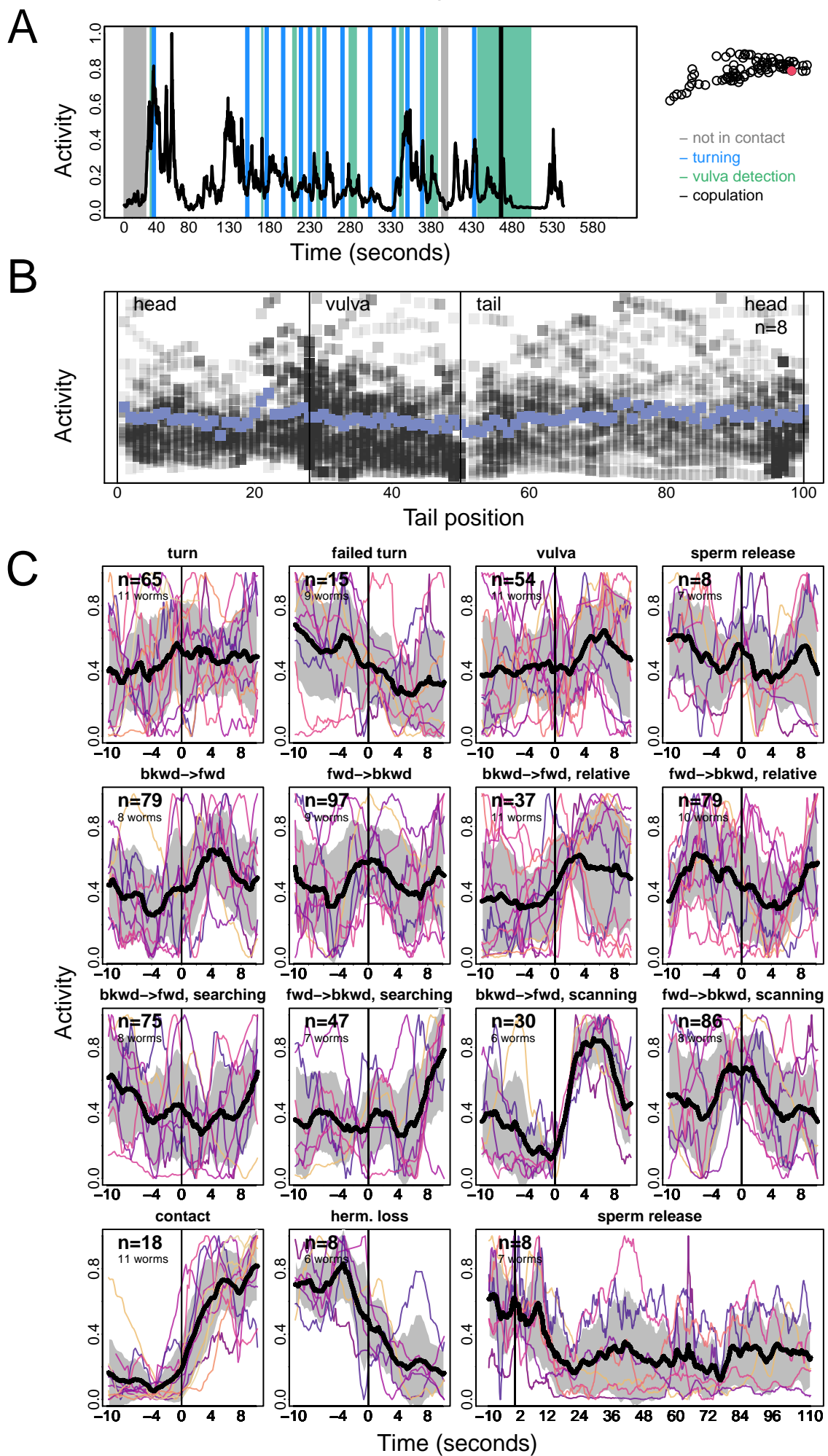
R3A



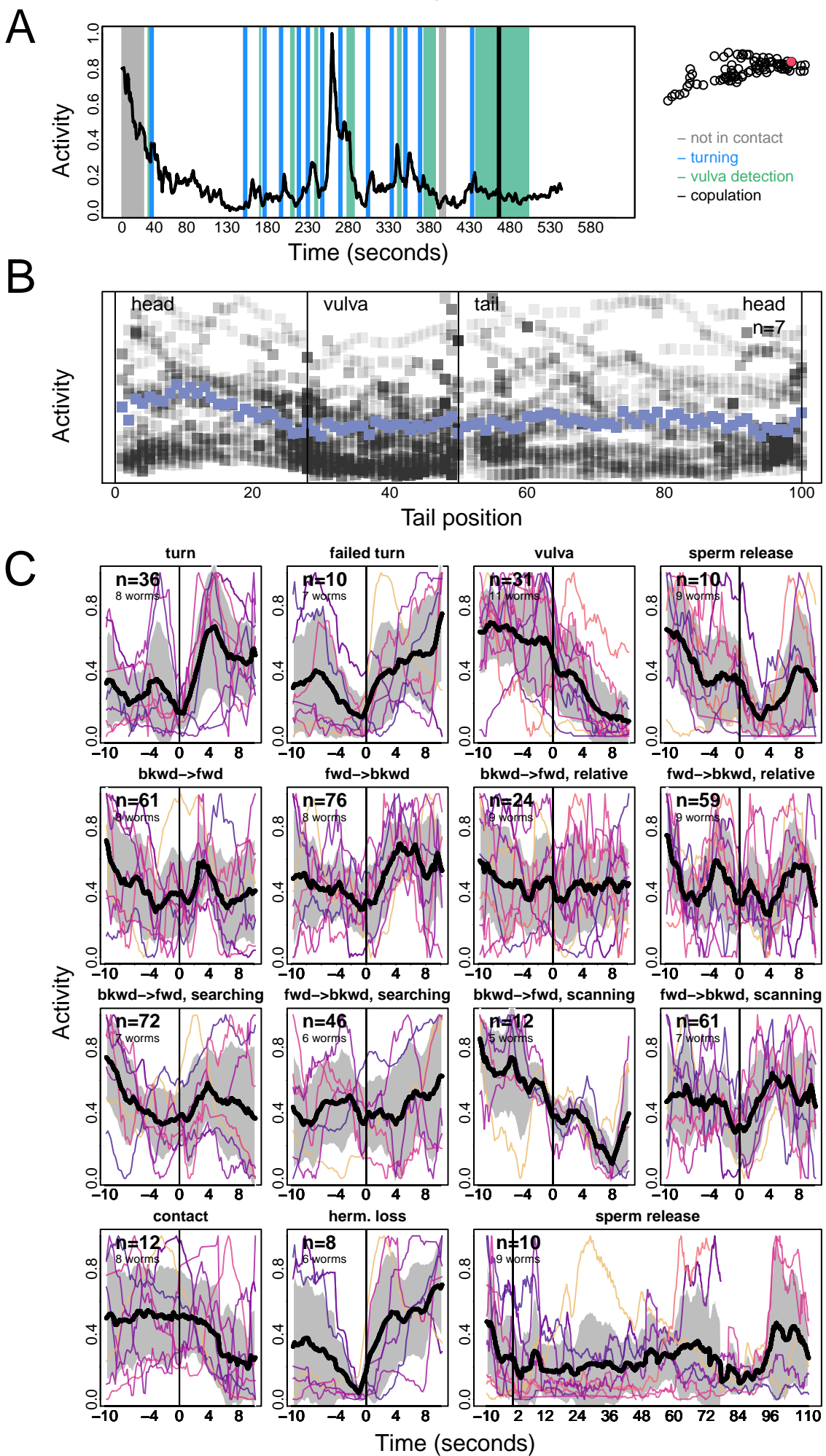
R4A



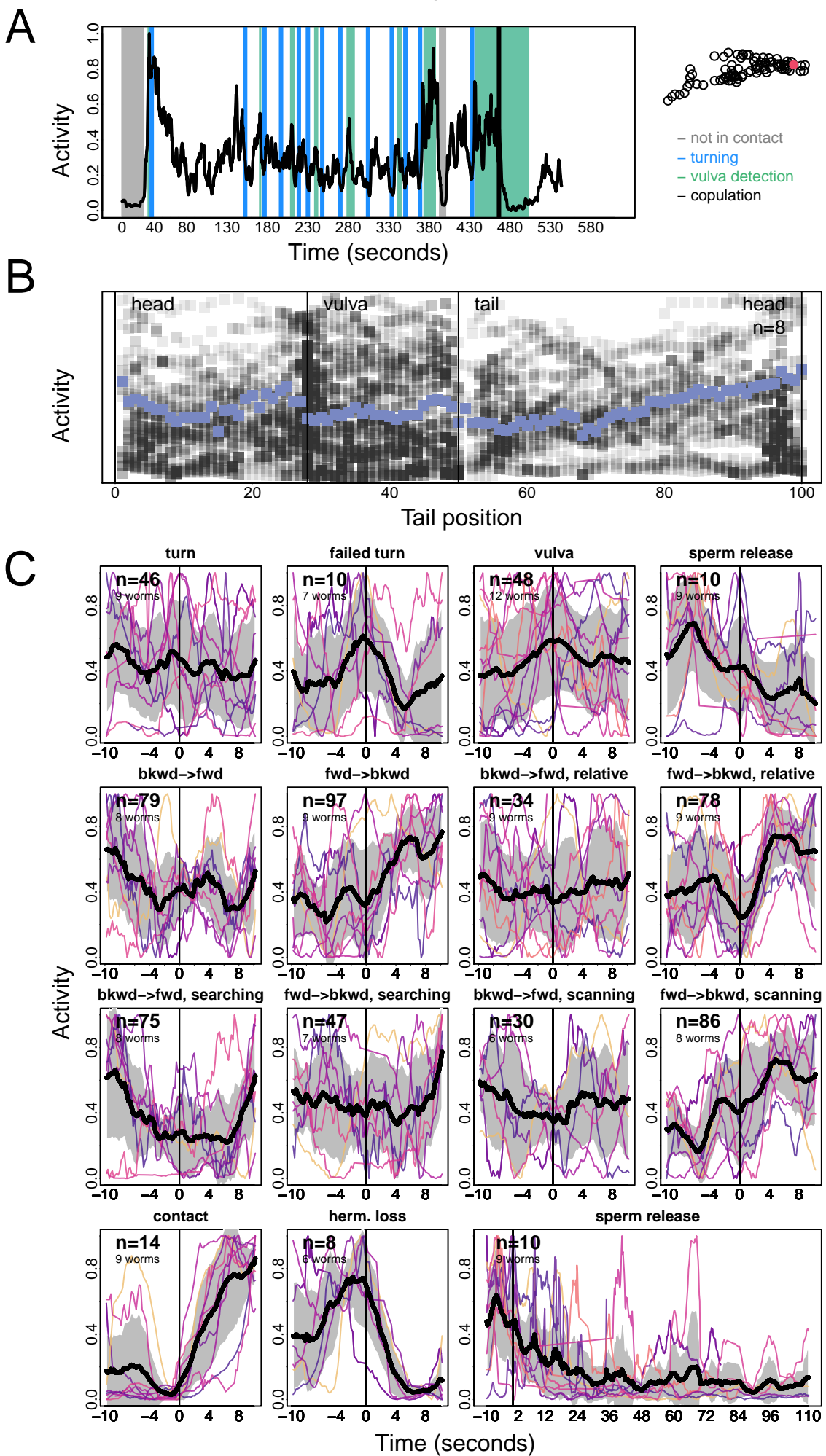
R6A



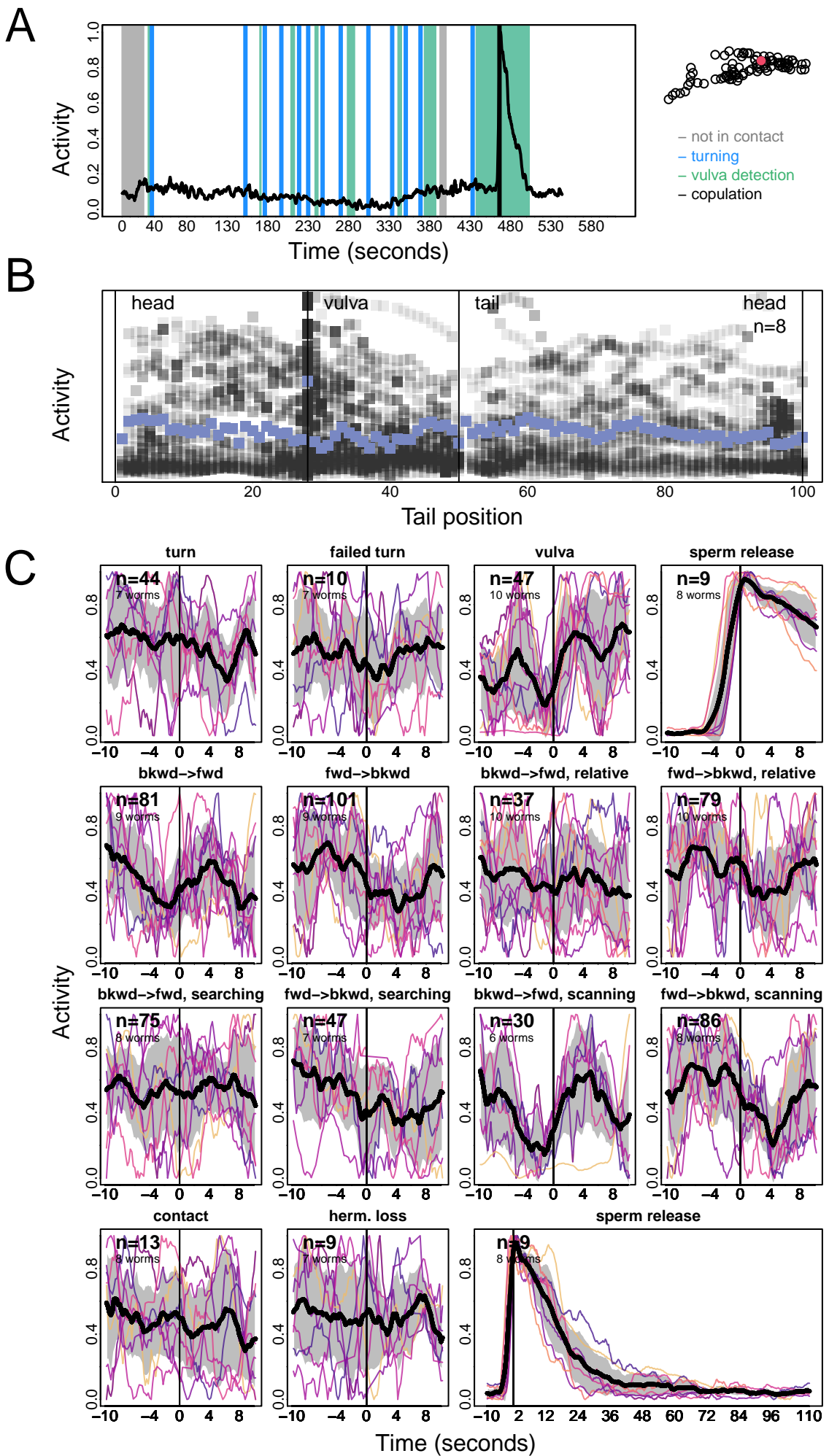
R8B



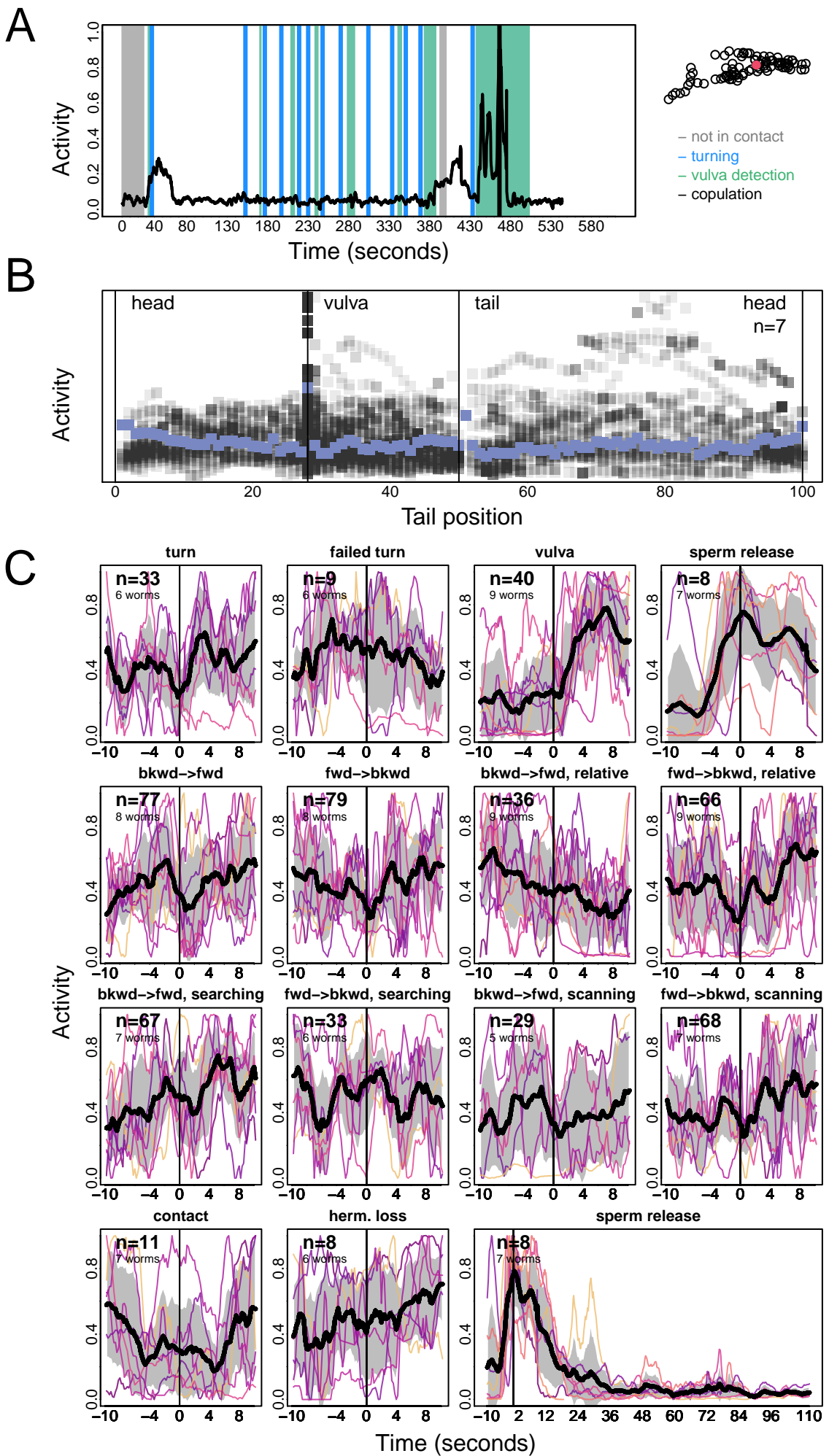
R9B



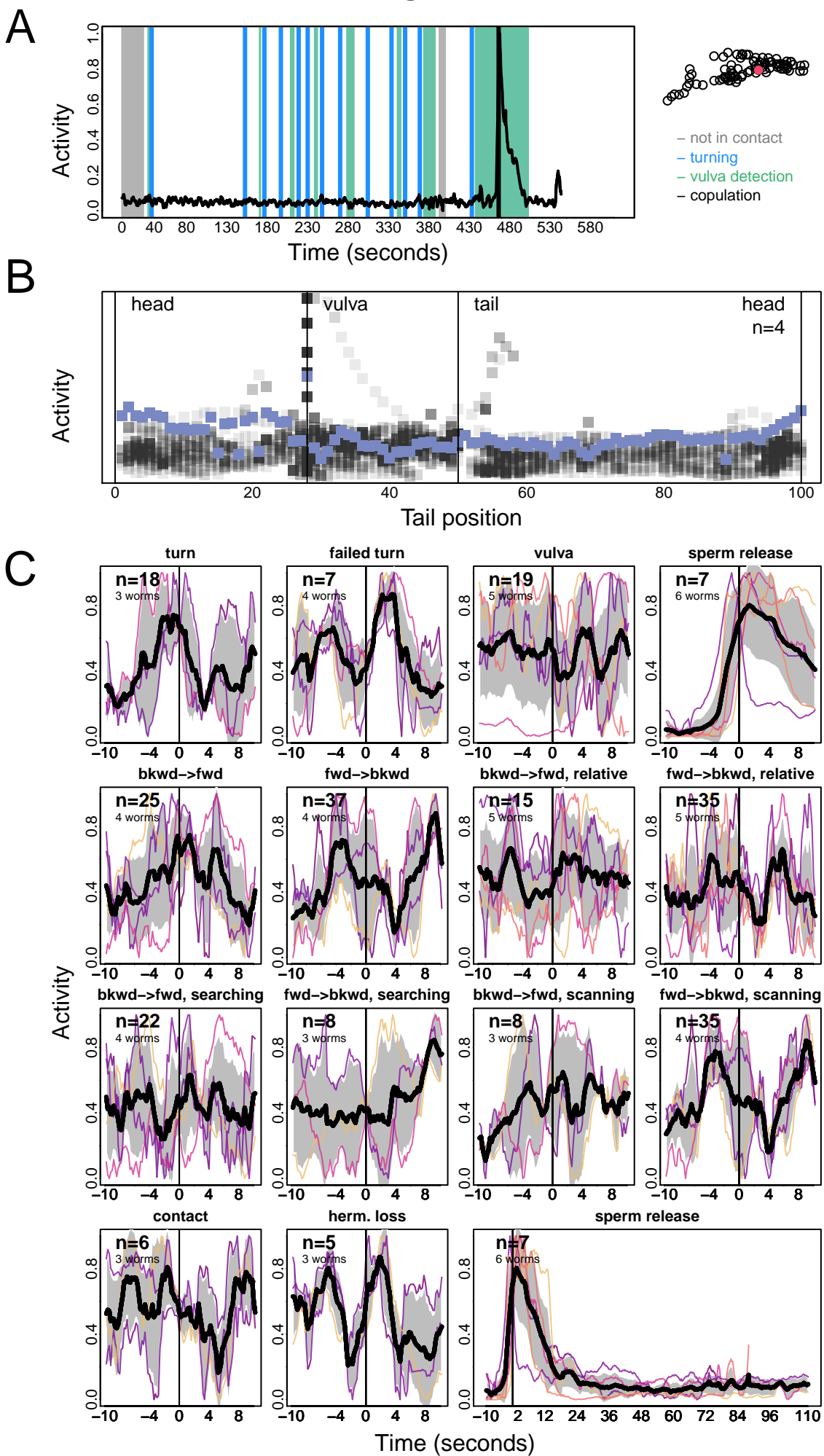
SPC



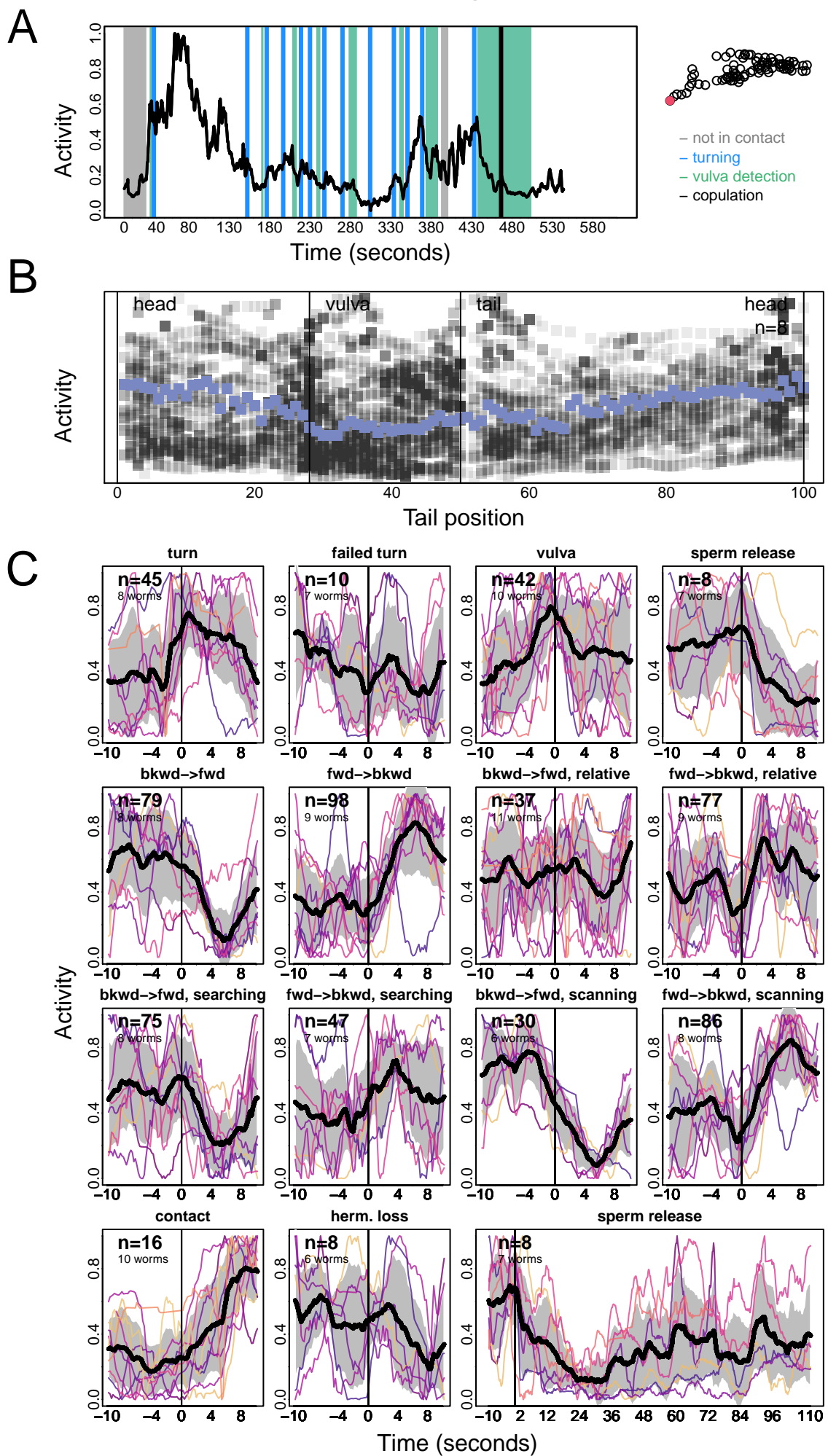
SPD



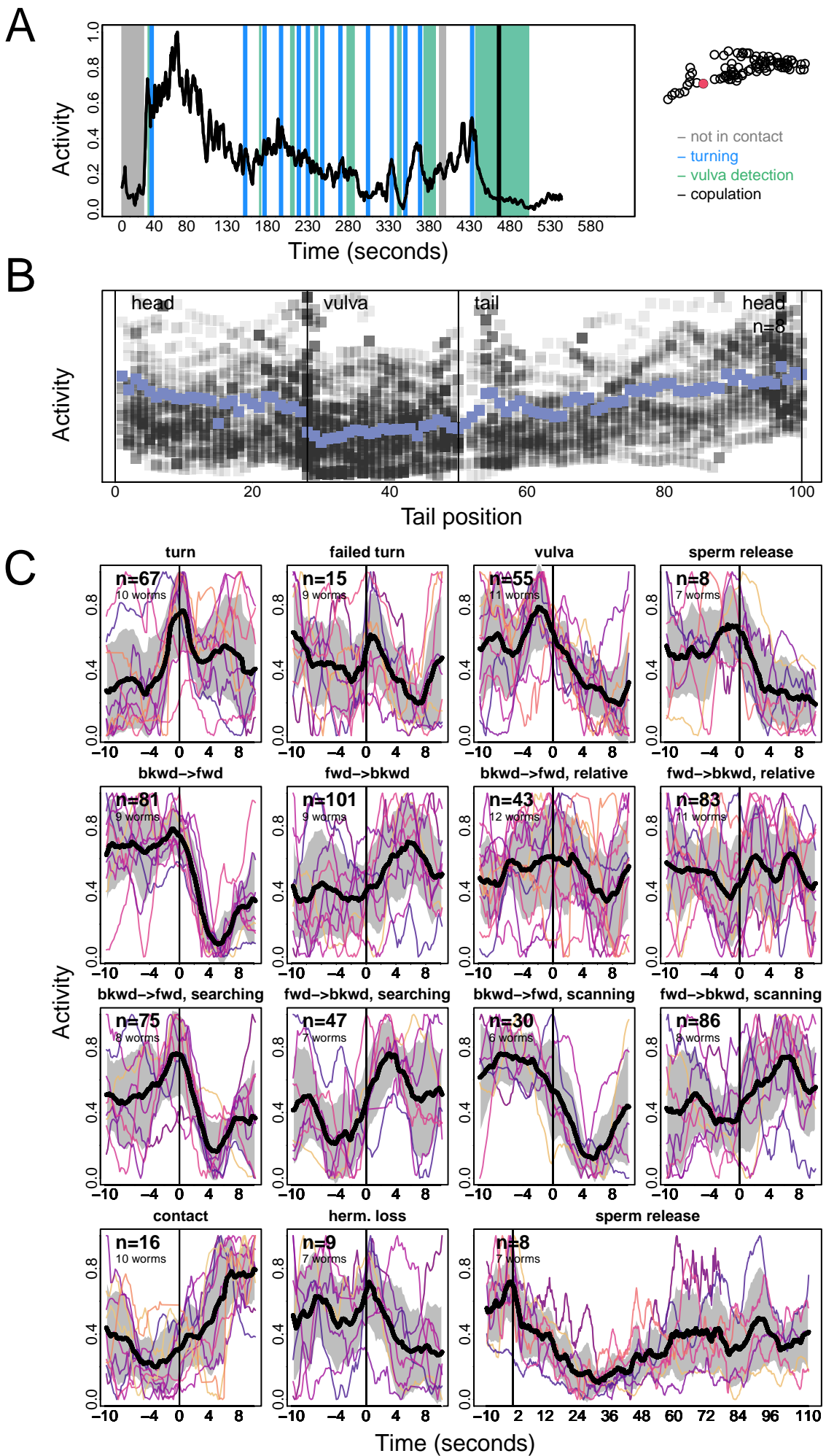
SPV



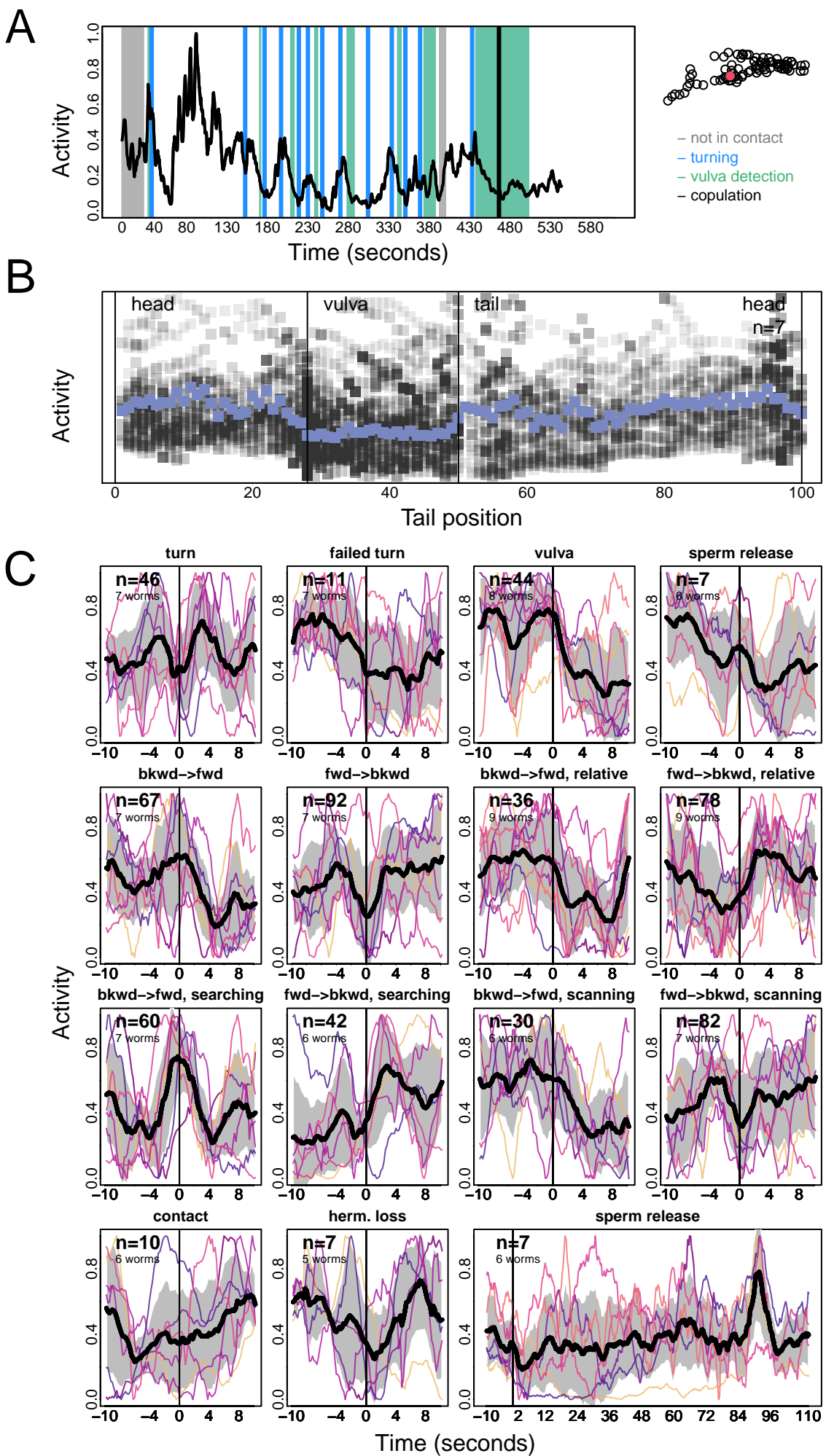
VA10



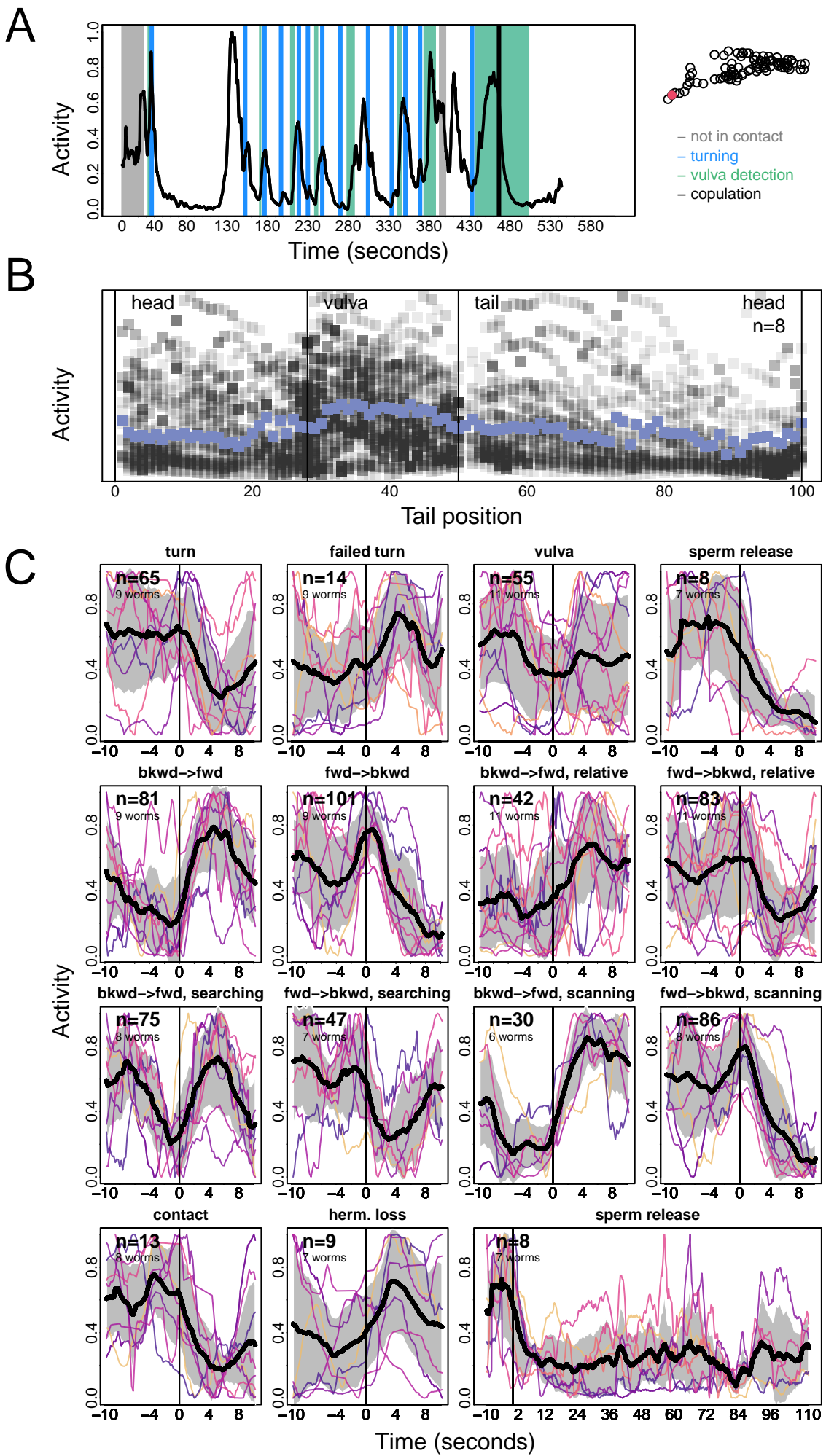
VA11



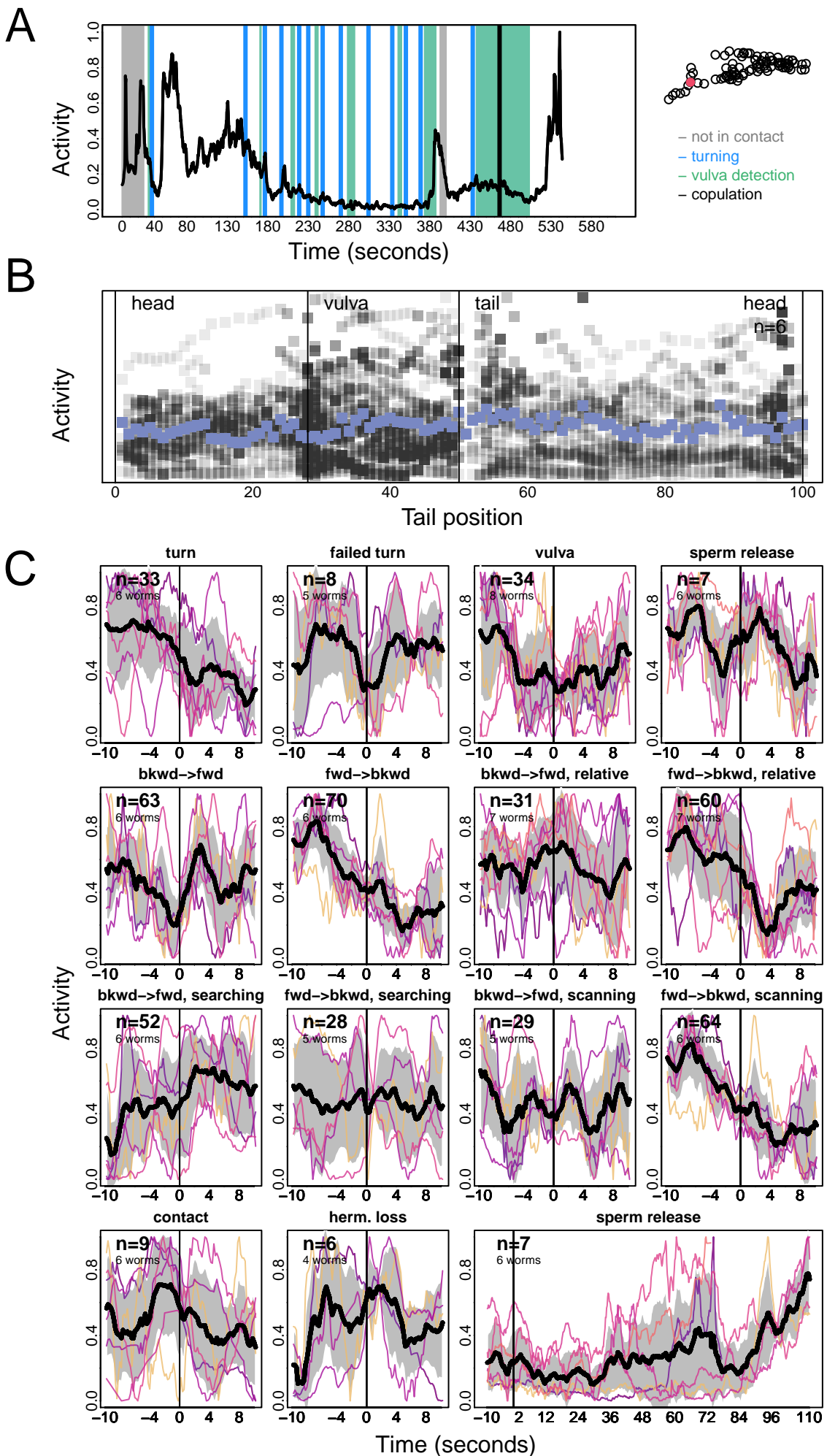
VA12



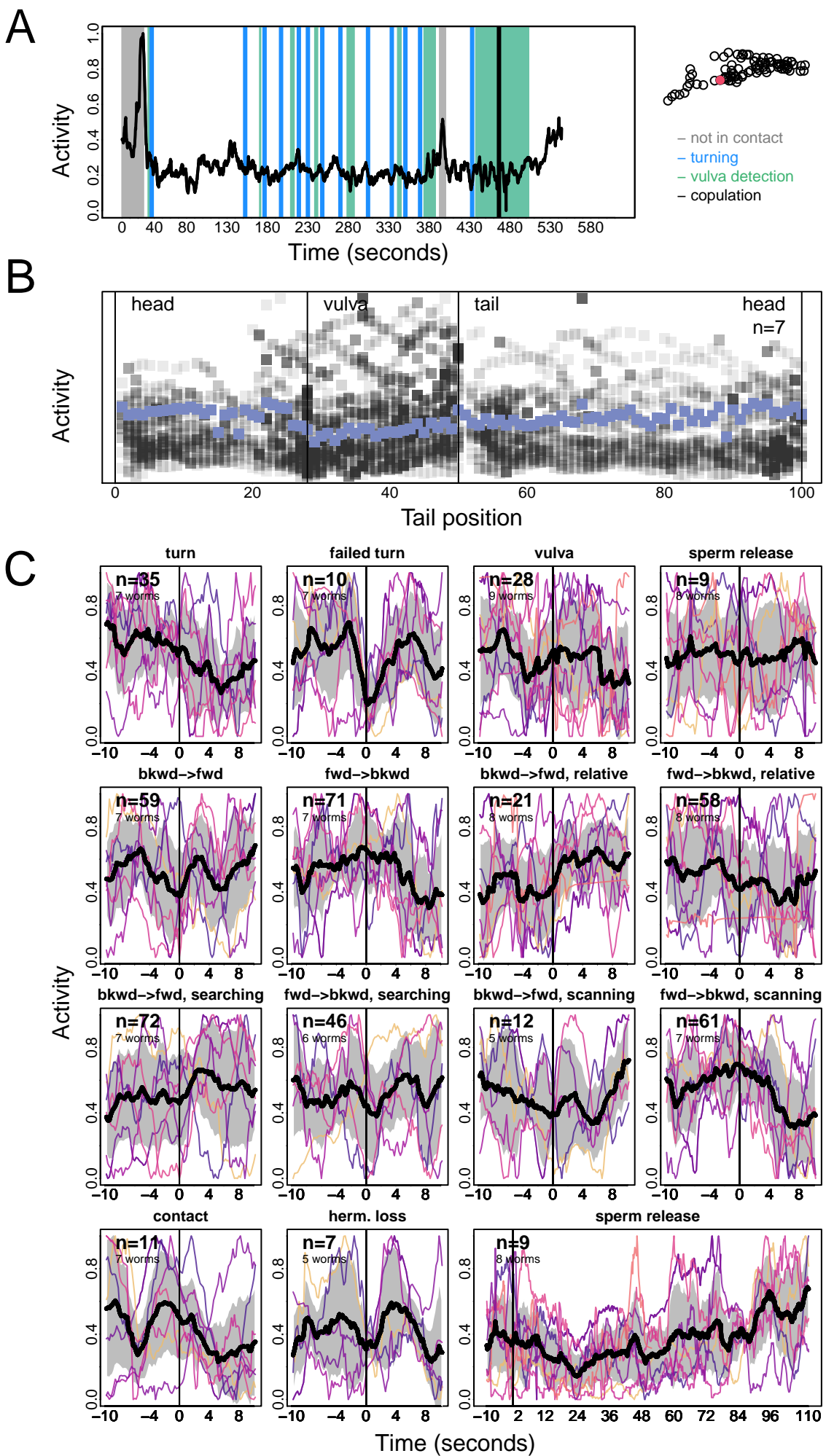
VB11



VD11



VD12



VD13

